SCUOLA INTERNAZIONALE SUPERIORE STUDI AVANZATI (SISSA)

INTERNATIONAL SCHOOL FOR ADVANCED STUDIES (ISAS)

PHD COURSE IN FUNCTIONAL AND STRUCTURAL GENOMICS

Academic Year 2014/2015

THE IMPACT OF FOXG1 ON HUMAN CORTICO-CEREBRAL ASTROGENESIS

THESIS SUBMITTED FOR THE DEGREE OF "DOCTORAL PHILOSOPHIAE"

ACADEMIC YEAR 2014/2015

Candidate:

Clara Grudina

Supervisor:

Prof. Antonello Mallamaci

“To my granny Livia

and my aunt Silva who I know that has guided me though from afar”

ABSTRACT

Foxg1 is a transcription factor gene involved in key steps of early corticocerebral development, including specification of the telencephalic and cortical fields, tuning of proliferation/differentiation kinetics, radial migration of projection neurons and laminar specification of them. Its allele dosage is crucial. Hemizygosity for *Foxg1* and duplication of it result into two devastating nosological entities, namely the Rett and West syndromes, respectively. We previously showed that *Foxg1*, like its Drosophila m. ortholog sloppy paired, also antagonizes gliogenesis.

Aim of this study was to investigate the role of *FOXG1* in human cortex, in particular the early commitment of pallial precursor cells towards glial fates and subsequent implementation of the astrocytic differentiation program.

For this purpose, we followed two approaches: (1) we modulated the expression of *Foxg1* by lentiviral vectors in human pallial precursor cells originating from the embryonic W8 of the gene in early commitment and astrocytic differentiation; (2) we generated human induced pluripotent stem cells (hiPSCs) starting from somatic non neural cells of patients affected by the *FOXG1* linked variant of the WS, then we forced these iPSCs to differentiate to cortical precursors to score their histogenetic properties.

We found that *Foxg1* overexpression in pallial precursor cells reduces their astroglial output, in particular S100β^+population. An opposite effect is elicited by halving *Foxg1* gene dosage. Moreover *Foxg1* overexpression also interferes with selected aspects of late astrocyte differentiation, possibly jeopardizing anti-excitotoxic capability of these cells.

These findings may help to reconstruct the molecular logic underlying normal articulation of astrogenesis. Moreover they provide useful hints about pathogenetic mechanisms leading to neurological disorders triggered by altered FOXG1 dosage.

INDEX

1. INTRODUCTION

1.1 *Foxg1* gene

Forkhead box G1 (FOXG1), formerly known as Brain factor-1 (*BF-1*) is a regulatory gene of the forkhead family, encoding for a winged-helix transcription factor (TF). The Forkhead family of transcription factors is characterized by a conserved DNA-binding domain called the 'Forkhead box', or FOX. The origin of the name 'Forkhead' comes from a study in Drosophila where a mutation in this gene caused the formation of an ectopic head structure that looks like a fork. Sometimes the forkhead proteins can be refered to as 'winged helix' proteins because X-ray crystallography revealed that the DNA-binding domain features a 3D structure with three α-helices flanked by two characteristic loops that resemble butterfly wings. The family contains more than a 100 members in humans displaying very diverse functions.

The gene is located on human chromosome 14 in position 13 on the long (q) arm (Figure I.1). *Foxg1* is an ancient transcription factor gene specifically expressed in the developing rostral brain. In particular, Foxg1 protein usually acts as a transcriptional repressor through DNA binding either in a direct or indirect manner.

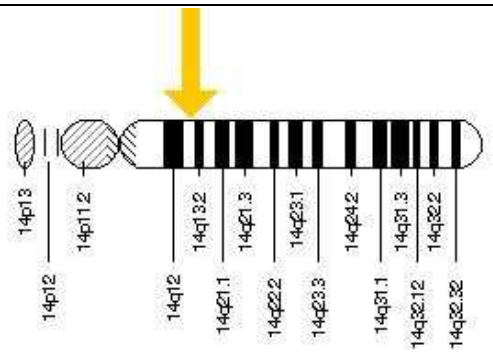

Figure I.1. *Foxg1* locus on chromoson 14

It is implicated in genetic control of multiple aspects of cerebral cortex morphogenesis, including early distinction between pallial and subpallial fields, dorsoventra lpatterning of the pallium, regulation of the balance between neural proliferation and differentiation, neocortical layering and tuning of astrogenesis rates. Proper *Foxg1* allele dosage is crucial for normal brain morphogenesis and function.

1.2 *FoxG1* in the developing telencephalon

The Central Nervous System (CNS) develops during embryogenesis as a simple sheet of neuroepithelial cells. This sheet then forms the nascent telencephalon that arises at the anterior end of the neural plate (Figure I.2). The telencephalic neuroepithelium becomes patterned into distinct progenitor regions which later give rise to specific neuronal subtypes.

The regulation of the rates of cell proliferation, differentiation and apoptosis of telencephalic precursors and the types of neurons that they generate, depend on several extrinsic factors secreted from signaling centers and intrinsic factors of the neuroepithelial cells. The extrinsic factors include members of the fibroblast growth factor (FGF), bone morphogenetic protein (BMP), and Wnt families as well as Sonic Hedgehog (SHH). The intrinsic factors, which are more specific to the developing anterior nervous system, include factors encoded by: *Foxg1, Gli3, Pax6, Lhx2,Gsx2,Nkx2.1* and *Emx2* genes.

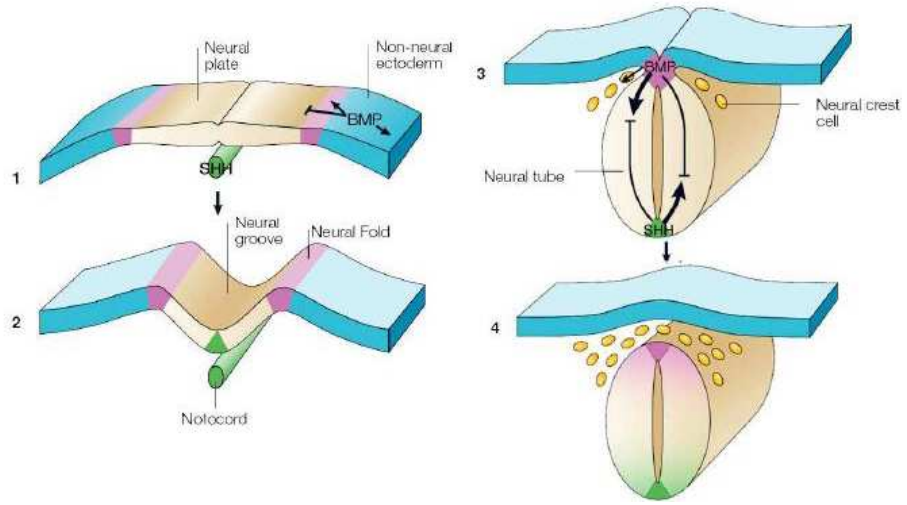

Figure I.2 Schematic view of the neural tube 1) opened neural plate 2) neural grove formation 3) closed neural tube 4) delaminating neural crests. Modified from (Gammill and Bronner-Fraser, 2003).

The initial formation of the telencephalon shares features with the induction of other tissues. In general, a discrete group of adjacent cells acts as an organizer to induce the formation of these tissues. In the mice telencephalon, the inducing cells are those of the anterior neural ridge (ANR). The ANR is located between the most anterior part of the neural plate, the anlage of the anterior commissure and the non-neural ectoderm. The telencephalon arises from cells at the rostrolateral end of the neural plate (Cobos et al., 2001);(Eagleson et al., 1995);(Inoue et al., 2000), which express *Foxg1.* In other words, *Foxg1* expression in the anterior neuroepithelium specifically marks telencephalic precursor cells and delineates most of the embryonic telencephalon. The ablation of the ANR from the anterior neuroepithelium prevents the expression of *Foxg1* (Shimamura and Rubenstein, 1997).

In addition to *Foxg1*, *Fgf* genes (including *Fgf8*) which are expressed by the ANR, help in organizing the telencephalon. Some evidences confirm the interaction between Fgfs and *Foxg1*. In particular, if Fgf signaling is suppressed in the anterior neural plate by knocking out three Fgf receptor genes (*Fgfr1-2-3*) most or all *Foxg1*-expressing cells are lost and as a result

the telencephalon does not form (Paek et al., 2009). Consistently, the replacement of *Fgf8* with hypomorphic and null alleles affects to various extents telencephalic development (Storm et al., 2006).

Once the anterior neural plate has acquired a telencephalic fate, it becomes further subdivided into domains distinguishable by the expression of specific molecular markers. These markers include genes encoding for transcription factors that are expressed in certain telencephalic subdomains, such as Nkx2.1,Gsx2,Pax6, and Emx2, as well as extracellular factors that are expressed in signaling centers at the edges of these subdomanis, such as Shh, FGFs, Wnts and Bmps (Figure I.3).

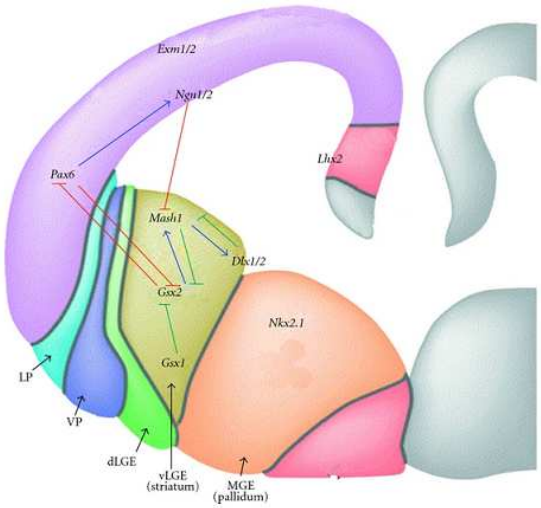

Figure I.3 Schematic coronal section through the developing telencephalon at E12. The dorsal and ventral subdomains are shown and defined by unique gene expression patterns. Dorsal telencephalic markers shown are Emx1/2, Ngn1/1, and Pax6. The ventral telencephalic markers shown can be split into identifying the LGE or MGE. Mash1 (Ascl1), Gsx1/2, and Dlx1/2 are associated with the LGE (specifically the vLGE), and Nkx2.1 is associated with the MGE. Adapted from (Wilson and Houart, 2004).

Prior to neural tube closure, two broad ventral and dorsal domains can already be distinguished molecularly. The dorsal telencephalic domain (the pallium) will give rise to the archicortex (subiculum, hippocampus and dentate gyrus), the paleocortex (olfactory piriform cortex and enthorinal cortex) and the neocortex, the largest region of the telencephalon. The ventral

telencephalon (the subpallium) will mainly generate basal ganglia and a part of amigdala (Figure I.4).

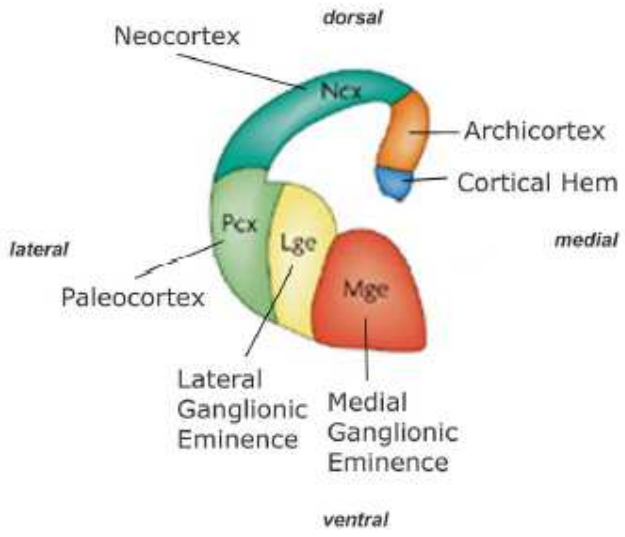

Figure I.4. **Sagittal view of the embryonic vertebrate telencephalon at E12**. Image modified from (Molyneaux et al., 2007).

1.3 *FoxG1* in Dorso-ventral (D-V) specification

Two main factors play a key role in establishing dorsal-ventral patterning. The dorsal Gli3, a zinc finger transcription factor and the ventral Shh, a secreted signaling protein. Indeed, the dorsal telencephalon fails to develop normally in Gli3 mutant mouse (Grove et al., 1998). Whereas in *Shh*$^{-/-}$ mouse embryos, all ventral telencephalic precursors are missing and the size of telencephalon is reduced due to the lack of cell proliferation and survival (Ohkubo et al., 2002). Shh controls the relative size of dorsal and ventral domains of the telencephalon in large part by restricting the dorsalizing function of Gli3. In other words, Shh function promotes ventral identity by preventing dorsalization. However the rescue of early ventral development in the Shh mutant by elimination of Gli3 implies that other factors function independently or downstream of Shh generate ventral precursor cells (Rallu et al., 2002). *Foxg1* and *Fgfs* are both required for generating ventral precursors independently of *Shh*. In mice, knockout of *Foxg1* determines the loss of

ventral precursor cells (Danesin et al., 2009) and ventral cells are not rescued by removal of *Gli3*. This suggests that *Foxg1* acts downstream of *Shh* and *Gli3.* In the *Foxg1;Gli3* mouse double mutant the whole telencephalon is missing. This indicates that both *Gli3* and *Foxg1 a*re essential for generating the dorsal and ventral subdivisions of the telencephalon, respectively (Hanashima et al., 2007). As for Fgf signaling, it also contributes to normal ventral telencephalic development (Gutin et al., 2006). FGF is necessary and sufficient to promote *Foxg1* expression (Shimamura and Rubenstein, 1997). *Fgf8* expression is reduced in *Foxg1*$^{-/-}$ embryos (Martynoga et al., 2005) and *Foxg1* is reduced in *Fgf8* mutants (Paek et al., 2009). In this way both signals promote the nascent telencephalon forming a positive feedback loop.

Studies in Zebrafish (Danesin et al., 2009) show that *Foxg1* directly inhibits Wnt/b-catenin pathway through transcriptional repression of *Wnt* ligands. Wnts have an important role for telencephalic dorsalization. Together with FGFs, Wnts progressively induce more mature dorsal identities to telencephalic precursor cells in chick embryos (Gunhaga et al., 2003) (Figure I.5).

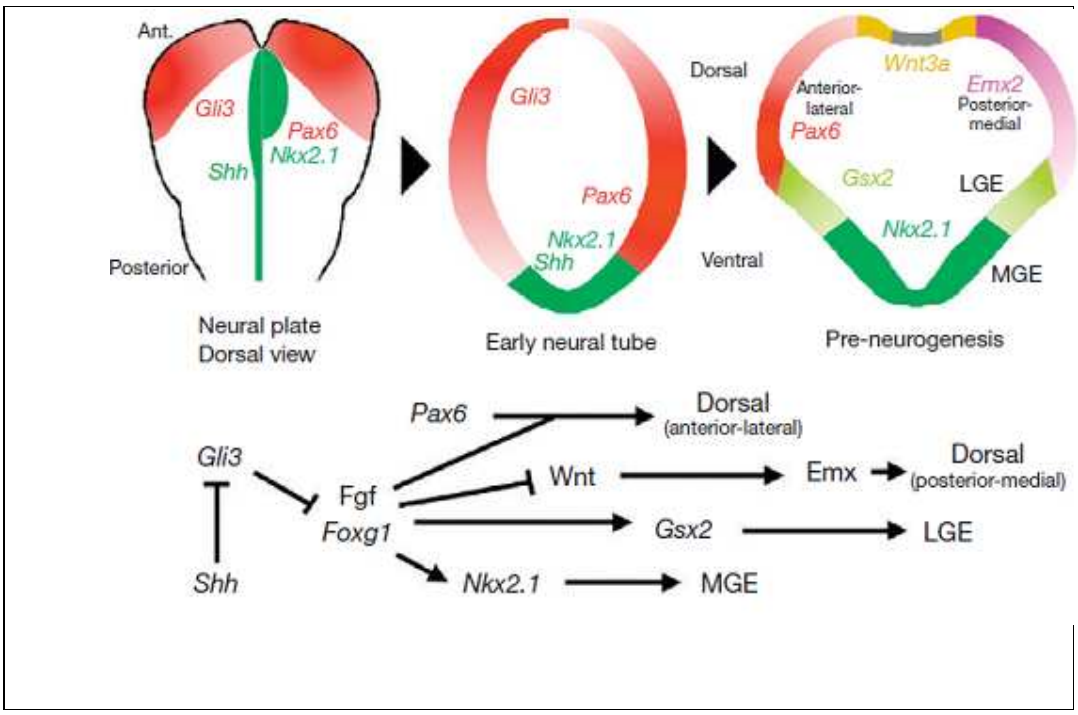

Figure I.5 Early expression patterns of key factors in the developing telencephalon from the neural plate stage (dorsal view), to the early neural tube stage (cross-section), to a stage that corresponds to midgestation (preneurogenesis) in the mouse. Salient interactions between these factors. Adapted from (John Rubstenstein and Pasko Rakic, 2013).

FoxG1 usually functions as an transcriptional repressor in direct and indirect way (Li et al., 1995);(Bourguignon et al., 1998); (Dou et al., 1999); (Yao et al., 2001);(Seoane et al., 2004). For example, FoxG1 can inhibit the TGF-β signaling by binding to Smad and FoxO transcription factor (Dou et al., 1999); (Seoane et al., 2004). In other cases, FoxG1 gets in direct contact with DNA. More specifically a protein-protein interaction is needed for its effect on positive proliferation, whereas an intact DNA binding domains is needed for its differentiation negative effect on (Dou et al., 2000; Hanashima et al., 2002).

Another example of FoxG1 physical interaction is with a member of the Groucho/Transducin-like enhancer-of-split (TLE) family, TLE2. The interacting mechanism between FoxG1 and TLE2 is accomplished by a conserved FoxG1 N-terminal motif, whereas the C-terminal domain is not required, although it has been previously proposed to be the biding site of TLE (Roth et al., 2010). When FoxG1 or TLE is knocked down, ventral telencephalon is disrupted.

1.4 *FOXG1* in hippocampus specification

The hippocampus is situated at the medial-temporal edge of the neocortex and harbors the neural circuitry essential for cognitive functions such as learning and memory (Lisman, 1999). The cortical hem lies at the dorsomedial border of the hippocampal field. It gives rise to different type of cells including Cajal-Retzius cells (C-R) in the cortical marginal zone. These C-R cells are one of the earliest neuronal cell types generated in the developing telenchephalon. They are essential for cerebral development because they produce the extracellular glycoprotein Reelin (Alcántara et al.,

1998). Reelin is an important signal for the guidance of later born cells that populate the cortical laminae. It organizes the radial migration of cortical neurons (Marín-Padilla, 1998), facilitate the development of hippocampal connectivity (Del Río et al., 1997) and modulate the morphology of radial glial cells (Supèr et al., 2000).

It has been hypothesized that Wnts and Bmps can regulate hippocampal development from the cortical hem (Grove et al., 1998). Moreover, several transcription factors have been found critical to decide the correct development of the hippocampus. In *Lhx2-null* mutants, the cortical hem and antihem are expanded at the expense of the pallial structures (Bulchand et al., 2001). Conversely, in *Foxg1-null* mutants, the cortical hem and the archipallium, i.e. the forerunner of hippocampus, are expanded at the expense of the neopallium and more ventral structures (Muzio and Mallamaci, 2005) (Figure I.6). Therefore, a suppression of both *Lhx2* and *Foxg1* is essential for the specification of the cortical hem, whereas expression of the former and suppression of the latter are needed to specify the hippocampus.

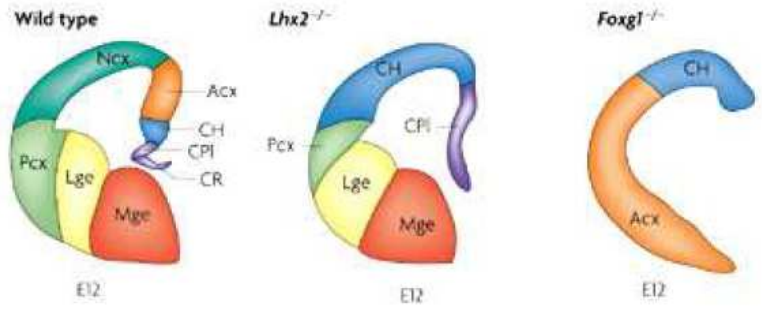

Figure I.6 Mutant phenotypes of mice knock-out for the Lxh2 and Foxg1, transcription factor involved in cortical specification. Abbreviations: CH, cortical hem; CR, choroidal roof; ChP, choroid plexus; Cx, cortex; Lge, lateral ganglionic eminence; Mge, medial ganglionic eminence; Pcx, paleocortex. Adapted from (Molyneaux et al., 2007).

1.5 *Foxg1* in neocortical projection neuron progenitor domain specification

Upon induction of the telencephalon by gradients of extracellular signaling molecules such as Shh, Fgfs, and Bmps, the interactions between several repressive transcription factors establish a dorsal (pallial), and ventral (subpallial),progenitor identity (Figure I.7) .

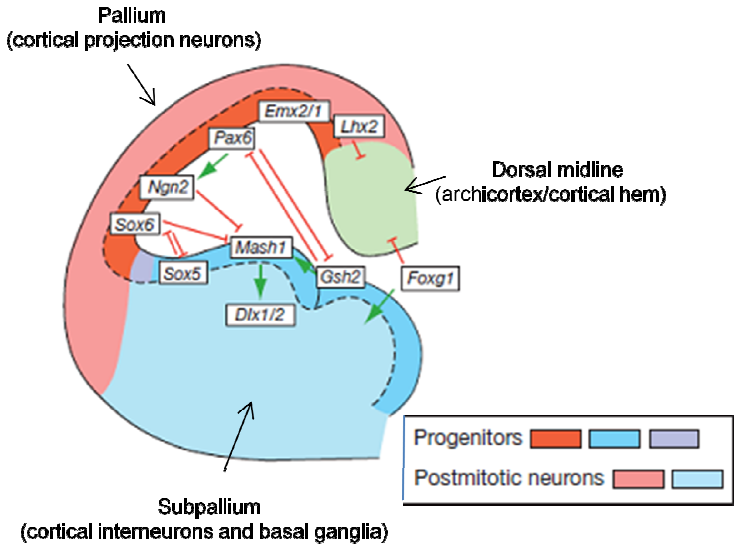

Figure I.7 A set of the key transcriptional regulators that establish the pallial progenitor domain. Adapted from (John Rubstenstein and Pasko Rakic, 2013).

These transcription factors include *Lhx2, FoxG1, Emx2, Pax6,* and *Sox6*, each of which has essential roles in specifying the progenitors that give rise to projection neurons of the neocortex. The five transcriptional regulators establish the neocortical progenitor domain. In particular, *Lhx2* and *FoxG1* repress dorsal midline while *Emx2, Pax6*, and *Sox6* regulate subpallial fates. This cooperation represents a critical first step in the specification of neocortical projection neuron identity.

In the absence of *FoxG1*, neocortical progenitors are not specified, while progenitors of the archicortex (which give rise to the hippocampus and

other evolutionarily older cortical regions) and the cortical hem (one major source of C-R cells) are expanded (Dou et al., 1999; Muzio and Mallamaci, 2005). Experiments in which *Foxg1* is conditionally inactivated at E13.5, a stage when cortical progenitors have already generated, have induced supernumerary cells with features of C-R cells (Hanashima et al., 2004). In vitro experiment by attenuating Foxg1 signaling in isolated cortical progenitor cells confirms that *Foxg1* negatively regulates C-R cell fate (Shen et al., 2006). In fact, in culture conditions, cortical progenitors that would normally generate cortical neurons of more advanced phenotype restarted the production of C-R cells.

These results provide evidence that *Foxg1* regulates the generation of C-R neurons after their normal birthday during early phases of cortical neurogenesis. Therefore, although cortical progenitor cells are competent to produce C-R neurons during later neurogenesis, *Foxg1* normally acts to inhibit this early-born cell fate during the subsequent generation of the cortical laminae.

1.6 Development of neocortex

The mammalian neocortex is a highly organized six layered structure that contains different neuronal cell types and a diverse range of glia cells (Ramon and Cajal, 1997). There are two main classes of cortical neurons: interneurons, which make local connections; and projection neurons, which extend axons to distant intracortical, subcortical and subcerebral targets. Projection neurons are glutamatergic neurons characterized by a typical pyramidal morphology that transmit information among different regions of the neocortex and to other regions of the brain. During development, they are generated from progenitors of the neocortical germinal zone located in the dorsolateral wall of the telencephalon (Anderson, 2002)(Gorski et al., 2002). By contrast, GABAergic interneurons and C-R cells are generated primarily from progenitors in the ventral telencephalon and cortical hem, respectively, and migrate for a long distance to their final locations within the neocortex.

During early development, the neuroepithelium in the dorsolateral wall of the rostral neural proliferate by repeating symmetric cell division, where each neuroepithelial cell divides into two neuroepithelial cells (Alvarez-Buylla et al., 2001);(Fishell and Kriegstein, 2003); (Fujita, 2003);(Götz and Huttner, 2005);(Miller and Gauthier, 2007). As the wall of the neural tube becomes thicker, neuroepithelial cells elongate and become radial glia cells (RGCs), which have cell bodies in the ventricular zone, and radial marginal processes reaching the pial surface. RGCs were previously thought of as specialized glial cells that guide neuronal migration. Later, it was found that RGCs undergo asymmetric cell division, where each RGC divides into two distinct cell types: a RGC and an immature neuron or a basal progenitor (neurogenic phase) (Malatesta et al., 2000);(Miyata et al., 2001);(Noctor et al., 2001). Immature neurons migrate outside of the ventricular zone along radial fibers into the cortical plate, where these cells become mature neurons, whereas basal progenitors migrate into the subventricular zone (SVZ) proliferate further and give rise to more neurons. RGCs give rise to many different types of neurons, initially deep layer neurons and then superficial layer neurons later, by repeating asymmetric cell division (Figure I.8). RGCs also give rise to astrocytes, oligodendrocytes and ependymal cells (gliogenic phase).

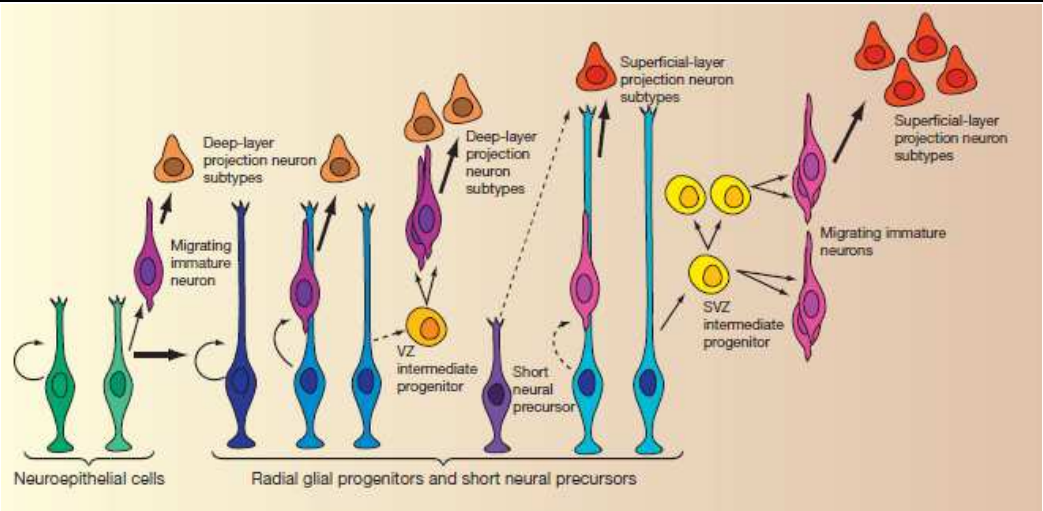

Figure I.8 The diversity of divisions cells during cortical development. Adapted from (John Rubstenstein and Pasko Rakic, 2013).

Both neuroepithelial and RGs are considered neural stem/progenitor cells. It was recently shown that the developing human neocortex has an expanded outer region in the SVZ (OSVZ), and that progenitors in this region (OSVZ progenitors) divide multiple times and generate a large number of neurons (Fietz et al., 2010);(Hansen et al., 2010). These cells seem to play a major role in the expansion of the cortex. OSVZ progenitors have radial glia-like morphology and extend radial fibers to the pial surface. However, they lack long apical processes and are not in contact with the ventricular surface (Figure I.9).

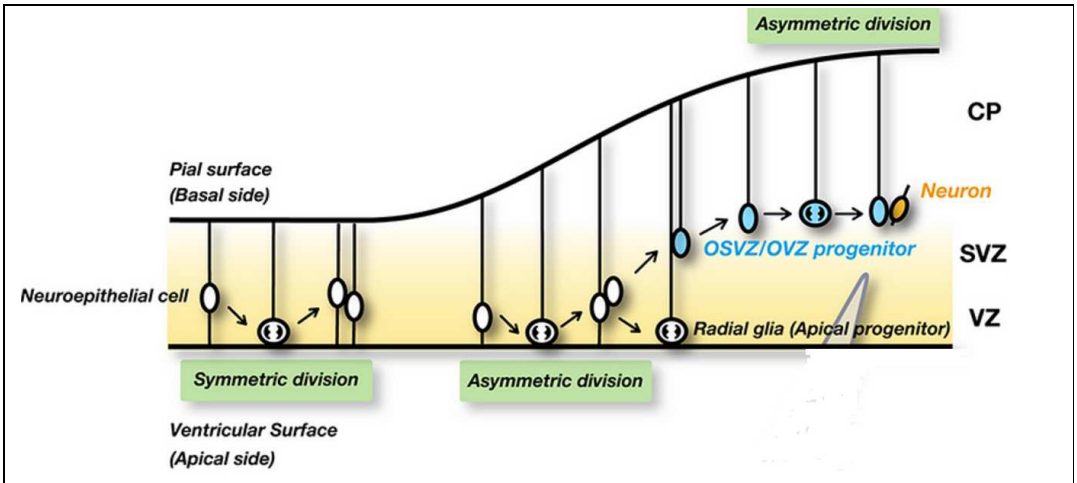

Figure I.9 Generation of OVZ progenitor. Adapted from (Shimojo et al., 2011).

Similar cells called outer ventricular zone (OVZ) progenitors are found also in the developing mouse cortex (Shitamukai et al., 2011). OVZ progenitors are located outside of the ventricular zone and retain radial fibers reaching the pial surface (basal processes) (Figure I.10). These cells undergo asymmetric cell division, where each OVZ progenitor divides into a daughter cell that inherits the radial fiber (OVZ progenitor) and the other that does not. The one that inherits the radial fiber seems to repeat asymmetric cell division multiple times, while the other differentiates into post-mitotic neurons.

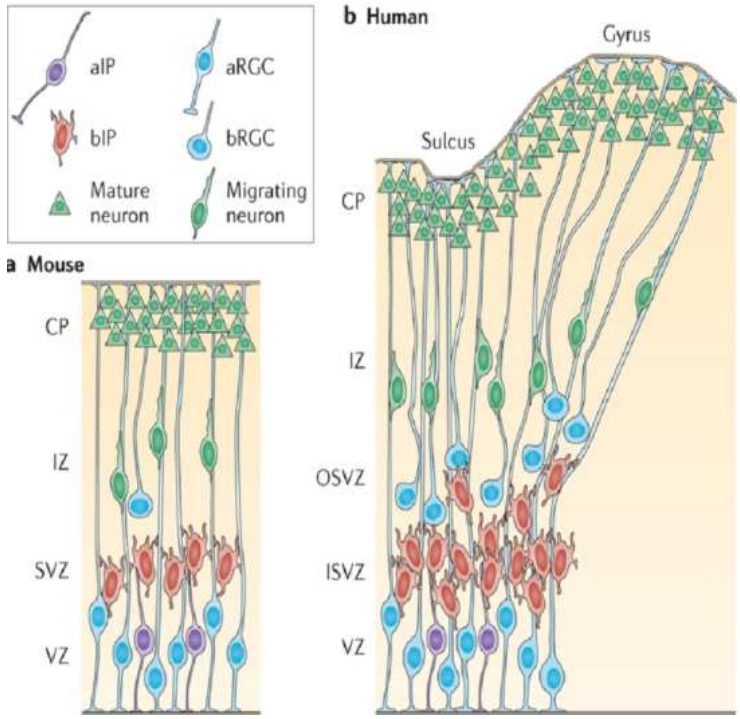

Figure I.10 Human vs mouse cortical neurogenesis. Basal IPs (bIPs) are mostly positioned in the subventricular zone (SVZ) in the mouse cortex and in the inner SVZ (ISVZ) in the human cortex. Basal RGCs (bRGCs) are identified in the SVZ in the mouse cortex and the outer SVZ (OSVZ) in the human cortex. Migrating neurons mostly appear in the intermediate zone (IZ), whereas mature neurons form an inside-out six-layered structure in the cortical plate (CP). Adapted from (Sun and Hevner, 2014).

Progenitors residing in the VZ and SVZ produce the projection neurons of the different neocortical layers in a tightly controlled temporal order from embryonic day (E) 11.5 to E17.5 in the mouse (Angevine and Sidman, 1961), and postmitotic neurons position themselves in the developing neocortex through defined modes of radial and tangential migration (Britanova et al., 2006). Around E10.5 the earliest born neurons appear and form a layered structure termed the preplate (PP); incoming CP neurons split the PP into the superficial marginal zone (MZ) which develops into layer 1 of the postnatal cortex, and the deeper subplate (SP), which is situated below layer 6 (Molliver et al., 1973). The cortical plate is developed between MZ and SP and will give rise to the multilayered neocortex. As neurogenesis progresses, diverse

subtypes of projection neurons are generated sequentially and their migration into the mantel layers occurs in an “inside-out” manner, meaning that later born neurons will occupy the more superficial layers than one is generated before (Rakic, 1974); (Frantz and McConnell, 1996) (Figure I.11). Hence neurons of the deepest layers (6 and 5) are generated at the earliest stages, followed by neurons of layers 4, 3 and 2.

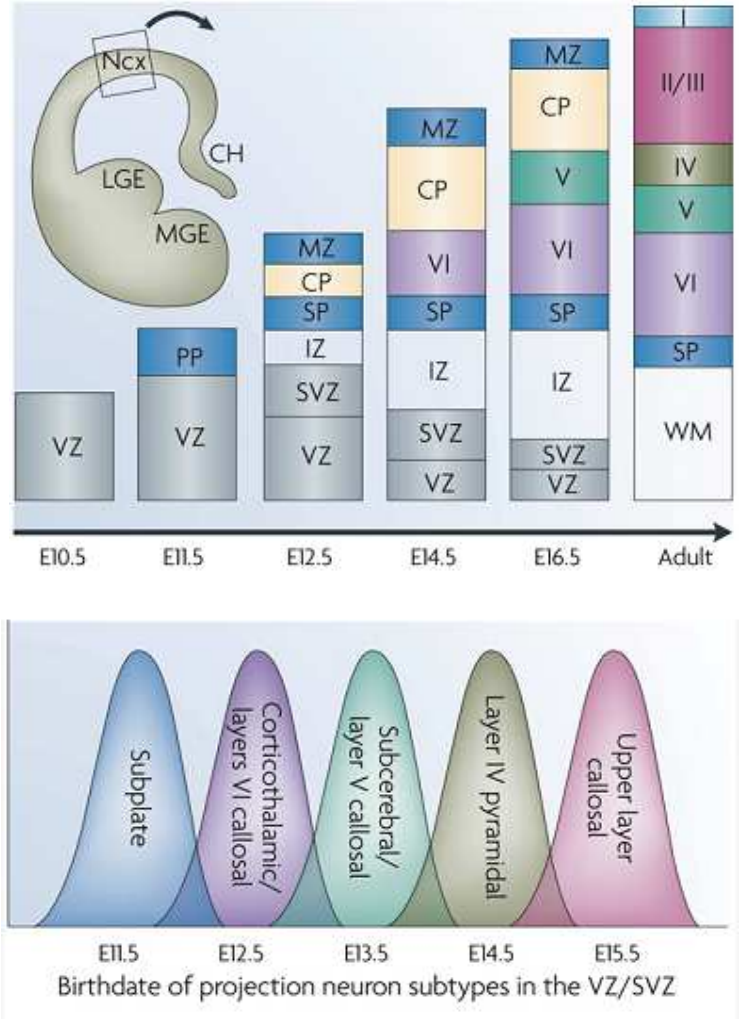

Figure I.11 At the top lamination of cerebral cortex during mouse development. At the bottom neuronal subtype specification in the cerebral cortex. Adapted from (John Rubstenstein and Pasko Rakic, 2013).

The classic view concerning Upper layer (UL) neurogenesis was that neural stem cells, known as radial glial cells (RGCs), undergo successive rounds of asymmetric cell division to produce the principal layer-specific subtypes (preplate, deep-layer (DL), and UL neurons) in a fixed order determined by temporal changes in cell competence (Frantz and McConnell, 1996); (Desai and McConnell, 2000);(Yu et al., 2009). The lineage relation between DL and UL subtypes has only recently been directly assessed (Yu et al., 2009;(Franco et al., 2012); (Yu et al., 2012); (Guo et al., 2013). In particular, the presence of UL-committed progenitors from the earliest phase of corticogenesis has provided an alternative view of cortical neurogenesis (Franco et al., 2012). It knows that specific patterns of gene expression are correlated with the changes in cortical progenitor cells, and in their progeny, over time. Genetic studies have indicated that the segregation between the principal layer subtypes of the cerebral cortex is established on a closed transcriptional network, in which cross-repression between the four TFs, namely, Fezf2, Ctip2, Satb2, and Tbr1, is sufficient to establish the subcerebral, intracortical, and corticothalamic projection identities within the postmitotic neurons (Alcamo et al., 2008); (Britanova et al., 2006); (McKenna et al., 2011); (Srinivasan et al., 2012). For example, *Tbr1* is expressed in the preplate and layer 6 during early corticogenesis (Bulfone et al., 1995). Indeed, in the absence of *Tbr1*, the expression of reelin by C-R cells in the marginal zone is reduced (Hevner et al., 2001). Recently studies have demonstrated that *Foxg1* might switch the transcriptional program to acquire projection neuron identity and, concomitantly, to confer the sequence of DL and UL neurogenesis (Toma et al., 2014) (Figure I.12). These data demonstrate that cortical progenitors have a restricted competence window *in vivo*, such that UL competence strictly follows DL competence and is terminated by gliogenic competence. In particular, *Foxg1* confers the sequence of DL and UL neurons competence through *Tbr1* repression within a closed transcriptional cascade (Toma et al., 2014).

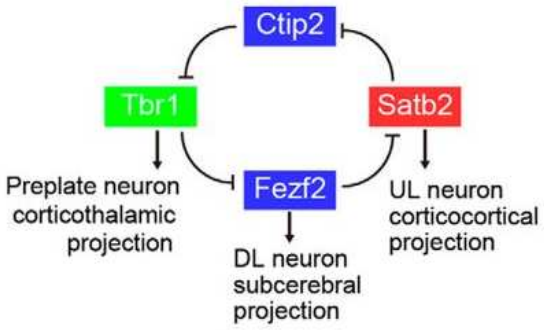

Figure I.12 Schematic model of identified genetic interactions between the layer-subtype TFs. Adapted from Toma et al., 2014.

1.7. Migration of neocortical projection neurons and neocortical inhibitory interneurons

The radial migration of projection neurons towards the CP include phases of temporary migratory arrest and retrograde migration prior to entering the CP (Noctor et al., 2004). During these phases, migrating neurons transition between bipolar and multipolar morphologies (LoTurco and Bai, 2006). Several genes control different aspects of neuronal migration and own mutation can lead to dramatic brain malformations. The mechanisms of neuronal migration mainly control the fundamental aspects of glial-guided neuronal motility, including cell-cell interactions, cytoskeletal dynamics, leading process extension, somal translocation and migration termination.

Cortical neurogenesis is essentially completed during the embryonic period, followed by gliogenesis, which occurs largely in the first month of postnatal life (Bystron et al., 2008).

Inhibitory interneurons of the cerebral cortex are generated from distinct progenitor cells in the germinal zones of the ventral forebrain, mainly within the medial and caudal ganglionic eminences. In human neocortex, some interneurons seems to derive from dorsal progenitors (Yu and Zecevic, 2011), other are probably generated in the ventral telencephalon and enter the cortex via tangential migration (Fertuzinhos et al., 2009). Upon arrival in

the neocortex, interneurons migrate radially to enter the CP (Nadarajah and Parnavelas, 2002) and segregate into their layer destinations based on their molecular subtype, origin and birth date during early postnatal development (Miyoshi and Fishell, 2011).

1.8 *FoxG1* regulate the migration of pyramidal neuron precursors into the cortical plate

The pyramidal neurons, which are generated locally within the cortical germinal zones (Götz and Huttner, 2005), were thought to achieve their appropriate laminar positions exclusively through vertical migration along radial glial fibers. However, it is now recognized that pyramidal neuron precursors, like interneurons, tangentially disperse during their integration into the developing cortex (O'Rourke et al., 1992). During this phase, pyramidal neuron precursors within the intermediate zone transiently assume a characteristic ''multipolar'' morphology, detach from the radial glial scaffold, and initiate axonal outgrowth (Barnes et al., 2008) prior to entering the cortical plate (Noctor et al., 2004);(Tabata and Nakajima, 2003). Recently studies have demonstrated that dynamic regulation of *Foxg1* activity is required during the postmitotic period, when pyramidal neurons transit through their multipolar phase of development (Miyoshi and Fishell, 2012). This multipolar cell transition phase is critical for the migration of cells through the intermediate zone and their integration into appropriate cortical layers. In utero electroporation experiments show that a down regulation of *Foxg1* occurs precisely at the beginning of the multipolar cell phase at a time coincident with when NeuroD1 expression is initiated, "early phase" (Figure I.13 A).

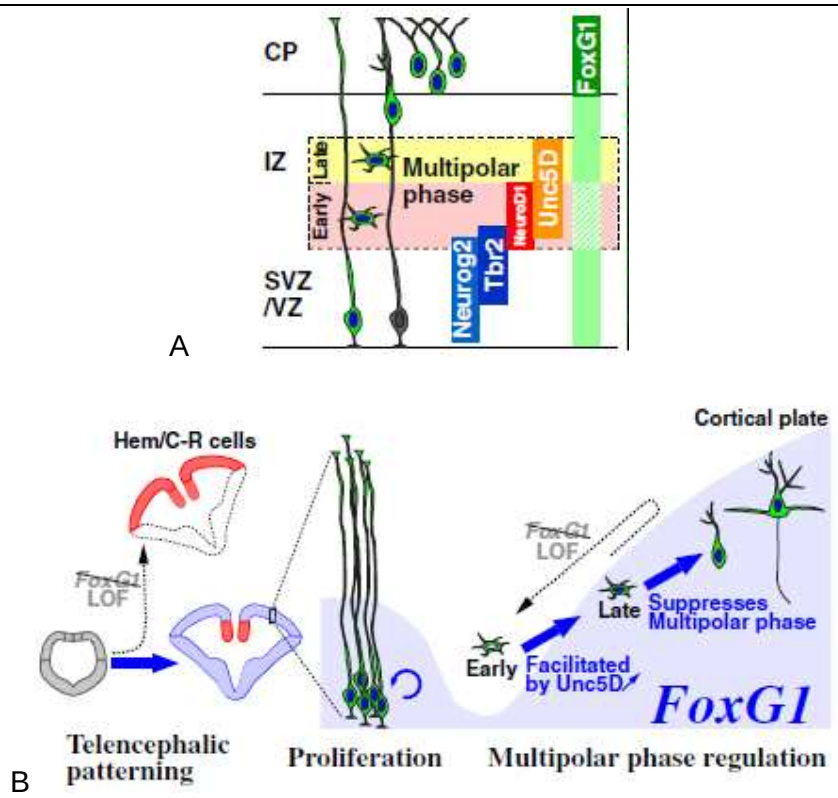

Figure I.13 Dynamic *FoxG1* expression during the postmitotic multipolar cell phase coordinates pyramidal neuron development. A) *FoxG1* expression is dynamically regulated throughout pyramidal neuron development. **B)** Model diagram summarizing the roles of *FoxG1* during pyramidal neuron development. *FoxG1* expression and function (arrows) are indicated in blue. Adapted from (Miyoshi and Fishell, 2012).

FoxG1 seems to regulate Unc5D, which is crucial for the rapid transition from the early to late phase. Deficiency to down regulate *Foxg1* delays cells from entering the cortical plate and results in a superficial shift with location and marker profiles indicating a shift in their laminar identity. On the other hand, failure to re-express *FoxG1* at this late phase results in a regression of pyramidal neuron precursors into the early multipolar phase and permanently prevents them from entering the cortical plate (Figure I.13B). Hence *FoxG1* has iterative roles during pyramidal neuron development in patterning, proliferation and postmitotic regulation of the multipolar cell phase.

1.9 *Foxg1* controls cell proliferation and neuronal differentiation

Neural precursors proliferate and differentiate to assure the intact population of neurons and glial cells in the cortex at the end of the embryonic life. Cell cycle progression plays a major role in this complicated process which is responsible for the final outputs of all cell types. It has been shown that both the length of cell cycle and the fraction of cells exiting from cell cycle (Q) increase during the neurogenesis process. Particularly, prolonged G1 phase is accountable for the lengthening of cell cycle (Takahashi et al., 1995) and the increase of Q is due to a shift of progenitors from self-renewing state to a more differentiated state. As the G1 phase length increases, the cell division switch from the symmetrical self-renewal pattern to the asymmetrical neurogenic differentiated one and finally to asymmetrical, fully differentiative one (Calegari and Huttner, 2003);(Götz and Huttner, 2005). Therefore, the G1 to S phase transition seems to be crucial for proliferative and differentiative fate choices. Cdk-cyclin complex inhibitors of the Kip/Cip family (p21Cip1, p27Kip1, p57Kip2) and Ink4 (p16Ink4, p15Ink4, p19Ink4, p18Ink4) could exert major roles in the balance between the two processes. p21Cip1 knockout leads to exhaustion of proliferative pools in embryonic cortical progenitor in vitro culture (Kippin et al., 2005) (Figure I.14).

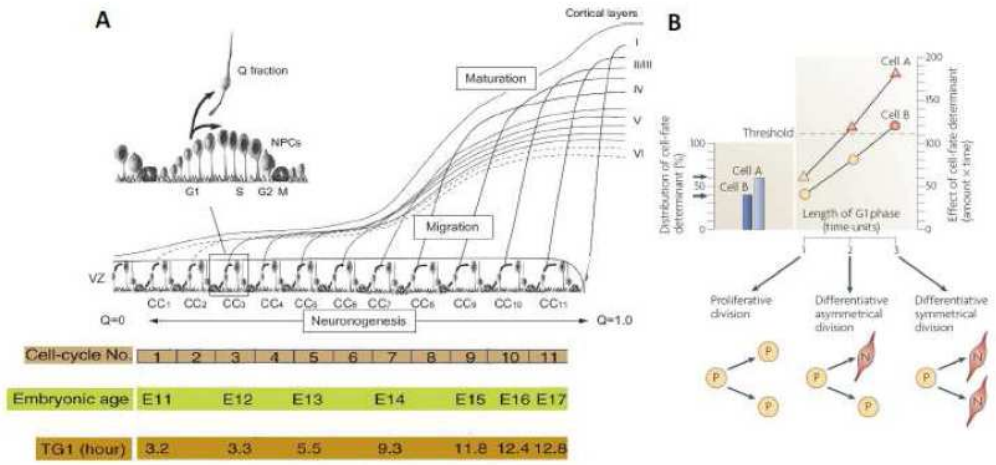

Figure I.14 Cell cycle and division pattern control in cortical histogenesis. (A) During the neurogenic period (E11-E17) the velocity of the cell cycle is not constant, there is an

increase of time of G1 phase (TG1). At the same time, the fraction of cell leaving cell cycle (Q) increases from 0 to almost 1. Modified from (Caviness et al., 2009); (Mitsuhashi and Takahashi, 2009).

Studies demonstrated that *Foxg1* null mutation leads to a marked reduction in the size of the cerebral hemispheres. The growth of the ventral telencephalon is more severely affected that of dorsal telencephalon. Moreover, it is present a reduction in the proliferation rate of the dorsal and ventral telencephalic neuroepithelium as well as alterations in the timing of neuronal differentiation in the cerebral cortical neuroepithelium. In particular, *Foxg1* reduces the progenitor-pool by premature cell-cycle exit and neuronal differentiation (Xuan et al., 1995), especially towards layer 1 neurons (Hanashima et al., 2004). Reduction of *Foxg1* by short hairpin RNA (shRNA) in cultured cortical progenitors resets the timing of cortical neurogenesis (Shen et al., 2006). At the molecular level, it is well established that *Foxg1* acts as a transcriptional repressor. It interacts with different gene including cell-cycle inhibitors, such as p27Xic in *Xenopus* (Hardcastle and Papalopulu, 2000) and p21Cip in mouse (Seoane et al., 2004). For example, *Foxg1* haploinsufficiency reduces the population of cortical intermediate progenitor cells by an increased expression of p21 (Siegenthaler et al., 2008). In addition, overexpression of Bmi-1, a cell cycle inhibitor, enhances the proliferation and self-renewal of neural progenitor cells (NPCs) including NSCs. This overexpression is accompanied by an early and sustained increase in *Foxg1* (Fasano et al., 2009). In fact, experiment of *Foxg1*-overexpression in neuronal stem cell compartment, give rise an enduring enlargement of this compartment, possibly due to increased NSCs self-renewal, promote progenitor survival and delay neurogenesis. Therefore *Foxg1* promotes the enlargement of NSC compartment and at the same time, reduces gliogenic commitment of NSC with a dramatically impaired progression of early born glial progenitors (GPs) toward more mature glial profiles (Brancaccio et al., 2010).

In Drosophila it is reported that *Foxg1* orthologs, Sloppy paired-1 and -2 (Slp1 and Slp2), promote neuronogenesis at expenses of gliogenesis (Bhat

et al., 2000) and *Foxg1* rescues the Slp1&2 null phenotype (Mondal et al., 2007).The precise mechanism is still unclear, it might be a correlation with Hes1, a key promoter of NSC self-renewal. Transient misexpression of basic helix-loop-helix (bHLH) genes *Hes1* or *Hes5* in the embryonic brain inhibits both neurogenesis and gliogenesis. These genes seem to have an important role in the maintenance of neural stem cells (Ohtsuka et al., 2001). *Foxg1* GOF might originate from unbalanced expression in the key gliogenesis promoters Coup-tf1, Nf1a, and Olig2 (Naka et al., 2008); (Ono et al., 2008). NP-restricted *Foxg1* overexpression elicited a progressively more prominent enlargement of this compartment probably due to a reduction of cell death, a doubling expansion rate and a decrease of neuronal differentiation. When *Foxg1* is overexpressed under the control of the neuronal lineage-specific Tubulin alpha 1 promoter (pTα1) NPs are forced to keep proliferating and newborn neuron maturation is dramatically impaired. In contrast, if the transgene is shut down, NPs exit cell cycle and massively differentiate as neurons (Brancaccio et al., 2010). Hence *FoxG1* overexpression in neuronal cultures, determines an increase of neurite growth and imbalanced ratio between neurons and glial cells (increasing neurogenesis and reducing gliogenesis).

1.10 West Syndrome (WS)

In 1841, Dr W. J. West first described a peculiar type of convulsion in his own four month old son. The infant exhibited significant mental retardation and died at 20 years of age; an autopsy revealed no cause of death (Lux, 2001).

Now WS is recognized as an epileptic syndrome in infancy, which is characterized by brief tonic spasms, a peculiar set of electroencephalographic findings termed hypsarrhythmia, and arrest of psychomotor development (ILAE Task Force, 1989). It is the most common epileptic syndrome causing neurological impairment in childhood around 2,500-3,000 children. In some case, this syndrome exhibits a normal development (Riikonen, 2001), indicating that developmental arrest is not obligatory for the diagnosis of WS.

Epidemiology

West Syndrome constitutes 2% of childhood epilepsies but 25% of epilepsy with onset in the first year of life. The incidence is about 1 per 2000 to 4000 live births (Hrachovy and Frost, 1989). Males are affected by WS slightly more often than females (60:40). 90% of patients begin in infants younger than 12 months. Peak onset is at age 4-6 months (Zupanc, 2003).

Clinical manifestations

In nine out of 10 children, infantile spasms occur in the first year of life, typically between three and eight months old. To begin with, the attacks are usually brief and infrequent and do not occur in clusters. The first diagnosis is often colic because of the pattern of the attacks and the cry that a child gives during or after an attack.

The typical pattern is of a sudden flexion (bending forward) in a tonic (stiffening) fashion of the body, arms and legs. Sometimes, the episodes are different, with the arms and legs being flung outwards (these are called 'extensor' spasms).

Typically, each episode lasts just one or two seconds, there is then a pause for a few seconds followed by a further spasm. While single spasms may happen, infantile spasms usually happen in 'runs' or 'clusters' of several in a row. It is common for babies who have infantile spasms to become irritable and for their development to slow up or even to go backwards until the spasms are controlled. These infants can also behave as if they cannot see.

The type of spasms, whether in flexion, extension, or mixed does not seem to be affected by etiology. In contrast, whether the spasms are symmetrical or not is important because asymmetry contributes to indicate some kind of cortical brain damage (Vigevano et al., 1993). Asymmetrical spasms consist of lateral deviation of the head or eyes.

The diagnosis of infantile spasms is made by a combination of the typical features with a typical EEG. The EEG shows a much disorganized pattern called 'hypsarrhythmia', with a continuous, irregular, random, ever-changing, high-voltage spike and slow wave activity (Figure I.15). It may be present during wakefulness and non-REM sleep or may be present only

during sleep (Watanabe et al., 1993). During deep sleep, it may be discontinuous (Blume and Dreyfus-Brisac, 1982).

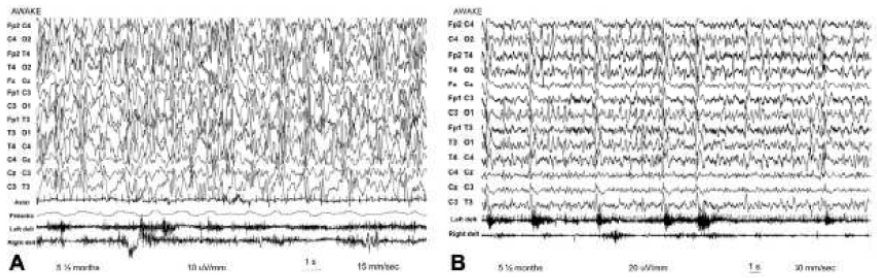

Figure I.15 EEG recorded from a West syndrome patient. (A) EEG and polygraphic recordings during wakefulness: slow waves of large amplitude mixed with almost continuous, independent and multifocal, high amplitude spikes, with a slight tendency to become synchronous, configuring a modified hypsarrhythmia. **(B)** clusters of asymmetrical epileptic spasms. Adapted from (Bertossi et al., 2014).

The psychomotor impairment, mental retardation signs and symptoms are very difficult to evaluate at early age such as WS infants. The most common features are:

- loss of hand grasping and simple muscular movements
- axial hypotonia and dysphonia
- no visual attention and abnormal ocular movement
- no social response

Among these symptoms, loss of eye contact has a negative prognostic significance.

Etiology

WS is due to many etiological factors including hereditary and non-hereditary conditions, such as neonatal asphyxia, meningoencephalitis, cerebral dysgenesis, and congenital metabolic disorders. This syndrome is now classified into two groups: symptomatic and cryptogenic. The symptomatic group is characterized by the previous existence of signs of brain damage (psychomotor retardation, neurological signs, radiological signs, or other types of seizures) or by a known etiology (ILAE Task Force, 1989).

The cryptogenic group is characterized by lack of previous signs of brain damage and of known etiology (Matsumoto et al., 1981); (Vigevano et al., 1993). On the other hand, an idiopathic group has been proposed, and WS in patients in this group is presumed to have resulted from an age-related multifactorial genetic predisposition (ILAE Task Force, 1992). Familial recurrence of WS without known etiology has been reported with uneven distribution to males indicating X-linked inheritance (Feinberg and Leahy, 1977);(Dulac et al., 1993); (Sugai et al., 2001). In particular, it has been found mutations of two genes, ARX and CDKL5, in patients with X-linked familial WS (Strømme et al., 2002); (Weaving et al., 2004). A polyalanine expansion mutation of the ARX gene has also been found in a patient with sporadic cryptogenic WS (Kato and Dobyns, 2003). Male mice deficient in ARX have abnormal differentiation and deficient non-radial or tangential migration of GABAergic (γ-aminobutyric acid) interneurons in the ganglionic eminence, neocortex, and hippocampus (Kitamura et al., 2002). Instead, the phenotype of CDKL5 mutation is similar to Rett syndrome caused by MECP2 mutation, but the former is characterized by early-onset seizures and association with WS (Weaving et al., 2004); (Evans et al., 2005). In addition, lissencephaly caused by LIS1 or DCX mutation frequently results in WS (Guerrini, 2005). Both LIS1 and DCX participate in the development of GABAergic interneurons as well as pyramidal neurons.

1.11 Relationship between WS and FOXG1

Recently, it has been reported that a number of microduplications of chromosome 14q12 sharing the *FOXG1* locus are associated with developmental delay, delayed/absent speech, and infantile epilepsies (Bertossi et al., 2014);(Pontrelli et al., 2014). In particular, in 14dup(14) patients, the size of duplication varied from 88Kb to 84Mb and 9/14 patients developed seizures in the first month of life. Moreover, most of them (8/9) presented infantile spasms and hypsarrhythmia EEG patterns (Bertossi et al., 2014). Taking in consideration this observation and the fact that *FOXG1* has a key role in brain morphogenesis leads to the new hypothesis that duplication of *FOXG1* might very likely cause of WS phenotype. However, some

individuals with 14q12 duplication including *FOXG1*, report anormal phenotype, intellect and no apparent evidence of epilepsy (Shaikh et al., 2009);(Amor et al., 2012). It is commonly accepted that these phenotypic variabilities might be explained by an incomplete penetrance of *FOXG1* duplication, the variable involvement of its regulatory elements, other genes in the duplicated region and genetic mosaicism (Brunetti-Pierri et al., 2011); (Tohyama et al., 2011); (Falace et al., 2013). Moreover, it has been found that *Foxg1* overexpression in neuronal cultures, promotes the neurite growth with an imbalanced ratio between neurons and glial cells (Brancaccio et al., 2010). Increasing neurite growth (including axons and dendrites) may determine the hyperexcitabilities of the cortex, by enlarging the afferent (and efferent) basin of neurons and therefore favoring the spreading of excitatory waves through cortical neural networks. Besides, lowering the astrocytes/neurons ratio could also exacerbate neuronal hyperactivity, due to defective neurotransmitter and potassium clearance upon neuronal firing. These phenomena may substantially contribute to abnormal electrical activities within the brain (hypsarrhythmia) and therefore strengthen the putative role of *FOXG1* in WS.

1.12 Glia from NSCs in the Developing Brain

The classical model of cell generation in the CNS, proposes that astrocytes are mainly generated after neurons and before oligodendrocytes (Figure I.16).

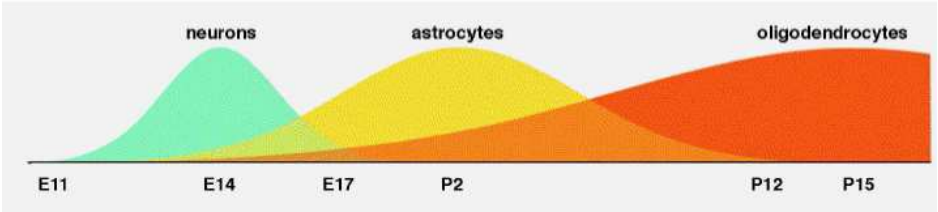

Figure I.16 Murine cortico-cerebral histogenesis.

For long time, glial cells and neurons were considered to take their origin from separated precursor pools diverging early during development. Conversely, the process is more complicate and elaborate than previously

thought. Even if committed progenitors may emerge very early, recent studies in the developing brain have given evidence of the fact that one single population called *radial glia* (RG) operate as primary precursor pool, which is now considered as *neural stem cells population* (NSCs). Moreover, NSCs give rise to transit amplifying *intermediate progenitors* (IPCs) before generating one of the extraordinary different specific neural subtypes (Figure I.17).These intermediate progenitors are lineage restricted and coexist not only in the embryo but also in some germinal regions in the adult (Kriegstein and Alvarez-Buylla, 2009).

Like neuroepithelial cells, RG cell bodies form a pseudostratified epithelial layer lining the ventricle, the ventricular zone (VZ), and while their radial processes span from the ventricular to the pial surfaces, their nuclei oscillate within the VZ in synchrony with the cell cycle in a movement known as interkinetic nuclear migration (INM). In detail, nuclei going through S-phase, place themselves in a layer quite distant from the ventricle, while nuclei in M phase, line up along the surface of the ventricle, and finally nuclei in G1 and G2 phases pass through the mid region of M and S phases (Sauer FC., 1935).The self-renewed RG cell inherits the basal process, and the daughter progenitor cell, referred to as an IPCs, generally migrates to the subventricularzone (SVZ) and divides symmetrically to produce a pair of neurons (Noctor et al., 2004). Intermediate progenitors differ from RG: they are not coupled by adherens or gap-junctions, and they lack the radial polarity of RG.

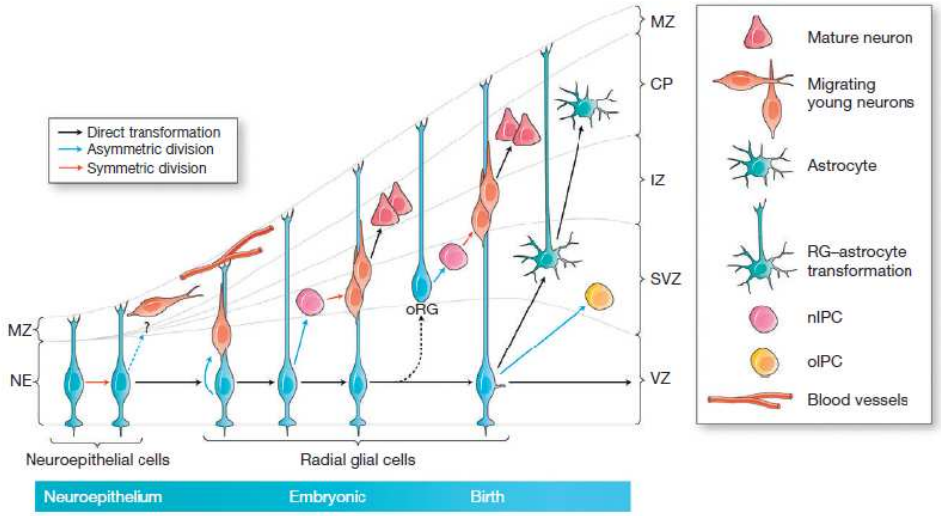

Figure I.17 Summarizing cartoon about neurogenesis during cortical development. Adapted from Kriegstein and Alvarez-Buylla, 2009.

Within the developing neocortex, Notch signaling maintains RG cell identity and self-renewal (Gaiano et al., 2000);(John Rubstenstein and Pasko Rakic, 2013).

Around E11 early radial glial cells within dorsal telencephalon proceed to generate *neuronal intermediate progenitors* (nIPCs) which in turn will originate the almost totality of cortico cerebral *glutamatergic* neurons. The second output of *dorsal* telencephalic RG cells is represented by astrocytes, which are generated to a large extent after neuronogenesis completion, by differentiation of RG cells via committed progenitors. In this respect, some astrocytes, still locally dividing before terminal differentiation are often referred to as aIPCs. Although there is a peak in the production of astrocytes just after birth and a global fading of this phenomenon around the end of the second week of postnatal life, the process of astrocytic amplification may happen also in the postnatal murine cortex (Hajós et al., 1981);(Ichikawa et al., 1983).The situation is more complex for cortico-cerebral oligodendrocytes, as their progenitors (oIPCs) are born in different telencephalic regions. Finally, late radial glial cells (lRG) get largely converted into ependymal cells (Figure I.18).

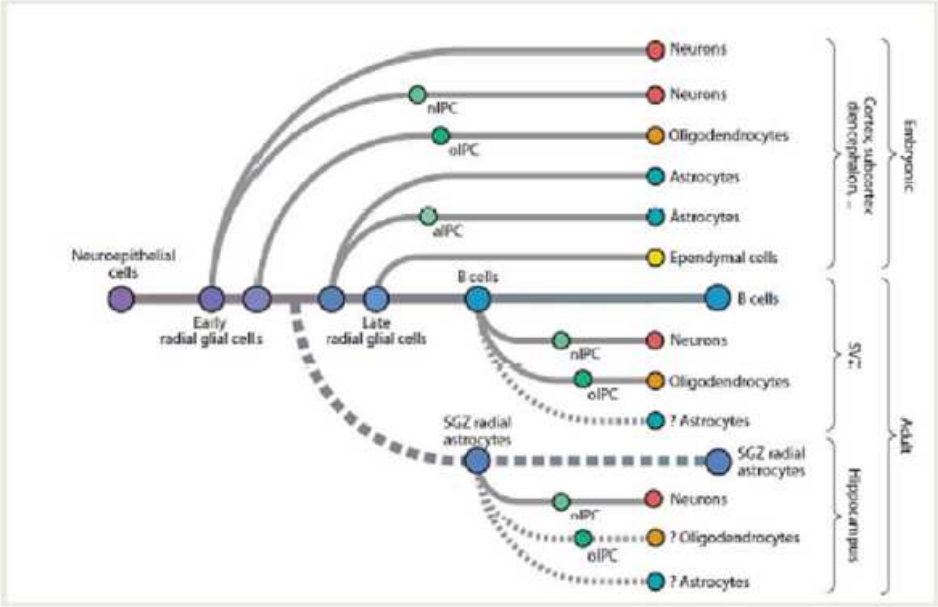

Figure I.18 Different cell lineages originating from neuroepithelial cells in the developing CNS . Adapted from Kriegstein and Alvarez-Buylla, 2009.

1.13 The astrocytogenic lineage

As already mentioned above, astroglial cells are derived from a population of progenitor cells (NSC) in the neuroepithelium of the developing central nervous system. In mammals, most RG cells become astrocytes. This is also strongly suggested by the fact that disappearance of RG coincides with the appearance of an increasing population of astrocytes. Also, RG and astrocytes share the expression of the same markers (such as RC1) (Mission et al., 1991). RG cells undergo some structural changes that switch their morphology from bipolar to an unipolar, typical of astroglial cell. Again, the production of astrocytes, can be also facilitated by a local division before terminal differentiation, which involves of course a transit amplifying subpopulation of intermediate precursors, called aIPC. Anyway, the situation remain extremely intricate and still entirely clear.

One more controversial point concerning astrocytes development is whether astrocytes are spatially restricted to specific locations depending on their site of origin or they migrate widely to their final position.

The basic assumption is that, just as with neuronal cell specification, canonical signaling factors like Sonic Hedgehog (SHH), Fibroblast growth factor (FGFs), WNTs and bone morphogenetic proteins (BMPs), provide positional information to developing macroglial cells through morphogen gradients along the dorsal–ventral, anterior–posterior and medial–lateral axes.

Finally, astrocytes take cortical positions reflecting the inside-out pattern of cortical neurons: later-born glia take superficial positions (Ichikawa et al., 1983). According to in vitro studies some markers define evolving population from NSC to astrocytes. The first one is the nestin-neural enhancer, which is expressed in NSCs and in part of glia-restricted progenitors (GRP, or IPCs). Cd44 is an even more specific marker which has been found in astrocytes restricted progenitors. Finally S100b and GFAP are the most common markers found in mature astrocytes.

1.14 Molecular mechanisms controlling astrocytogenesis

Several molecular mechanisms are at play in what turns out to be an exquisite control of astrocytogenesis. Exhaustive studies of transcriptional regulation of a selection of astroglial markers, including GFAP and S100b, have deepened the global knowledge of the system. There are at least four independent primary pathways trans-modulating astrocytic promoters (GFAP, S100b), but numerous modulatory controls can also impinge on these ones. Also, other pathways control the epigenetic state of astrocytic promoters.

Jak/STAT pathway

The main signaling pathway that promotes astrocyte differentiation is the the Jak/STAT pathway (Figure I.19). It regulates astrogenesis by promoting the expression of key astrocyte genes such as GFAP and S100B. The astrogenic cytokine Cardiotrophin 1 (Ct1) binds to its co-receptor ciliar neurotrophic factor receptor a (CntfRa) and activates Jak receptor, which is composed of two transmembrane chains: glycoprotein 130 (gp130) and Lif-receptor b (LifRb). Upon receptor activation, phosphorylation and acetylation activate the signal transducer and activator of transcription STAT3. STAT3 dimerizes and translocates to the nucleus to activate gene transcription. The

transcription factor STAT3 binds to its binding site at the promoter of the astrocyte genes GFAP and S100B. The activation of astrocytic gene expression initiates astrocyte differentiation. On the other hand, during neurogenesis, several mechanisms inhibit STAT3 activity and in turn astrocytic JAK/STAT signaling to prevent astrogenesis.

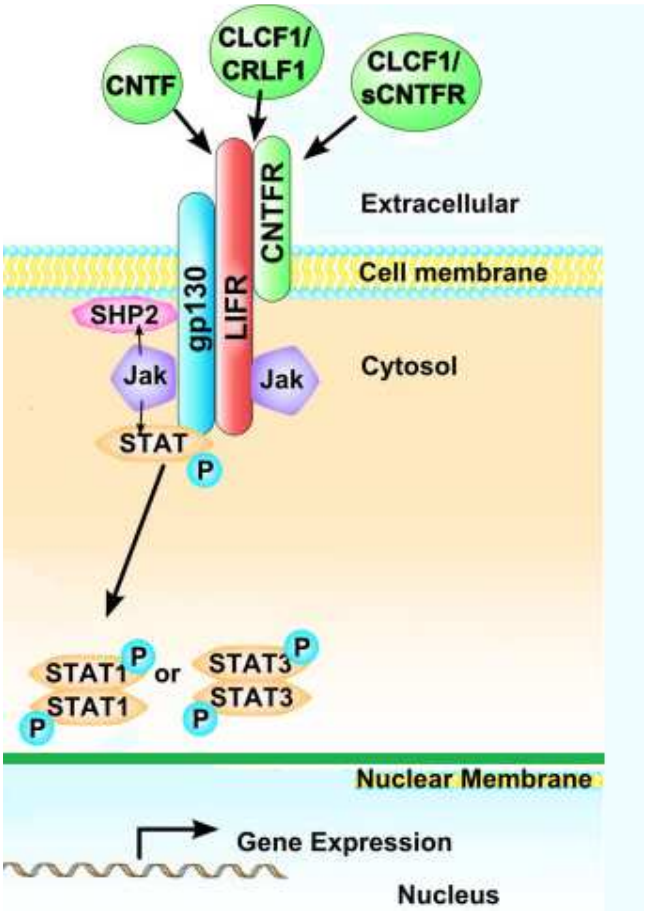

Figure I.19 JAK-STAT pathway. Adapted from (Mikelonis et al., 2014).

Notch signaling

Notch signaling is a key regulator of the NSC fate. During the neurogenic phase, Notch is critical to maintain the NSC pool by repressing neurogenesis through its downstream targets hairy enhancer of split (Hes),

Hes1 and Hes5 (Kopan and Ilagan, 2009). Newly born neurons express Notch ligands such as Jagged 1 and Delta-like 1 and by doing so they activate Notch signaling in those same NSCs (Namihira et al., 2009). Moreover, Notch activation is both necessary and sufficient to push NSCs to astrocyte fate. Thus Notch signaling is a master regulator of astrogenesis. However, little is known on how the Notch response switches from being self-renewing to astrogenic during the course of development (Figure I.20). The canonical signaling pathway is activated by the Notch ligands Jagged and Delta-like proteins. Upon ligand binding, Notch is cleaved by the γ-secretase complex and Notch intracellular domain (ICD) is released and translocates into the nucleus. In the nucleus the transcription of Notch target genes is regulated by DNA binding proteins. As for astrogenesis, Notch signaling induces epigenetic remodeling of the GFAP promoter and, in turn, its expression.

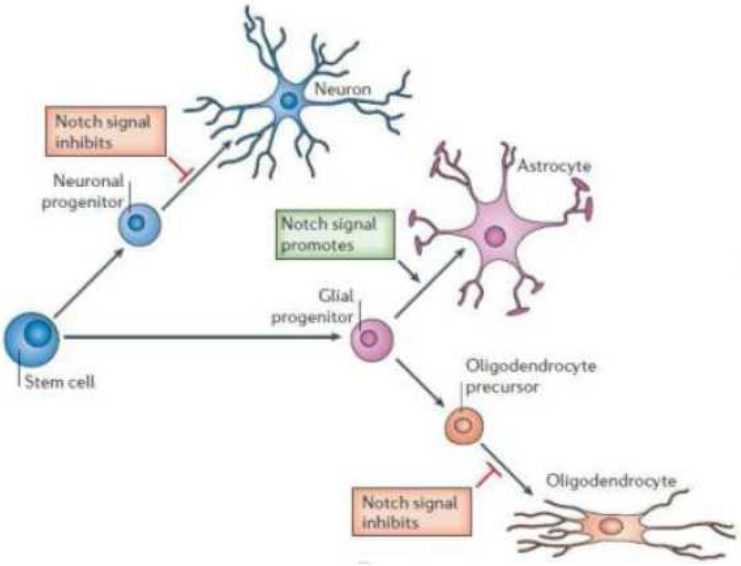

Figure I.20 Notch signaling plays many roles in cell differentiation process. Adapted from (Louvi and Artavanis-Tsakonas, 2006).

PACAP/Dream pathway

Calcium signaling is also involved in the stimulation of astrogenesis. Mainly, the cAMP-dependent pituitary adenylatecyclase-activating polypeptide (PACAP) activates intracellular cAMP and so provoking the entry of calcium in

NSCs. Being a potent intracellular messenger, calcium activates the transcription factor downstream regulatory element antagonist modulator also known as DREAM. Activated DREAM binds to responsive elements in the GFAP promoter and stimulates transcription. The PACAP-DREAM and the Jak/STAT pathway act in synergy, relying on the transcription factor NF1A, a downstream factor of Notch signaling (Figure I.21). In other words, calcium signaling and growth factor- regulated pathways cooperate to activate astrogenesis. Interestingly, the Pacap pathway seems to act independently of Jak-Stat3.

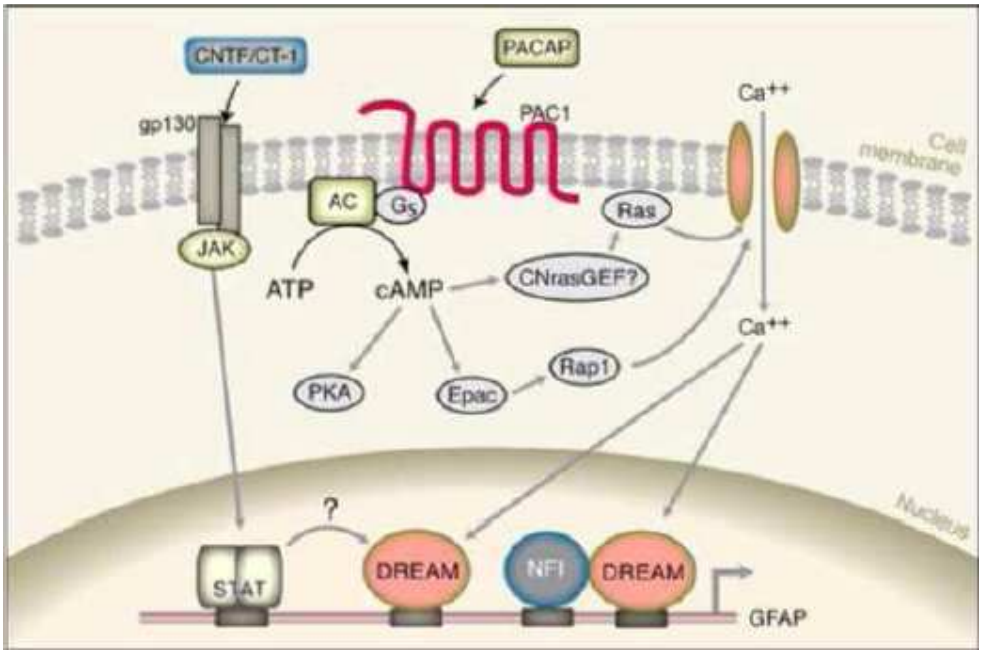

Figure I.21 PACAP/DREAM pathway and JAK/STAT pathway interact in synergy. Adapted from (Vallejo, 2009).

Nrg1/ErbB4 pathway

A major role in setting up the proper onset of astrogenesis is played by the ligand Neurogulin 1 (Nrg1), expressed by neurons and neural precursors, and its ErbB4 receptor, transducing its signal whitin cortico-cerebral precursors. ErbB4 is a plasma membrane tyrosine kinase receptor of the EGF

receptor family that forms are pressor complex with NcoR. Following receptor activation, the intracellular domain of the ErbB4 receptor, translocates into the nucleus, together with NcoR and TAB2, and inactivates GFAP expression (Sardi et al., 2006)(Figure I.22). This pathway is crucial to prevent premature astrogenesis in vivo.

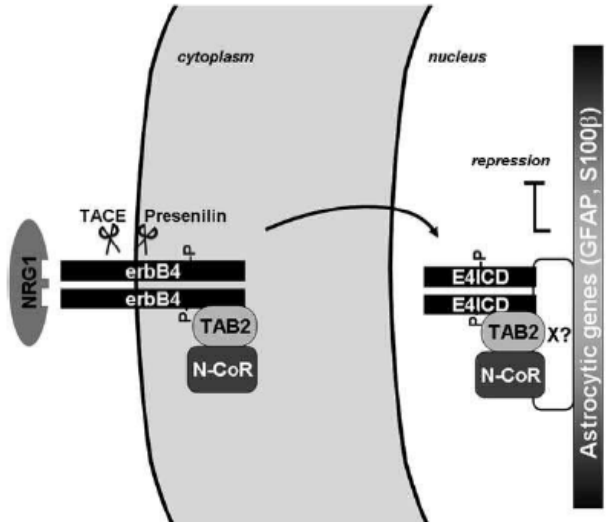

Figure I.22 Nrg1/ErbB4 signaling. Adapted from (Sardi et al., 2006).

1.15 Astrocytes

Astrocytes (“Astro” from Greek “astron” = star and “cyte” from Greek "kyttaron" =cell) are the most numerous cells in the mammalian brain and play many more roles in neural function than had previously been appreciated. Detailed morphological studies revealed the first broad category of astrocyte heterogeneity based on location in the white versus gray matter. Fibrous astrocytes populate the white matter show typically regular contours and cylindrical processes, yielding the more classic ‘star-like’ appearance, and they have dense glial filaments that stain with the intermediate filament marker GFAP. When they are in close proximity to capillaries they physically connect to capillary walls with their prolongations known as "vascular feet".

Protoplasmic astrocytes are found in the gray matter and have more irregular processes, and typically express few glial filaments (Bignami et al., 1972);(Vaughn and Pease, 1967)(Vaughn and Peters, 1967) (Figure I.23).

In addition, there are two types of specialized ‘radial’ astroglia recognized in the CNS. Bergman glia are found in the cerebellum; their cell bodies are in the purkinje cell layer and they extend processes into the granule cell layer that terminates at the pial surface (Hoogland et al., 2009). Muller cells are the primary glial cell in the retina and are oriented radially, spanning the photoreceptor layer to the inner retinal surface (Metea and Newman, 2006). Both these cell types are morphologically reminiscent of the radial glia cells present during development; in fact, Bergmann glia serve an analogous function in helping to guide migrating granule cell precursors .

However, in the adult CNS, these glia are functionally thought to resemble protoplasmic astrocytes in that they associate with and enwrap synapses, and may act to modulate synaptic function (Reichenbach et al., 2010).

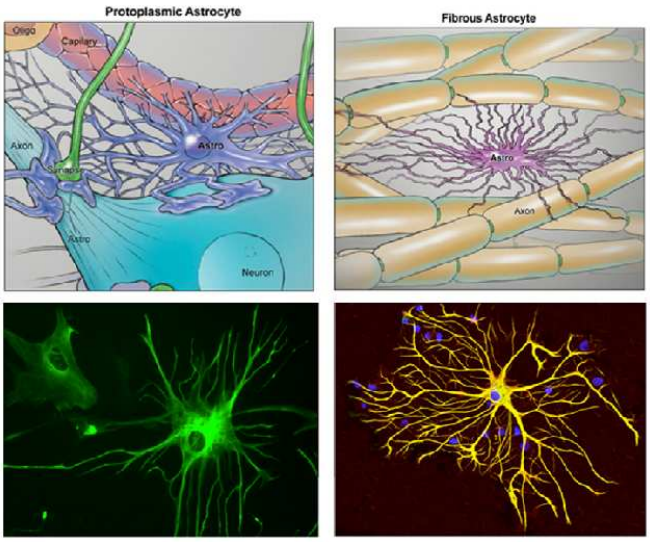

Figure I.23 Protoplasmic and fibrous astrocytes.

Astrocytes influence multiple aspects of synaptic transmission by maintaining extracellular homeostasis, including recycling neurotransmitters and modulating extracellular potassium concentrations (Parpura and Haydon,

2008). As a result, astrocytes are critical to promoting neuronal survival in the context of neuroinflammation (Saijo et al., 2009) and hypoxia (Vangeison and Rempe, 2009), among others. More recently, many groups have proposed a more active role for astrocytes in synaptic transmission, arguing that astrocytes engage in information processing in parallel to and modulating neuronal information processing.

1.16 Astrocytes and Epilepsy

Historically epilepsy research has predominantly focused on dysfunction of neurons that either generate too much excitation or fail to provide enough inhibition. However, there is a substantial amount of evidence that implicate glial dysfunction as a major contributing factor to epileptogenesis. Epileptogenesis is characterized by abnormal and excessive neuronal firing, each seizure represents a rapid loss of homeostatic equilibrium, with altered energy and molecular gradients, and a corresponding interruption of normal behavior and consciousness.

The involvement of astrocytes in the pathogenesis of epilepsy is based on the discovery that astrocytes modulate synaptic transmission not only by the release of gliotransmitters such as glutamate, ATP and D-serine (Haydon and Carmignoto, 2006), but also by the reuptake of neurotransmitters such as glutamate (Coulter and Eid, 2012) or neuromodulators such as adenosine (Boison, 2012). Hence astrocytes regulate or modulate a number of neuronal functions including excitability, synaptic transmission, and plasticity.

Glia communicate with each other, are equally numerous compared to neurons in the human cerebral cortex, and assume a role that is upstream of neuronal function. Perturbations of glial function can affect entire neuronal networks (Herculano-Houzel, 2011).

Here below find the most important functions of astrocytes and their critical role in pathogenesis of neurological disorders such as epilepsy.

Glutamate-glutamine homeostasis

Excitatory amino acid transporters 1 (EAAT1) a.k.a. Glutamate Aspartate Transporter (GLAST) and excitatory amino acid transporters 2

(EAAT2) a.k.a. the Glial Glutamate Transporter 1 (GLT-1), are astroglial glutamate transporters that clear excess of glutamate from synapses. In particular, EAAT1 is present exclusively on astrocytes (Lehre et al., 1995), EAAT2 is mainly present on astrocytes but can also be found at low levels in neurons (Furness et al., 2008).

It is estimated that astrocytic glutamate transporters accomplish more than 80% of the extracellular clearance of glutamate (Anderson and Swanson, 2000). Glutamate homeostasis in the brain depends on a glutamate-glutamine cycle in which astrocytes convert the transported glutamate into glutamine via glutamine synthetase. Glutamine is transported back into neurons, where it is transformed into glutamate or GABA (Shigeri et al., 2004);(Pow and Robinson, 1994) (Figure I.24).

Increased levels of synaptic glutamate may in part be attributed to reduced expression of glutamate transporters on the astrocytes membrane or reduced glutamine synthetase. Glutamate accumulation produces, as a final effect, neuronal hyperexcitability and decrease seizure threshold.

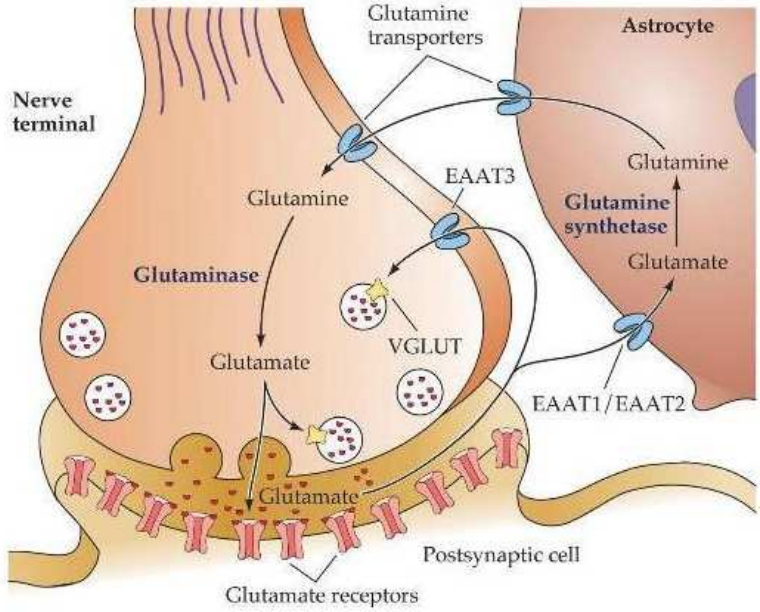

Figure I.24 Glutamate and glutamine cycle between neurons and astrocytes. From website *StudyBlue.*

Release of Glutamate

Astrocytes signal to neurons by releasing a number of gliotransmitters that can have both excitatory and inhibitory actions. In rodents this gliotransmitter release is stimulated by neuronal activity-dependent elevation of intracellular Ca^{2+} (Halassa et al., 2009);(Petzold et al., 2008) and may occur through Ca^{2+} dependent exocytosis (Bezzi et al., 2004); (Chen et al., 2005). In normal brain Ca^{2+} elevations in astrocytes are mediated mainly by metabotropic receptors. The metabotropic glutamate receptor (mGluR) family consists of eight members, which couple to G-proteins. mGluR3 and mGluR5 are the predominant subtypes expressed by astrocytes and have been described in cultured cells and *in situ* (D'Antoni et al., 2008); these subtypes are also found in human hippocampal astrocytes. Activation of these receptors affects cAMP accumulation and leads to increase in intracellular Ca^{2+}. The $[Ca^{2+}]$ may oscillate and initiate Ca^{2+} wave propagation within the astrocyte network, activate Ca^{2+}-dependent K^+ channels, and induce glutamate release from astrocytes that activates neuronal receptors (Bezzi et al., 1998). Activation of mGluRs induced other astrocyte responses, including swelling, activation of phospholipase D and glutamine synthetase, release of arachidonic acid, cAMP-dependent block of K^+ currents, modulation of proliferation, and regulation of the expression of the glutamate transporter GLAST. Hence changes in mGluR expression influence the neuronal excitability, in particular an upregulation is observed in many pathological diseases such as epilepsy. This might indicate an astroglial involvement in seizure generation or spread (Seifert and Steinhäuser, 2013); (Seifert et al., 2006); (Aronica et al., 2003).

K + Homeostasis

Increased extracellular K^+ concentration $[K^+]_o$ is known to be associated with seizures in epilepsy. In addition, high $[K^+]_o$ can directly generate epileptiform activity *in vitro*.

Kir channels are abundantly expressed by astrocytes and represent a prerequisite for the regulation of the K^+ homeostasis (Orkand et al., 1966). Among the Kir subunits identified in the CNS, Kir4.1 is selective expresses in glia where it is mainly localized to astroglial processes wrapping synapses

and blood vessels. The significance of Kir4.1 for spatial buffering and control of excitability has been confirmed through general (Kofuji et al., 2000) or conditional knockout of Kir4.1 (Chever et al., 2010). Genetic downregulation of Kir4.1 profoundly reduced the ability of astrocytes to remove glutamate and K^+ from the extracellular space, both in cell culture (Kucheryavykh et al., 2007) and in vivo (Djukic et al., 2007). In addition to spatial buffering, transient K^+ accumulations can be counterbalanced by net K^+ uptake through Na,K-ATPase and the Na-K-Cl cotransporter (NKCC1), at the cost of cell swelling due to concomitant water influx (Kofuji and Newman, 2004). In rodent hippocampus, the Na-K-ATPase was reported to have a potential role in maintaining the low $[K^+]_o$ level and to clear elevations in $[K^+]_o$ after epileptiform activity (D'Ambrosio et al., 2002); (Xiong and Stringer, 2000).

Ultrastractural analyses in rat demonstrated a spatial overlap of Kir4.1 and the water channel acquaporin 4 (AQP4) (Nielsen et al., 1997). This finding gave rise to the hypothesis that K^+ clearance through Kir channel might be critically dependent on concomitant transmembrane flux of water to dissipate osmotic imbalances due to K^+ redistribution. During normal periods of neuronal activity, much of the potassium released into extracellular space (ECS) by spiking neurons is taken up by astrocytes and neurons. The notion is that normally potassium uptake is accompanied by water influx via AQP4 into astrocytes in the perisynaptic space and then excess water is dumped via AQP4 at perivascular endfeet (Figure I.25).

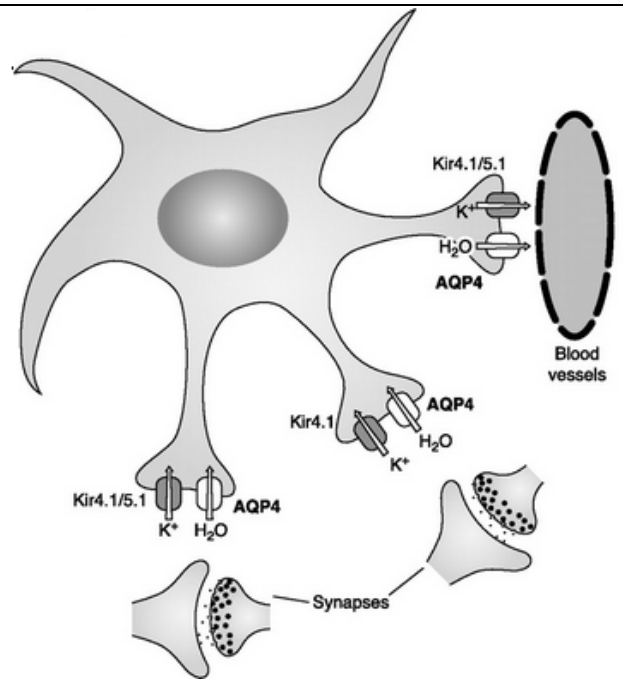

Figure I.25 Astrocytes membrane distribution of Kir4.1 and AQP4 at synapses and blood vessels. Adapted from (Hibino et al., 2010).

Gap junctions (GJ) and hemichannels (HC)

GJ are membrane specializations consisting of dense aggregates of large pore channels that extend from one cell into an adjacent cell and mediate direct cytoplasm-to-cytoplasm communication. They are formed by a family of proteins, called connexins (Cxs). These channels are poorly selective for ions and small molecular weight signaling molecules, and allow extensive ionic and biochemical exchanges between cells. In the mammalian brain, astrocytes express mainly Cx43, from embryonic stages to adulthood, and Cx30 from postnatal day 10 (Kunzelmann et al., 1999). Under certain conditions Cxs can also operate as hemichannel (HC), that represent another functional state providing a pathway suitable for autocrine as well as paracrine interactions. Membrane channels may also be formed by proteins called pannexins (Panxs) that have some properties that are similar to Cx HCs (Phelan and Starich, 2001). Three Panx isoforms (1-3) have been found in

mouse and human; Panx1 and Panx2 have been detected in the brain (MacVicar and Thompson, 2010) (Figure I.26).

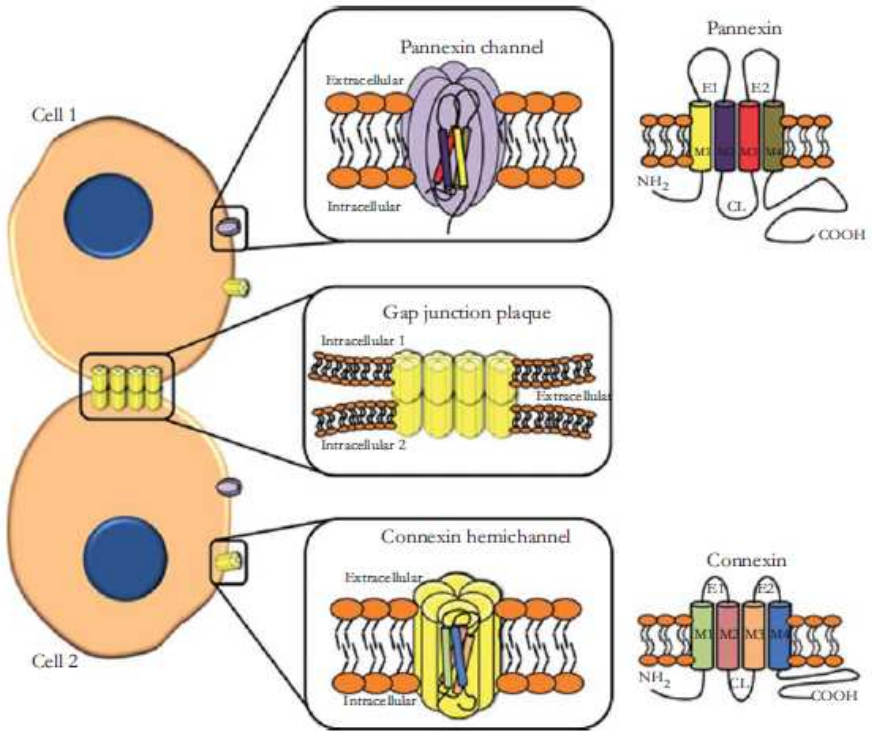

Figure I.26 ***Gap Junction and Hemichannel Molecular Organization.*** Each GJC is formed by two Cx HCs docked together and rotated 30° with respect to one another. Panx channel that do not form GJCs, and a Cx HC have four transmembrane domains (M1-4) with amino (NH2) and carboxy (COOH) termini on the cytoplasmic side, two extracellular loops (E1 and E2), and one cytoplasmic loop (CL). Modified from (Orellana and Stehberg, 2014).

Astrocytes coupled together by GJCs were initially assumed to form a nonspecific glial syncytium (Mugnaini E., 1986);(Theis et al., 2005), but recent evidence suggests they are organized in a more complex and restricted manner forming networks of communicating cells with rules governing their functional status and plasticity (Giaume and McCarthy, 1996); (Giaume, 2010). Glial Cx channels are regulated by a number of releasable bioactive molecules, and their expression is modified by brain pathologies (Giaume, 2010).

Ions clearly pass through GJCs, in this way they contribute to K^+ homeostasis during neuronal activity (Kuffler et al., 1966);(Wallraff et al., 2006), and assist in the intracellular homeostasis of Na^+ (Ye et al., 2003). Little is known about the expression and possible functions of unopposed gap junction hemichannels in the brain. Emerging evidence suggests that gap junction hemichannels can act as stand-alone functional channels in astrocytes. With immunocytochemistry, dye uptake, and HPLC measurements, we show that astrocytes in vitro express functional hemichannels that can mediate robust efflux of glutamate and aspartate. Functional hemichannels were confirmed by passage of extracellular lucifer yellow (LY) into astrocytes in nominal divalent cation-free solution (DCFS) and the ability to block this passage with gap junction blocking agents. Glutamate/aspartate release (or LY loading) in DCFS was blocked by multivalent cations (Ca^{2+}, $Ba^{2+,}$ $Sr^{2+,}$ $Mg^{2+,}$ and La^{3+}) and by gap junction blocking agents (carbenoxolone, octanol, heptanol, flufenamic acid, and 18alpha-glycyrrhetinic acid) with affinities close to those reported for blockade of gap junction intercellular communication. Glutamate efflux via hemichannels was also accompanied by greatly reduced glutamate uptake. Glutamate release in DCFS, however, was not significantly mediated by reversal of the glutamate transporter: release did not saturate and was not blocked by glutamate transporter blockers. Control experiments in DCFS precluded glutamate release by volume-sensitive anion channels, P2X7 purinergic receptor pores, or general purinergic receptor activation. Blocking intracellular Ca^{2+} mobilization by BAPTA-AM or thapsigargin did not inhibit glutamate release in DCFS. Divalent cation removal also induced glutamate release from intact CNS white matter (acutely isolated optic nerve) that was blocked by carbenoxolone, suggesting the existence of functional hemichannels in situ. Our results indicated that astrocyte hemichannels could influence CNS levels of extracellular glutamate with implications for normal and pathological brain function (Ye et al., 2003)(Rose and Ransom 1997). Neural activity generates transient increases in $[K^+]_o$ and the glia cells participate in moving extracellular K^+ from areas in which it accumulates secondary to neural activity, to distant areas in which the K^+ is not elevated (Orkand et al., 1966). Strong astrocytic coupling would extend the distance

over which this K^+ distribution system could operate and increase its efficiency (Mobbs et al., 1988). Thus released K^+ or glutamate can induce an activity-dependent plasticity of astrocytic networks (Roux et al., 2011). This plasticity might help preserve synapse independence and protect from excitotoxicity. Therefore, the increased Cx expression and/or GJ coupling reported in some human epileptic patients and animal models of epilepsy (Lee et al., 1995);(Collignon et al., 2006) may be interpreted as an adaptative change to clear-up the excess neuroactive substances released in the extracellular space, and thus may limit the development of aberrant bursting activity. In contrast, neuronal hyperactivity during epileptic state creates an enhanced metabolic demand, which can be substained, by nutrient supply through astroglia network (Rouach et al., 2008). In addition, intercellular Ca^{2+} waves in astroglial networks may also contribute to the generation of aberrant bursting by promoting neuronal synchronization through release of glutamate at extrasynaptic sites (Angulo et al., 2004);(Tian et al., 2005).

Unlike GJCs, HCs are directly exposed to extracellular ions and are gated by extracellular, as well as intracellular, ionic changes. Pannexins form hemichannels that mediate regulated exchange of second messenger molecules, such as adenosine triphosphate (ATP), between cytoplasm and the extracellular space. Cx43 hemichannels are also able to pass ATP molecules in response to phosphorylation, intracellular and extracellular calcium change and other stimuli (Kang et al., 2008);(Bao et al., 2012). Pannexin channels actively interact and are regulated by P2Y/P2X purinergic receptors. It is the major conduit for ATP release in response to a variety of physiological and pathological stimuli. Once ATP is released, it acts as potent transmitter triggering rises in Ca^{2+} in neighboring cells by activation of P2Y receptors, resulting in long-distance increases in Ca^{2+} (Goodenough and Paul, 2003).Normally, HCs are opened in absence of extracellular divalent cations (Ye et al., 2003).

Purinergic signaling in neuron and glia network

Purines are chemical substances that have been regarded as the major intracellular energy sources. Recently they are associated to heterotypic communication between neurons and astrocytes (Zhang et al., 2003) as well

as, to homotypic communication, among astrocytes (Guthrie et al., 1999). Purines play a preponderant role in stress situations and evidence suggest that astrocytes sense the severity of damage by the amount of ATP released from damaged cells (Fields and Burnstock, 2006).

The purine receptors are divided into P1 (metabotropic receptors, activated by adenosine: A1, A2A, A2B and A3) and P2 receptors (activated by different nucleotides such as ATP [adenosine 5'-triphosphate] or ADP [adenosine 5'-diphosphate]). P2 receptors are further subdivided into seven ionotropic P2X receptors (P2X1-7) and twelve metabotropic P2Y receptors (P2Y1, P2Y2, P2Y4, P2Y5, P2Y6, P2Y8, P2Y9, P2Y10-14). P1 and P2 effector responses are usually antagonistic and as such negatively regulate each other, resulting in a tightly regulated system (Figure I.27) (Burnstock, 2007); (Köles et al., 2011).

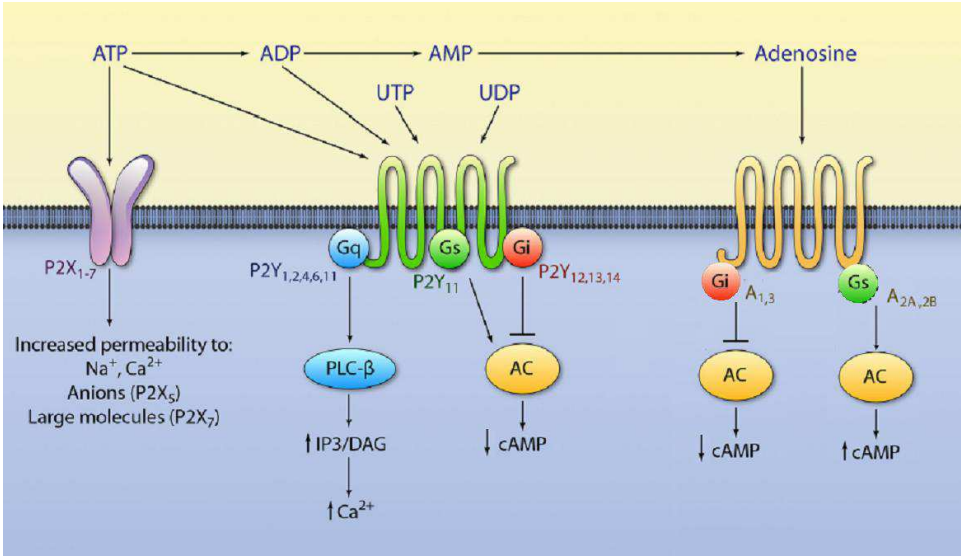

Figure I.27 The purine receptors and their specific ligands. *Adapted and modified from* (Yang and Liang, 2012).

ATP is the main purinergic player: it is released from astrocytes by a variety of different mechanisms, such as exocytosis, transporters and diffusion through membrane channels. Once released, various ectonucleotidases sequentially dephosphorylate it to ADP, AMP (adenosine 5'-monophosphate) and adenosine, also signalling molecules in the purinergic

pathway. One type of the ectonucleotidase family are E-NTPDases (ectonucleoside triphosphate diphosphohydrolases). In the brain there are three ectonucleotidases: E-NTPDase 1, 2 and 3 (Braun et al., 2000). Expression in the brain of E-NTPDase 1 (also called CD39) is restricted to microglial cells and vascular endothelium of blood vessels. E-NTPDase 1 rapidly converts both ATP and ADP to AMP, thereby depleting the extracellular space of ligands for P2X and P2Y receptors. E-NTPDase 2, expressed by astrocytes, converts preferentially ATP into ADP, but it has a much lower hydrolysis rate for ADP, which can lead to ADP accumulation and subsequent activation of ADP-specific P2 receptors. E-NTPDase 3 is present in hypothalamic neurons. Instead, the degradation of AMP into adenosine is due to the enzymeecto-5'-nucleotidase (5'-NT) (Figure I.28).

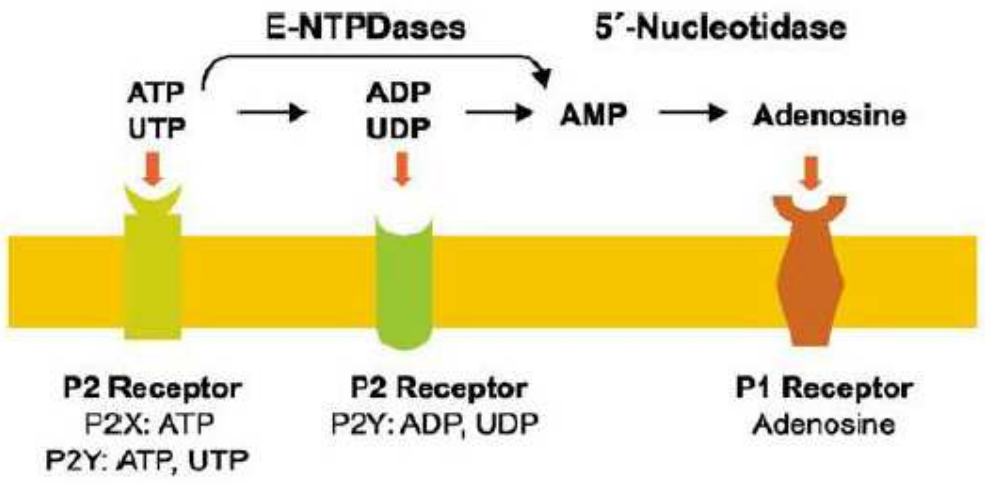

Figure I.28 ATP degradation, Purinergic Receptors, and their signaling pathways. ATP undergoes degradation and is converted into various breakdown products including ADP, AMP, adenosine. Adapted from (Robson et al., 2006)Robson et al., 2006

Yet, among these enzymes, adenosine kinase (ADK) is prominently expressed in astrocytes (Studer et al., 2006) and serves as a key regulator for adenosine metabolism. ADK eliminates and converts adenosine into AMP and its astrocytic expression has further hinted the importance of glial purinergic signaling in regulating various synaptic events.ADK was found to be upregulated and causing adenosine deficiency in epileptogenic sclerotic

tissue in a variety of rodent models of epilepsy as well as in human specimen resected from patients with temporal lobe epilepsy (TLE) and hippocampal sclerosis (Aronica et al., 2011). In experimental epilepsy, seizure induction results in the upregulation of ADK, while genetic reduction of ADK prevents seizures (Li et al., 2008).

2. AIM OF MY WORK

An in vitro study by (Brancaccio et al., 2010) showed that overexpression of *Foxg1*, a transcription factor gene involved in key steps of early cortico-cerebral development, halves the astroglial output of murine pallial stem cells, due to an impaired commitment of these cells to glial fates and a defective progression of early glia committed progenitors to more advanced cell types. This echoed the results of a previous study, performed in Drosophila, where *Foxg1* orthologs, Sloppy paired-1 and -2 (*Slp1* and *Slp2*), promote neurogenesis at the expense of gliogenesis (Bhat et al., 2000).

Rare microduplications of chromosome 14 fragments including *FOXG1* are associated to a variant of the West Syndrome (WS), namely a devastating infantile pathological entity, including an highly aberrant electroencephalo-graphic profile and a severe impairment of cognitive abilities.

I suspected that the neuronal hyperexcitability characterizing patients affected by this pathology may largely arise from an impaired astrocytic functionality. Therefore aim of my study was to investigate the role of *Foxg1* in early commitment of cortical precursor cells towards glial fates and subsequent implementation of the astrocytic differentiation program. Findings originating from this study may provide useful hints about pathogenetic mechanisms leading to neurological disorders triggered by altered *Foxg1* dosage. Moreover they may help to reconstruct the molecular logic underlying normal articulation of astrogenesis, a poorly explored field in vertebrates and mammals.

3. MATERIALS AND METHODS

3.1 Lentiviral production

Third generation self-inactivating (SIN) lentiviral vectors (LTVs) were produced as previously described (Follenzi and Naldini, 2002) with some modifications. Briefly,293T cells were co-lipofected (LipoD293TM, SigmaGen) with the transfer vector plasmid plus three auxiliary plasmids (pMD2 VSV.G; pMDLg/pRRE; pRSV-REV).The conditioned medium was collected after 24 and 48hs, filtered and ultracentrifuged at 50000 RCF on a fixed angle rotor (JA 25.50 Beckmann Coulter) for 150 min at 4℃. Vir al pellets were resuspended in PBS without BSA (Gibco).

LTVs were generally titrated by Real Time quantitative PCR after infection of HEK293T cells, as previously reported (Sastry et al., 2002). One end point fluorescence-titrated LTV was included in each PCR titration session and PCR-titers were converted into fluorescence-equivalent titers throughout the study.

3.2 Lentiviral plasmids construction

Basic DNA manipulations (extraction, purification, and ligation) as well as bacterial cultures and transformations, media and buffer preparations were performed according to standard methods. Restriction and modification enzymes were obtained from New England Bioloabs and Promega;DNA fragments were purified from agarose gel by the QIAquick Gel Extraction Kit(Qiagen); small and large scale plasmid preparations were done by DNA plasmid purification kit (Qiagen). Plasmids were grown in E.Coli, Xl1-blue or ElectroMAX™ Stbl4™ Competent Cells (Invitrogen).

A description of each transfer vector construction follows.

LV_Pgk1p-rtTA2S-M2 is the "driver lentivirus"described in (Spigoni et al., 2010)

LV_pTα1-rtTA2S-M2 (Brancaccio et al., 2010)

LV _pNes/hsp68-rtTA2S-M2 (Brancaccio et al., 2010);

LV_TREt-Foxg1 (Raciti et al., 2013);

LV_TREt-IRES2-EGFP derived from LV_TREt-luc-IRES2-EGFP(Brancaccio et al., 2010), via deletion of the luc cassette

3.3 Generation of lentiviral miRNA expressors

The plasmid encoding for the constitutive lentiviral miR expressor, pLVmiR.23, was assembled as described (Diodato et al., 2013). Briefly, the "BfuAI-stuffer" (5'TGC TTC GTG CAG GTC TGC AGG AAT TCA CCT GCG GAC CAG G3') was cloned into pcDNA^{TM}6.2-GW/EmGFP-miR (Invitrogen) and the DraI/EcoRV 155 bp fragment of the resulting plasmid was transferred into the ΔXhoI-ΔBamHI derivative of pCCL-SIN-18PPT.Pgk.EGFP-Wpre (Follenzi and Naldini, 2002) (gift from L. Naldini), cut by SalI and filled in by Klenow enzyme, in sense orientation. Then, pri-miR-cDNAs, designed by “BLOCK-iT™ RNAi Designer" (freely accessible at https://rnaidesigner.thermofisher.com/rnaiexpress/) and listed below, were cloned into BfuAI-digested LVmiR.23.

miRNA	*pri-miRNA cDNA insert (underlined the mature miR sequence)*
1690	TGCTGAAACGTTCACTTACAGTCTGGGTTTTGGCCACTGACTG ACCCAGACTGAGTGAACGTTT
2030	TGCTGTTAGGTTGTTCTCAAGGTCTGGTTTTGGCCACTGACTG ACCAGACCTTGAACAACCTAA

Finally, the negative control pri-miR expressor lentivector was obtained, by transferring the SalI-XhoI cDNA fragment from ‘‘pcDNA^{TM} 6.2-GW/EmGFP-miR_neg_control_plasmid" (Invitrogen) into SalI-digested pCCL-SIN-18PPT.Pgk.EGFP-Wpre, in sense orientation.

3.4 Mouse embryonic fibroblasts cultures

CD-1 Mouse Embryonic Fibroblasts (MEFs) were isolated from E14.5 embryos under a dissection microscope (Leica). The head, vertebral column (containing the spinal cord), dorsal root ganglia and all internal organs were removed and discarded. The remaining tissue was manually dissociated and incubated in 0,05 % trypsin (Sigma) for 10-15 min to create a single cell suspension. The cells were plated onto a 10-cm tissue culture dish in MEF

media (Dulbecco's Modified Eagle Medium; Invitrogen) containing 10% fetal bovine serum(FBS), and penicillin/streptomycin. Cells were grown at 37 ℃ for 3-4 days until confluent, and then split once before being frozen.

MEFs were used as feeders for induced pluripotent stem cells (iPSCs). For this reason, their ability to proliferate was inhibited by incubating them for 3 hours in medium containing 10ug/ml mitomycin C(Sigma), followed by 3 washes with PBS 1X.

3.5 Tissue isolation and derivation of human fibroblasts

The skin punch biopsy from a WS patient harboring a chromosome 14 duplication including *FOXG1* (Pringsheimet al., unpublished) was performed in Schön Klinik Vogtareuth-Neuropaediatrics Clinic (Germany). The sample was shipped at RT in 1X PBS. Within 24 hours from biopsy, it was transferred to the dissecting microscope in the laminar flow hood.The sample, a 4-mm round skin punch,was split into 12-15 evenly sized pieces with sharp edges, using a scalpel to hold the biopsy in place. During this step the tissue was kept in 1X PBS additionated with penicillin/streptomycin. Every piece was transferred into a well of a 6wells-plate,under a sterile glass coverslip, in 1 ml of RPMI 1640 (Sigma)/15% FBS/penicillin/streptomycin. Cells were cultured in a humidified 37℃, 5% CO_2 incubator and the medium was changed every 2 days taking care not to drive up the glass coverslip. Once fibroblasts were confluent in each well (around 2 weeks after biopsy), cells collected from the well bottom and the coverslip were trypsinized. Fibroblasts from one 6-well plate were transferred into two T75 flasks (so giving rise passage 1 cells).

3.6 Murine Embryonic Stem Cell (mESC)

Murine, R1 embryonic stem cells were a gift from W.Wurst. They were cultured on mitotically inactivated MEF feeder layers in mESC medium: KnockOut™ D-MEM, KnockOut™ Serum Replacement 20%, 2 mM glutamine, 1 mM pyruvate, 0.1 mM non essential amino acids, 0.1 mM 2-ME (Invitrogen), 1000 U/ml LIF (Millipore). In some cases,mESCs were cultured in feeder free conditions: plates were precoated with 0.1 % Gelatin (Sigma). In

general, the mESC medium was replaced every day and cells were trypsinized every other day.

When required, ESCs were acutely infected, at a concentration of 1000 cells/µL by a mix containing lentiviral vectors, each one at a multiplicity of infection (m.o.i) of 25. This m.o.i is sufficient to infect the almost totality of cells in such conditions, in the absence of overt signs of toxicity.

3.7 Reprogramming human fibroblasts into human induced pluripotent stem cells (hIPSCs)

The day before viral transduction (day -1), passage 3 human fibroblasts were plated at the density of 1×10^5 cells/well, onto a 0.1% Gelatine-coated 24-well plate.

On day 0, as cells reached 80-90% of confluency, they were infected with each of the four CytoTune™ Sendai reprogramming viruses (A1378001, Gibco), at m.o.i = 4, in 300µl of fibroblast medium. Infected cells were incubated at 37℃, 5% CO_2 overnight, the medium was changed 24 hours after transduction and, subsequently, every two days. Seven days after transduction, cells were additionated with 1µM Y-27632 and, one hour later, trypsinized by TrypLe Select (Gibco). They were replated at 5×10^4 cells per 60-mm MEF culture dish, in iPSC medium (KnockOut™ D-MEM/F-12, 20% KnockOut™ Serum Replacement (Gibco), 100µM MEM Non-Essential Amino Acids Solution, 1x GlutaMAX™-I Supplement,100µMβ-mercaptoethanol, 1x Penicillin-Streptomycin, 4ng/ml bFGF (Gibco), additionated for 48 hours with 1µM Y-27632 (Sigma). To improve the efficiency of reprogramming, some plates were cultured at 5% O_2 from the 7th to the 14th day (Yoshida et al., 2009).Around two weeks after transduction, iPSC colonies appeared on the plate. One week later, they had an appropriate size in order to be picked and transferred onto 24 well MEF culture plates. 48 hours after this last procedure, the iPSC colonies were cut into 3-4 pieces using a 25 gauge 1½ inch needle and transferred to a freshly prepared 24 well MEF culture plate. The medium was changed every day and colonies were passed every 6-7 days using Collagenase Type IV (Gibco), according to the manufacturer instructions. iPSCs cultured on MEF feeder layers were also adapted to feeder-free

culturing conditions in mTeSR™1 (Stemcell Technologies) on plate pre-coated with Matrigel (Corning), again according to the manufacturer's instructions.

After picking, different iPSCs clones were validated for a set of pluripotent genes by immunostaining (hNanog, TRA1-60) and quantitative RT-PCR (technical details are described later). Positive clones, after 10 passages, were analyzed by PCR to detect the absence of CytoTune® Sendai virus as described in the kit manual (A1378001, Gibco).

3.8 Human Neural Precursors (hNPs)

We used for our experiments hNPs provided by Dr. Stefano Pluchino (Cambridge University, UK). These cells were cultured as floating neurospheres at clonal density (13,000 cells/cm^2) in NS-A Proliferation medium: Neurocult™ NS-A Proliferation Kit (#05751,StemCell Technologies), 0.2% human Heparin (StemCell Technologies), 10ng/ml bFGF (Gibco), 20ng/ml EGF (Gibco). The growth factors were added every two days and cells were passaged by Accutase (Sigma) every two weeks. When required, they were acutely infected, at a concentration of 1,100 cells/µL by a mix containing lentiviral vectors, each one at a multiplicity of infection (m.o.i.) of 2. This m.o.i. is sufficient to infect the almost totality of cells in such conditions.

In order to obtain astrocytes, hNPs were dissociated at single cells and plated at 60,000 cells/cm^2 on multiwell plates pre-coated with Matrigel (Corning) in NS-A Differentiation medium: Neurocult™ NS-A Differentiation kit (#05752, StemCell Technologies) without any growth factors. The medium was changed by half every four days. When required, the astrocytes were infected at m.o.i.=4 on multiwell plates pre-coated with Matrigel (Corning) in NS-A Differentiation medium.

TetON-controlled transgenes were switched on by 9 ng/mL doxycycline (Sigma) added to the medium.

3.9 In vitro generation of cerebral neural precursors starting from ESCs/iPSCs

Three-dimensional cell aggregates known as "Serum-Free floating cultures of Embryoid Body-like, quick aggregates"(SFEBq's) were generated according to (Eiraku et al., 2008) and (Mariani et al., 2012), with minor modifications,in case of murine and human cultures, respectively.

murine SFEBq aggregates

As for mouse SFEBq's**,** mESCs were dissociated to single cells in 0.25% trypsin-EDTA (Gibco) and quickly reaggregated in differentiation medium (5,000 cells in 10 µl/well for the first 2 hours, followed by addition of further 140µl of medium/well), using 96-well "low cell-adhesion plates, round bottom" (Nunc). Differentiation medium was prepared as follows: DMEM supplemented with 10% Knockout Serum Replacement (KSR; Gibco), 2 mM glutamine, 1 mM pyruvate, 0.1 mM nonessentialamino acids, 0.1 mM 2-ME, 10µM XAV939 (Tocris Bioscience) [replacing 250 ng/ml recombinant Dkk1], and 10 µM SB431542 (Tocris Bioscience). On day 7, cell aggregates were transferred to a 10 cm bacterial-grade dish in DMEM/F12 supplemented with N2. The day on which ESCs were seeded to differentiate is defined as post aggregation day 0 (PAD0).

As for SFEBq analysis, in some cases the aggregates were fixed for 15 minutes in 4% PFA, washed 3 times in PBS, incubated in 30% sucrose over night and finally included into Killik (Bio-Optica)for cryostat sectioning. In other cases SFEBq's were disrupted by 0.25% trypsin-EDTA (Gibco), 0.1% DNase I (Roche). The resulting single cells were plated at 100,000 cells/well, onto poly-L-lysine-coated 24-well-plates, in neuronal differentiation medium: Neurobasal (Gibco), 1X B27, 2 mM glutamine,0.025 mM 2-ME, 0.025 mM glutamate.

Murine SFEBq's were made conditionally *Foxg1*-GOF, by manipulating their mESC forerunners via lentiviral and TetON technology.

In a former experimental setup, the *rtTA*^{M2}transactivator gene was driven by the artificial, neural stem cell-specific *pNes-promoter* (including the *rat nestin intron II neural enhancer* and the minimal *hsp68 promoter*). In turn, *Foxg1* was under the control of a tetracycline responsive element (TRE). The resulting *pNes*-rtTA^{M2}/TRE-*Foxg1*and control,*pNes*-rtTA^{M2}/TRE-luc genotypes were activated by 2μg/ml doxycycline, added to the medium during the neurogenesis phase, from PAD7 to PAD13, and subsequently removed until the analysis, at PAD 21.

In a latter similar setup, the *rtTA*^{M2} transactivator gene was alternatively driven by the neuronal lineage-specific *α1-tubulin* promoter (*pTα1*). The resulting *pTα1*-rtTA^{M2}/TRE-*Foxg1* and control *pTα1*-rtTA^{M2}/TRE-luc genotypes were activated by addition of 2μg/ml doxycycline to the medium, from PAD7to PAD13. As the transgene was switched off, SFEBq's were disaggregated (as described above). The resulting neural cells were cultured in neuronal differentiation medium for two weeks and finally analyzed.

human SFEBq aggregates

As for generation of human SFEBq's, hiPSCs maintained on Matrigel (Corning) and pretreated for at least 1 h with 50 μMY27632 compound (Sigma), were dissociated with TrypLe Select (Gibco) to single cells, which were plated onto low-attachment, U-shaped wells of 96-well-plates (Nunc), at 9,000 cells per well, in 150 μL differentiation medium. Differentiation medium was prepared as follows: DMEM/F12, 0.1 mM 2-ME, 0.1 MmNEAA, 2 mM L-glutamine, and 20% KSR, 20 ng/mL bFGF (Gibco), supplemented with 500 ng/mL recombinant DKK1 (R&D Systems), 1.5μg/mL human BMPRIA-Fc (R&D Systems), and 10 μM SB431542 (Tocris Bioscience). The cell aggregates were cultured in suspension for the first 18 days. On day 18, cell aggregates were transferred to ultralow-attachment six-well plates (Corning) and cultured in DMEM/ F12/GLUTAMAX-type medium, supplemented with 0.1 mM 2-ME, 0.1 mM NEAA, 1X N2 as well as DKK1, BMPRIAFc, and SB431542 (at the above reported concentrations) until day 24. On day 25 the floating cell aggregates were replated onto eight-well chamber slides (Nunc), sequentially precoated with50 μg/ml poly-L-ornithine (Sigma) for 6 hours,

followed by 60 μg/ml laminin (Sigma), and 10μg/ml fibronectin (Corning) overnight. Cell aggregates were cultured until day 70 in Neurobasal Medium (Gibco) supplemented with 2X B27 (without Vitamin A) and 2 mM glutamine as adherent cultures.The medium was changed every other day.

As for SFEBq analysis, in some cases SFEBq's were fixed for 5 hours in PFA 4 %, washed 3 times in PBS, incubated in sucrose 30% over night and finally included into Killik (Bio-Optica) for cryostat sectioning and straight immunoprofiling. In other cases, to get radial glial cell preparations, SFEBq's were disrupted by 0.25% trypsin-EDTA (Gibco), 0.1% DNase I (Roche) and plated in NS-A Proliferation medium (described above).

3.10 Quantitative RT- PCR

In each experimental session, almost 400,000 cells were processed for RNA extraction by Trizol® LS Reagent (Ambion™) according to manufacturer's instructions. RNA preparations were treated by TURBO™ DNase (2 U/μL) (Ambion™)1 hour at 37℃. At least 1. 0μg of genomic DNA-free total RNA from each sample was retro-transcribed by SuperScriptIII™ (Invitrogen) in the presence of random hexamers, according to manufacturer's instructions. 1/100 of the resulting cDNA was used as substrate of any subsequent qPCR reaction. Limited to intronless amplicons, negative control PCRs were run on RT(-) RNA preparations. PCR reactions were performed by the SsoAdvanced SYBR Green Supermix™ platform (Biorad), according to manufacturer's instructions. Per each transcript under examination and each sample, cDNA was PCR-analyzed at least in technical triplicate and results averaged. Averages were further normalized against *GAPDH.* Experiments were performed in almost biological triplicate and analyzed by Student's t test.

Oligos were as follows:

OCT3.4/F 5' GAG CCC TCA CTT CAC TGC ACT GTA CTC 3';
OCT3.4/R 5'TGG CAC AAA CTC CAG GTT TTC TTT CCC T3';
SOX2/F 5' CCC AGC AGA CTT CAC ATG TCC CAG C 3';
SOX2/R 5' TGC ACC CCT CCC ATT TCC CTC GTT TT 3';

NANOG/F 5’ ACA TCC TGA ACC TCA GCT ACA AAC AGG TG 3’;
NANOG/R 5’ TCC CTG GTG GTA GGA AGA GTA AAG GCT G 3’;
TERT/F 5’TCC AGA CGG TGT GCA CCA ACA TCT ACA AG 3’;
TERT/R 5’ ACA TCC CTG CGT TCT TGG CTT TCA GGA T 3’
FOXG1/F 5’CGA CCC TGC CCT GTG AGT CTT TAA G 3’
FOXG1/R 5’ GGG TTG GAA GAA GAC CCC TGA TTT TGA TG 3’
GAPDH/ F 5’ CAT CAC CAT CTT CCA GGA GCG AGA TCC 3’
GAPDH/R 5’ CAA ATG AGC CCC AGC CTT CTC CAT GG 3’
CX43/F 5’ CAT CCT CCA AGG AGT TCA ATC ACT TG 3’
CX43/R 5’ ACA CCT TCC CTC CAG CAG TTG AG 3’
CX30/F 5’ CAC TCC AGT GGG GTA GGA GAA GGA G 3’
CX30/R 5’ACC TTC CCG ATG CTG GTG GAG TG 3’
PANX1/F 5’AGA GCG AGT CTG GAA ACC TCC CAC TGT 3’
PANX1/R 5' TTC CAT GAT AAA CTT CAA GTC TGA GCA AAT ATG AG 3'
hSRR/F 5’ CTT CAA ATG TGA ACT CTT CCA GAA AAC AGG ATC TTT TAA 3’
hSRR/R 5’CAT GGT TTC CAC TGC TGT GAG TAA CAA CAG CTTT 3'
*GS/*F 5’GAC CAC CTC AGC AAG TTC CCA CT 3’
GS/R 5’AGT ACT GAG CCA TCG AAA TTC CAC 3’
GRIN1/ F 5' AGG GTA CCA GAT GTC CAC CAG ACT GAA GA 3'
GRIN1/R 5' TTG ACT GGG TCG CCG TTG ACT GTG AACT 3'
mGluR5/F 5'CAG CCT AGT CAA CCT GTG GAA GAG A3'
*mGluR5/*R 5'TTC TTT CTT GTT GAT GTG GAT GGA CAG3'
GLAST/F 5’ GCT GGG GAA TTC ACC TCG TTA CTG CTT 3’
GLAST/R 5’ CCC ATC TTG GGC TCT TCC CAT TGC TT 3’
GLT-1/F 5’ GTG GGC CTG CCA ACA GAG GAC AT 3’
GLT-1/R 5’ TAT CCC AGC CCC AAA AGA GTC ACC C 3’
*KIR4.1/*F 5’ CGC CCC GTC CGT CCA TCT GTC 3’
*KIR4.1/*R 5’TCT CAC GTT GCT GCG ACC ATC TTT TG 3’
ATP1A2/F 5' CTT CCC CTA CAG CCT CCT CAT CTT CAT CTA T 3'
ATP1A2/R 5' CCA TCA CCA TCC CCA CAA CAC CTC CAG 3'
ATP1B2/F 5' GGA CTC CAC CCA CTA TGG TTA CAG CAC T 3'
ATP1B2/R 5' CGG GGA ACA TGA CGA AGT TGC CGA GAT T 3'
KCC1/F 5' CGG AGC TCC ACG ACG AGC TGG AAA A 3'

*KCC1/*R 5' GTG ACC GCA GCA TCT CTG GTT GGA GTA 3'
ENTPD1/F 5' GGA AGG ATC AGG CAC TCT GGC AGA AAC T 3'
ENTPD1/R 5' GGT CAC TTA CGT TCA CTA CCT TCT TAT ATC CA 3'
*ADK/*F 5' GTG AAG TCA CTG CTT TTG CTG TCT TGG A 3'
ADK/R 5' GGA AGT CTG GCT TCT CAG GAA AGG T G 3'
P2RX7/F 5' CTA CTA CAG GAA GAA GTG CGA GTC CAT TGT G 3'
P2RX7/R 5' CCC TAG TAG CTG CTG GTT CAC CAT CCT AAT 3'
ADORA1/F 5' TGT GGA CCG CTA CCT CCG GGT CAA GAT 3'
*ADORA1/*R 5' GGT CAG TCC CAC CAC GAA GGA GAG GAT 3'
ADORA2A/F 5'CTC ACG CAG AGC TCC ATC TTC AGT CTC 3'
ADORA2A/R 5' CAC CCA GCA GAT GGC AAT GAT GCC CTT A 3'
*AQP4/*F 5'GCA TTG CAA CCA TGG TGC AGT GCT T 3'
*AQP4/*R 5' GCC AGT GAC ATC AGT CCG TTT GGA ATC 3'

3.11 Immunofluorescence

For immunocytofluorescence cells were fixed directly on coated 1 cm Ø glass coverslips in 24-multiwell plates by 4% paraformaldehyde (PFA) for 20 min at 4℃. Subsequently, cells were washed 3 times in 1X PBS.

For immunofluorescence on brain sections (controls not shown) and SFEBq's, slices were allowed to dry for at least one hour at RT, they were post-fixed 5 minutes in 4% paraformaldeyde at RT, followed by three washes in 1X PBS. In all cases, samples were subsequently treated with blocking mix (1X PBS; 10% FBS;1mg/ml BSA; 0.1% Triton X100) for at least 1 hour at RT. Then, incubation with primary antibody was performed in blocking mix, overnight at 4℃. The day after, samples were washe d in"1X PBS - 0,1% Triton X-100" 3 times and incubated with a secondary antibody in blocking mix, for 2 hours at RT. Samples were finally washed in PBS for 5 minutes, 3 times, counterstained with DAPI (4', 6'-diamidino-2-phenylindole) and mounted in Vectashield Mounting Medium (Vector).

In case of immunos with polyclonal anti-Aldolase C, anti-ALDH1L1 and monoclonal anti-S100β antibodies, antigen retrieval was performed by baking samples in 500 ml of 10 mM citrate buffer (pH6.0), at 700 W for 5 min, respectively.

In case of immunos with polyclonal anti-human Nanog, the cells were permeabilized in 0,1% Triton X-100 for 30 min before the incubation in blocking mix and the washing was performed in 1X PBS and 0,2% Tween 20.

The following primary antibodies were used: anti-Tubβ3, mouse monoclonal, (clone Tuj1, Covance, MMS-435P, 1:1000); anti-GFP, chicken polyclonal (Abcam, ab13970, 1:600); anti-NeuN mouse monoclonal (clone A60, Millipore, MAB 377, 1:200); anti-Sox2, rabbit polyclonal (Abcam, ab97959,1:500); anti-Aldolase C, rabbit polyclonal (Abcam ab87122, 1:50); anti-ALDH1L1 (Abcam ab56777, 1:200), anti-CNPase, mousemonoclonal, clone 11-5B antibody (Abcam ab6319, 1:200); anti-GFAP rabbit polyclonal (DAKO Z0334, 1:500); anti-GFAP mouse monoclonal (Chemicon, MAB360, 1:200); anti-Pax6, rabbit polyclonal (Covance PRB-278P, 1:300); anti-S100β, mouse monoclonal, clone 4C4.9 (Abcam ab4066,1:50); anti-S100β, rabbit polyclonal (DAKO Z0311, 1: 1000); anti-Foxg1 rabbit polyclonal (gift from G. Corte, 1:200); anti-Nanog rabbit polyclonal (Abcam, ab21624, 1:50) anti TRA 1-60 (Millipore, MAB4360, 1:200).

Secondary antibodies were conjugates of Alexa Fluor 488, and Alexa Fluor 594 (Invitrogen, 1:600).

3.12 Images acquisitions

Immunoprofiled cultured cells were photographed on a Nikon TI-E microscope,equipped with 20X or 40X objectives and a Hamamtsu C4742-95 camera.

Immunoprofiled iPSCs and SFEBq's were photographed on Leica confocal microscope equipped with 40X objectives. Samples were collected as 10µm Z-stacks.

All images were processed using Adobe 9.0.2 Photoshop 2 CS2 software, GIMP2.6 software and ImageJ Cell counter plug-in.

3.13 Neurite morphometry

After images acquisition, neuronal silhouettes, including somas and neurites, were generated by free hand by an operator blind of cell genotype, with GIMP2.6 software. These silhouettes were analyzed by the Neurphology (Ho et al., 2011) interactive plug-in, in ImageJ environment. Four parameters were measured: number of somas, total neurite length, number of attachment points, and number of endpoints. Numerical results were finally processed by Excel software.

3.14 Glutamate colorimetric assay

Human neural precursors made *Foxg1*-gain-of-function were plated at 300,000 cells/well in 12-well-plates and differentiated to astrocytes in NS-A Differentiation medium, as described above. The transgene was activated by 9ng/ml doxycycline. To maintain the right concentration of cells for every biological replicate, 0.5mM cytosine-1-β-D-arabinofuranoside (AraC) (Sigma) was added to the medium. 48 hours after transgene activation, the medium was changed to DMEM/F12 /10%FBS (500µl per well) with 0.5mM L-Glutamic Acid (G1251, Sigma). 40µl aliquots of medium were collected at 3-6-9-12 hours. The medium was centrifuged in order to eliminate debris; 30µl for every sample was conserved at -20℃ in the dark. All of s amples were co-assayed by a Glutamate Assay Kit (ab83389, Abcam), following manufacturer's instructions (20µl of sample diluted in 30µl of buffer). Optic reading of samples was performed by a Thermo Scientific Multiskan FC device.

3.15 Luminescent ATP detection assay

Human neural precursors made *Foxg1*-gain-of-function were plated at 200,000 cells/well in 12-well-plates and differentiated to astrocytes in NS-A Differentiation medium, as described above. The transgene was activated by 9ng/ml doxycycline and 0.5mM cytosine-1-β-D-arabinofuranoside (AraC) (Sigma) was added to the medium. The experiment was performed after 48 hours from transgene activation. Briefly, the medium was changed to synthetic medium: 148 mM NaCl, 5 mM KCl,1.8 mM $CaCl_2$, 1mM $MgCl_2$, 5mM glucose, 5mM HEPES pH 7.4 (Stehberg et al., 2012). Then 100µl aliquots of

synthetic medium were collected, at 10 and 20 minutes after medium change, and conserved at -20℃ in the dark. Upon last mediu m sample collection, every cell sample was lysed with the specific detergent of the Luminescent ATP detection assay kit (ab113849, Abcam) in the presence of 1x protease inhibitor cocktail (Roche).Then the luminescent ATP detection assay was run following kit instructions. Optic reading of samples was performed by a luminometer without injection at the ICGEB Institute facility (Trieste).

3.16 Statistical analysis of results

Generally, when not otherwise stated, experiments were performed at least in biological triplicate. Results were averaged and their statistical significance was evaluated by one-way ANOVA (* $p<0.5$; ** $p<0.01$; *** $p<0.001$).

4. RESULTS

4.1 Regulation of astrogenesis rates upon experimental manipulation of *FOXG1*-mRNA levels in human pallial precursors [Figures R1-4]

It was reported that *Foxg1* overexpression impairs pallial astrogenesis in the mouse (Brancaccio et al., 2010). Similar phenomena might occur in WS patients harboring a supranumerary copy of *FOXG1* and, therefore, presumably displaying increased expression of this gene. To evaluate the impact of *FOXG1* on human astrogenesis progression, we decided to manipulate expression levels of this gene in derivatives of human, *FOXG1*-wt, fetal pallial precursors.

These precursors were kept in pro-proliferative medium, as floating neurospheres. To better define their identity, we scored them for the expression of select neural markers (Figure R1A). The vast majority of these precursors were immunoreactive for the panastrocytic markers AldoC and AldH1L1. About one half of them expressed the EGFP reporter under the control of the rat nestin neural enhancer, normally firing in neural stem cells and their immediate derivatives (Figure R1B). All that suggests that these precursors were to large extent newborn, committed astroblasts. To confirm this hypothesis, we transferred them to a prodifferentiative medium and, one week later, we profiled them for markers specifically active in distinct neural types: Tubβ3 (neurons), S100β and AldoC (astrocytes), and CNPase (oligodendrocytes)(Figure R1A). As expected, almost all cells resulted to be immunoreactive for AldoC and approximately 2/3 of them positive for S100β. Only less than 10% of them expressed either Tubβ3 or CNPase, confirming that their precursors were primarily astroblasts (Figure R1C).

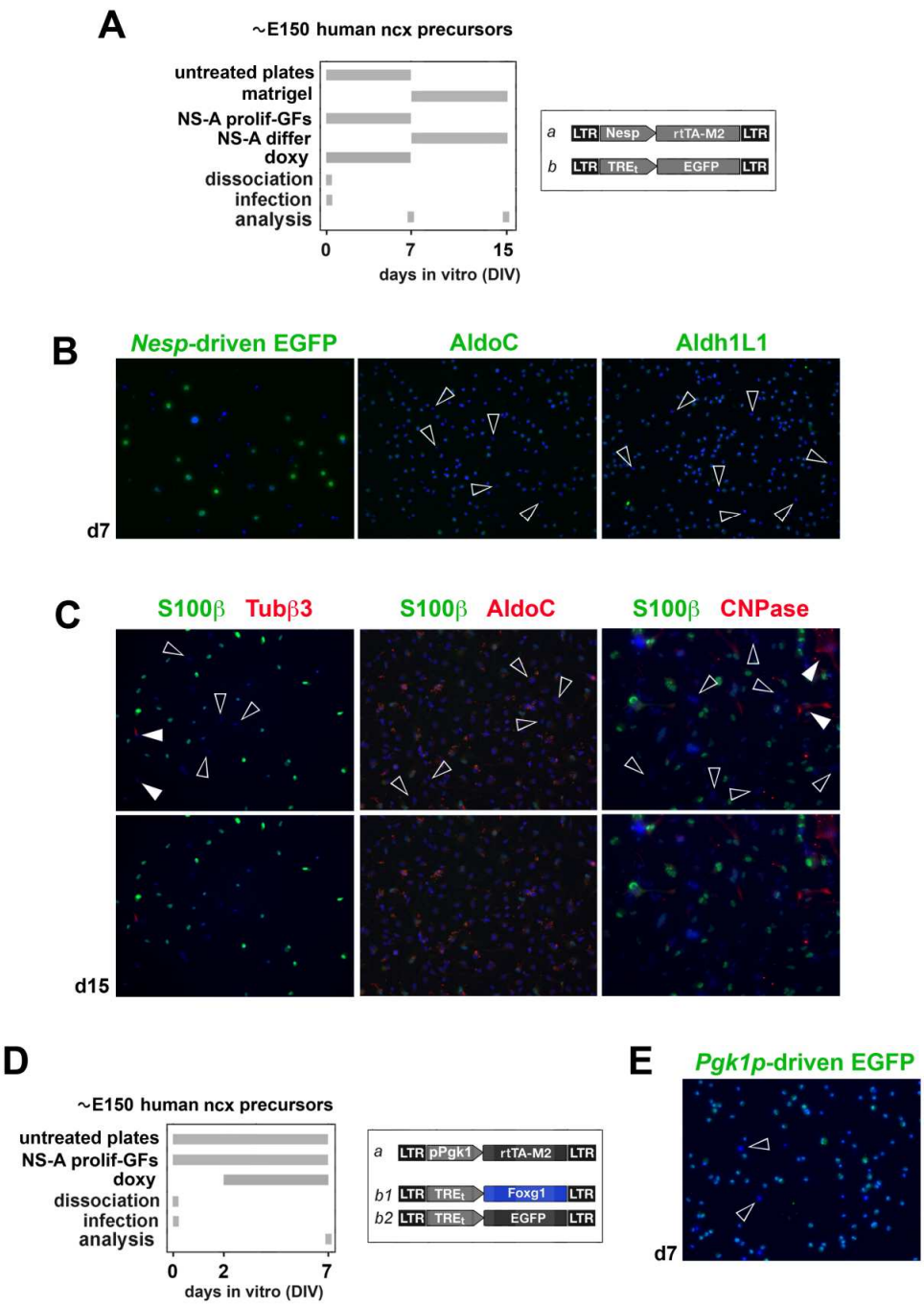

F *Foxg1*-mRNA expression gain

[doxy], ng/ml	*gain*	*p*	*n*
50	85,0	---	1,1
20	6,0	0,072	4,4
12	6,0	0,003	3,3
6	2,1	0,042	3,3

Figure R1. Histological characterization and conditional gain-of-function engineering of human fetal pallial precursors. (A) To the left, temporal articulation of histological characterization. To the right, the two recombinant lentiviruses (a,b) driving doxycycline-dependent expression of EGFP under the control of the "neural enhancer of *nestin* plus minimal *hsp68* promoter" (*Nes*p). These viruses label NSCs and their immediate progenies. **(B)** Immunoprofiling of pallial precursors kept 7 days under pro-proliferative conditions, for *Nes*p-driven EGFP and the pan-astrocytic markers AldoC and Aldh1L1. Empty arrowheads point to rare precursors not expressing AldoC or Aldh1L1.**(C)** Histogenetic output of pallial precursors further kept under pro-differentiative medium, for additional 8 days, and profiled for the pan-neuronal marker Tubβ3, the astrocytic markers AldoC and S100β, and the pan-oligodendrocyte marker CNPase. Solid and empty arrowheads point to cells positive and negative for the marker in order, respectively.**(D)** Assessment of the *Foxg1* expression gain obtained upon lentiviral transduction of pallial precursors by a *Foxg1* (b1) or an *EGFP* transgene (b2), driven by the constitutive *Pgk1*p (a) and tuned by doxycycline. **(E)** Example of EGFP protein expression referred to in (D). **(F)** Relationship among *Foxg1*-mRNA expression gain and doxycycline concentration. Data double normalized, against *GAPDH* and *EGFP* controls. Statistical significance (*p*) evaluated by t-test. *n* is the number of biological replicates.

Next, we set up the conditions for *FOXG1* upregulation to levels suitable for gain-of-function analysis. We infected proliferating pallial precursors by two lentiviruses, expressing the rtTA^{M2} transactivator under the constitutive *Pgk1* promoter and *Foxg1* under the rtTA^{M2}/doxycycline-responsive TREt promoter (Figure R1D). Each lentivirus was delivered at moi = 2, sufficient to transduce the almost totality of the neural culture (Figure R1E). We added different doxycycline concentrations to the medium, in the 6 to 50 ng/ml range. 5 days later, we measured the total *Foxg1/FOXG1* mRNA cell content, by qRTPCR (Figure R1D). The *FOXG1* expression gain, as evaluated against *EGFP* controls, varied between 85.0 and 2.1. In particular, it equaled 4, when doxycycline concentration was 9 ng/ml. We chose this last drug concentration for subsequent gain-of-function analysis. In fact, gene upregulation elicited by it, was satisfactorily robust (i.e. effective and reproducible), while being not too far from the 1.5 value presumably peculiar to WS patients.

To assess if *Foxg1* overexpression impairs pallial astrogenesis in humans, we delivered a *Foxg1* TetON-controlled transgene to human pallial precursors, and activated it according to the protocol illustrated in Figure R2A,B. In particular, the transgene was activated for 7 days in proliferating cells, kept as floating neurospheres, and 4 additional days in their derivatives, differentiating on matrigel. 15 days after transgene delivery, we scored the frequency of AldoC$^+$S100β$^+$ astrocytes. Remarkably, it was almost halved in *Foxg1*-GOF cultures, as compared to "*wt*" *EGFP* controls (Figure R2C,D).

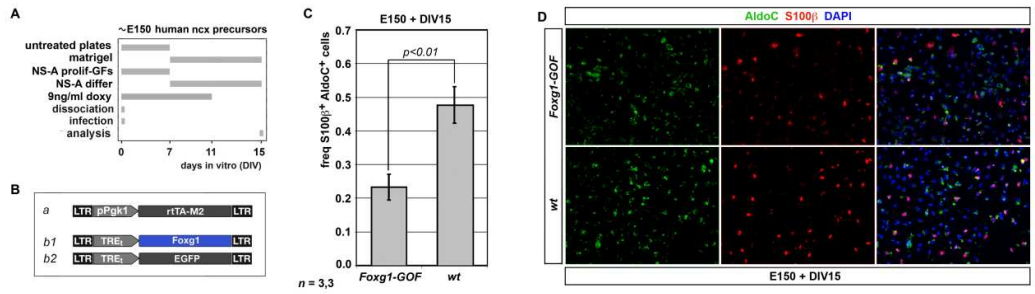

Figure R2. Inhibition of astrogenesis upon *Foxg1* overexpression in human pallial precursors. (A,B) Temporal articulation of the assay and lentiviral vectors employed for it. **(C)** Absolute frequencies of S100β$^+$AldoC$^+$ astrocytes in *Foxg1*-GOF and control cultures at DIV15. Statistical significance (*p*) evaluated by t-test. *n* is the number of biological replicates. **(D)** Example of S100β$^+$AldoC$^+$ astrocytes referred to in (C).

To rule out that this phenomenon could arise as a dominant-negative effect, we decided to measure the same histogenetic parameter in human pallial cultures loss-of-function for *FOXG1*.

For this purpose, we selected three potential *FOXG1*miRNA targets by Block-it Invitrogen software https://rnaidesigner.thermofisher.com/rnaiexpress and built lentiviral vectors driving constitutive expression of pri-miRNA-155-based, miRNAs against them (Figure R3A,B). We delivered these lentiviruses to proliferating pallial precursors at moi = 4. Five days later, we measured levels of *FOXG1*-mRNA by qRTPCR. miRNA-α*FOXG1*.2030 and miRNA-α*FOXG1*.1690 elicited a robust down-regulation of their intended target (about -50% and -40%, respectively) (Figure R3C). We chose the better performing one, miRNA-α*FOXG1*.2030, for our subsequent loss-of-function analysis.

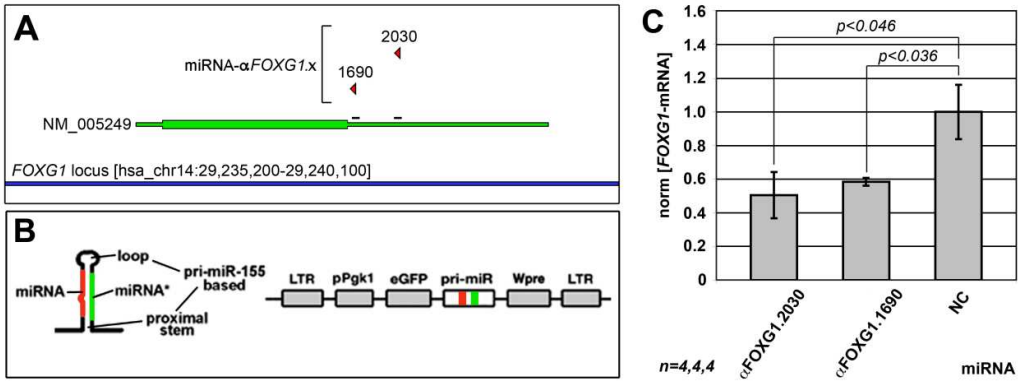

Figure R3. Down-regulation of *FOXG1* in human pallial precursors. (A) Localization of miRNA targets selected for FOXG1 down-regulation. **(B)** Schematics of pri-miR-155-based miRNA precursors and lentiviral vectors employed for their constitutive expression. **(C)** FOXG1 downregulation by αFOXG1.2030 and αFOXG1.1690 in proliferating human pallial precursors. Data double normalized, against *GAPDH* and "*miR(-)*" controls. Statistical significance (*p*) evaluated by t-test. *n* is the number of biological replicates.

Finally, human pallial precursors were infected with the miRNA-α*FOXG1*.2030-expressing lentivirus and allowed to differentiate to astrocytes, as shown in Figure R4A. Remarkably, *FOXG1* knock-down did not diminish the frequency of S100β$^+$ cells (Figure R4B), suggesting that the decrease of this frequency detected upon *Foxg1* overexpression was a genuine gain-of-function effect.

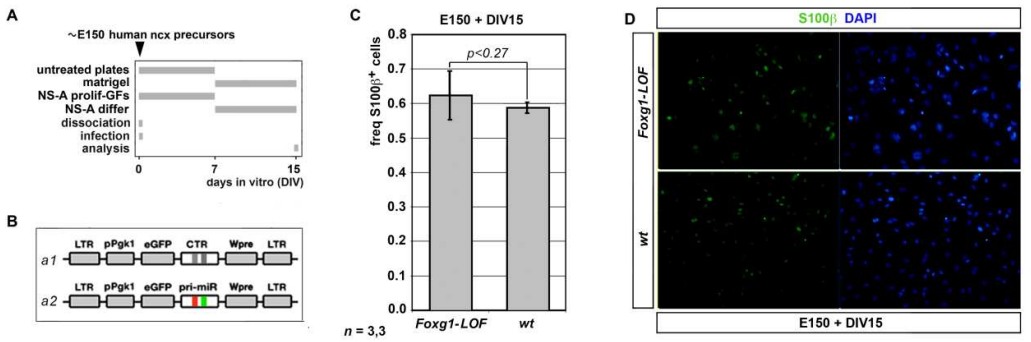

Figure R4. Unaffected astrogenesis rates from *FOXG1 knock-down* human pallial precursors. (A,B) Temporal articulation of the assay and lentiviral vectors employed for it. **(C)** Absolute frequencies of S100β$^+$ astrocytes in *FOXG1*-LOF and control cultures at DIV15.

Statistical significance (*p*) evaluated by t-test. *n* is the number of biological replicates. **(D)** Example of S100β$^+$ astrocytes referred to in (C).

4.2 Altered astroglial molecular differentiation upon modulation of *FOXG1*-mRNA levels in immature astrocytes [Figures R5-7]

Astrocytes exert fundamental functions crucial to proper tuning of neuronal activity. They remove excitatory neurotransmitters and K^+ ions which accumulate in the extracellular space upon bursts of neuronal activity. They release soluble gliotransmitters, modulating the activity of astrocytes themselves and neurons. They form large syncitia which take care of coordinating the chemo-electric behaviour of adjacent, coupled neurons (Anderson and Swanson, 2000)(Seifert and Steinhäuser, 2013). We wondered if *FOXG1* overexpression, in addition to impairing general progression of astroglial differentiation, could selectively perturb the expression of genes involved in the execution of these functions.

To test this prediction, we overexpressed *Foxg1* in cultures of differentiating human astrocytes in according to the protocol shown in Figure R5A,B and we profiled them for selected gene sets by qRTPCR. These sets include genes involved in: (1) formation of gap junctions and hemichannels (*CX43* and *PANX1*); (2) metabolism, translocation and sensing of gliotransmitters, such as D-serine (*SRR*), L-glutamate (*GLUL*, *GRIN1*, *mGLUR5*, *GLAST* and *GLT-1*), ATP and purines (*ADK*, *ENTPD1*, *P2RX7*, *ADORA1* and *ADORA2A*); (3) extracellular K^+ clearance (*KIR4.1*, *NKCC1*, *ATP1A2* and *ATP1B2*); (4) water flux (*AQP4*).

As expected, we found that some of these genes were misregulated. 7 out of 18 were upregulated: *CX43* (by 1.56±0.06), *PANX1* (by 1.36±0.13), *mGLUR5* (by 2.35±0.30), *ADK* (by 1.24±0.04), *ATP1A2* (by 2.79±0.34), *ATP1B2* (by 2.36±0.11), *AQP4* (by 1.34±0.04) (Figure R5C). Only one, *KIR4.1*, was downregulated (by 0.66±0.09) (Figure R5C).

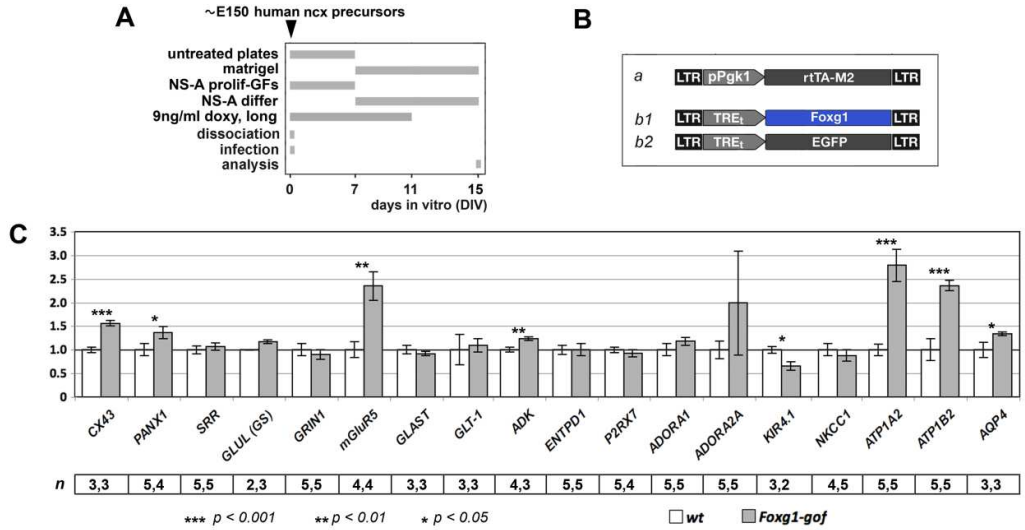

Figure R5. Biased transcriptional profiling of astrocytes originating from human pallial precursors gain of function for *Foxg1*.(A,B)Temporal articulation of the assay and lentiviral vectors employed for it. **(C)** mRNA levels of a selection of genes essential for proper function of astrocytes, as measured by qRTPCR. Data double normalized, against *GAPDH* and *EGFP* controls. Statistical significance (*p*) evaluated by t-test. *n* is the number of biological replicates.

To rule out that this phenomenon could arise as dominant-negative effects, we decided to monitor expression levels of these genes in human pallial cultures loss-of-function for *FOXG1*. As shown in Figure R6A, we infected astrogenic differentiating cultures of human pallial precursors with the miRNA-α*FOXG1*.2030-expressing lentivirus (Figure R6B) and, 2 weeks later, we profiled them by qRTPCR (Figure R6C).

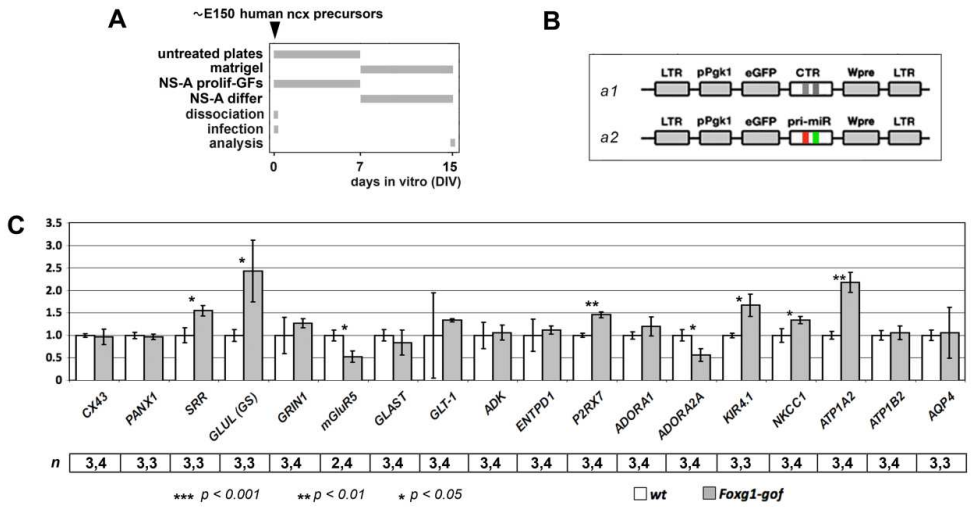

Figure R6. Biased transcriptional profiling of *FOXG1-knock-down* human pallial astrocytes. (A,B) Temporal articulation of the assay and lentiviral vectors employed for it. (C) mRNA levels of a selection of genes essential for proper function of astrocytes, as measured by qRTPCR. Data double normalized, against *GAPDH* and *EGFP* controls. Statistical significance (*p*) evaluated by t-test. *n* is the number of biological replicates.

All genes stimulated upon *Foxg1*-GOF manipulation were not upregulated following *FOXG1* knock-down, except *ATP1A2*, whose expression robustly arose (by 2.18±0.22). One of these genes, *mGLUR5*, was conversely downregulated (by 0.53±0.13), strengthening the hypothesis that *FOXG1* may physiologically stimulate its expression. Moreover, *KIR4.1*, depressed by *Foxg1* overexpression, went up following *FOXG1* knock-down (by 1.67±0.25), suggesting that *FOXG1* may physiologically inhibit its expression. Finally, as many as five genes apparently unaffected by *Foxg1* overexpression were sensitive to knock-down of this gene. Four of them, *SRR*, *GS*, *P2RX7* and *NKCC1* were upregulated (by 1.55±0.11, 2.43±0.68, 1.46±0.07, 1.34±0.08, respectively). One, *ADORA2A*, was downregulated (by 0.57±0.14).

To confirm potential biological relevance of the mRNA level alterations reported above, we monitored *Foxg1*-GOF astrocytes for expression and distribution of the protein product encoded by these mRNAs (Figure R7A,B). We were not able to detect any appreciable increase of PANX1 (Figure R7C),

while CX43 resulted to be dramatically upregulated in GFAP$^+$ astrocytes (Figure R7D).

All these findings suggest that key functional properties of astrocytes may be profoundly altered upon *Foxg1* overexpression. We can envisage an increase of gap-junction-mediated, intra-syncitial conductance, as well as an increase of hemichannel-mediated gliotransmitter release, due to CX43 misregulation. *ADK* and *mGLUR5* upregulation conversely point to increased production of the excitatory gliotransmitter ATP and higher sensitivity to L-glutamate, respectively. Finally, changes in *ATP1A2*, *ATP1B2* and *KIR4.1* as well as in *AQP4* levels are likely to lead to disorders in K$^+$ and water fluxes through the astrocyte plasmamembrane. These concepts will be addressed more in depth in the Discussion section.

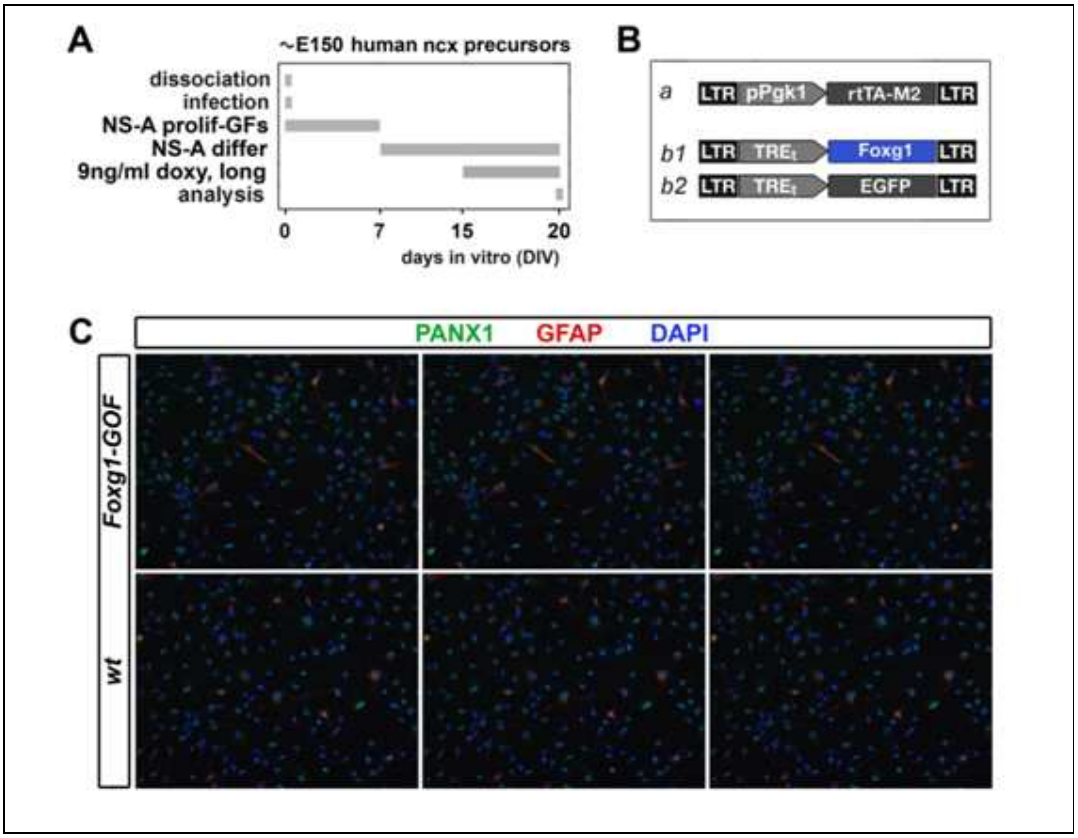

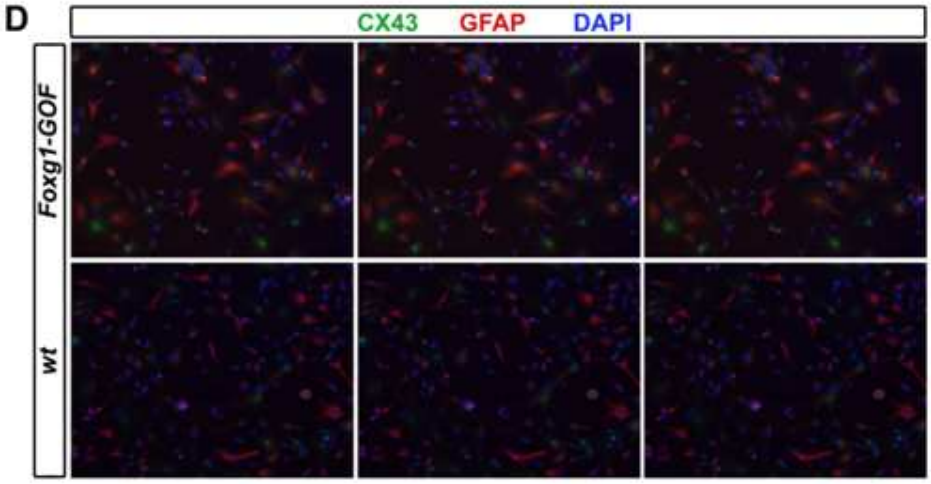

Figure R7. Biased immunoprofiling of astrocytes originating from human pallial precursors gain of function for *Foxg1.* (A,B) Temporal articulation of the assay and lentiviral vectors employed for it. Expression of PANX1 **(C)**, CX43 **(D)** in *Foxg1*-GOF and controls (wt). Throughout the figure, distribution of GFAP immunoreactivity is provided as internal reference.

4.3 Functional correlates of FOXG1 overexpression in human astrocytes [Figures R8-9]

ADK, *CX43* and *mGLUR5* upregulation, by potentiating ATP synthesis, release and its stimulation, respectively, could synergically increase the amount of ATP released by *FOXG1*-GOF astrocytes in the extracellular milieu. That might be a major determinant of neuronal hyperexcitation in WS patients. To address this issue, we compared temporal progression of extracellular ATP concentration, $[ATP]_o$, in cultures of *Foxg1*-GOF and control astrocytes (200,000 cells in 1 ml medium), by a luminometric assay. As expected, we found that *Foxg1* overexpression increased $[ATP]_o$, both 10 and 20 minutes after the initial medium change (75±14 nM vs 28±4 nM, with $p<0.015$ and n=3,3, and 127±7 nM vs 61±13 nM, with $p<0.050$ and n=3,3, respectively) (Figure R8).

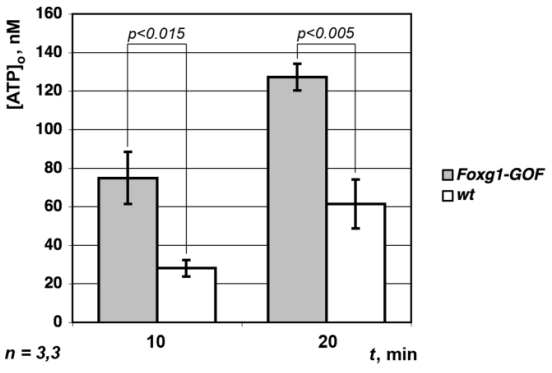

Figure R8. Extracellular ATP release by astrocytes gain-of-function for *Foxg1*. Astrocytes employed for the assays were prepared as described in Figure 7A,B. Pro-differentiative medium was replaced by synthetic medium and, 10 and 20 minutes later, extracellular ATP concentration, $[ATP]_o$, was evaluated by a luminometric assay. *EGFP*-transduced astrocytes were used as "wt" controls. Statistical significance (*p*) evaluated by t-test. *n* is the number of biological replicates

GLAST and GLT-1-mediated L-glutamate uptake from the extracellular space is coupled to Na^+ influx into astrocytes and K^+ exit from these cells, according to a well defined stoichiometry (Kanner and Schuldiner, 1987). Therefore, misregulation of *KIR4.1, ATP1A2* and*ATP1B2* (Figures R5 and R6), in addition to perturbing K^+ fluxes, might ultimately affect the capability of astrocytes to remove L-glutamate from the extracellular space. To address this issue, we compared temporal progression of extracellular glutamate concentration, $[glutamate]_o$, in cultures of *Foxg1*-GOF and control astrocytes (300,000 cells in 0.5 ml medium), upon initial glutamate addition up to 500µM, by a colorimetric assay. As expected, we found that *Foxg1* overexpression reduced the progressive $[glutamate]_o$ decline detectable in controls. In particular, 9 and 12 hours after the onset of the test, $[glutamate]_o$ was 368±5µM vs 292±18µM, with $p<0.007$ and n=3,3, and 364±5µM vs 259±23 µM, with $p<0.006$ and n=3,3, in *Foxg1*-GOF and control cultures, respectively (Figure R9).

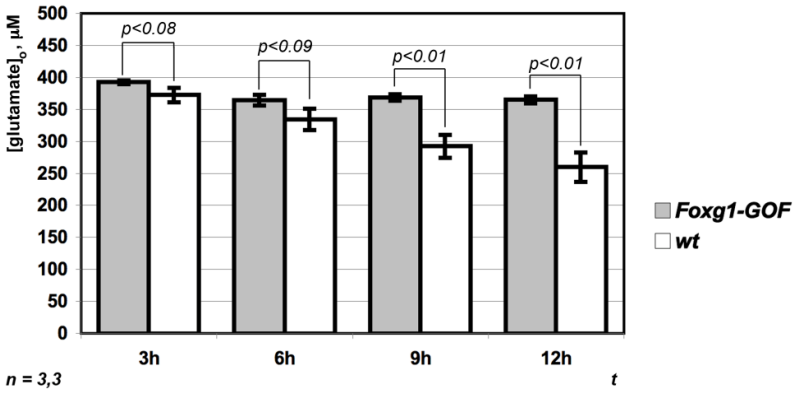

Figure R9. Clearance of extracellular glutamate by astrocytes gain-of-function for *Foxg1*. Astrocytes employed for the assays were prepared as described in Figure 7A,B. Pro-differentiative medium was replaced by DMEM/10% serum supplemented with 500 µM glutamate and, 3, 6, 9 and 12 hours later, extracellular glutamate concentration, $[glutamate]_o$, was evaluated by a colorimetric assay. *EGFP*-transduced astrocytes were used as "wt" controls. Statistical significance (*p*) evaluated by t-test. *n* is the number of biological replicates.

4.4 Generating WS patient-specific pallial tissue via fibroblast reprogramming to iPSCs and iPSCs differentiation to SFEBq's [Figures R10-12]

We wondered to which extent the disfunctions we observed in human wild type astroblasts upon *artificial* manipulation of *FOXG1* expression levels would reproduce what really happens within the developing human embryo with an extra-copy of this gene. In principle, this might be tested in vitro by de-differentiating somatic non-neural cells from WS patients to pluripotent induced stem cells (iPSCs), as described by (Takahashi and Yamanaka, 2006), and further differenting so-obtained pluripotent cells to "serum-free embryoid body quick" (SFEBq) pallium-like organoids, in agreement with the classical (Eiraku et al., 2008) protocol. However, due to the geometrical variability intrinsically associated to SFEBq's (our unpublished results), the capability of these organoids to reproduce subtle histogenetic anomalies caused by an altered *FOXG1* dosage is not granted. Moreover, compared to

mouse, human SFEBq generation is technically demanding and time-consuming. Therefore, to preliminarly assess the feasibility of this approach, we generated *murine* SFEBq's from ESCs made conditionally *Foxg1*-GOF, by lentiviral and TetON technology (Figure R10A). Then we inspected these organoids for three key features relevant to our interests. First, we verified that they are able to activate gliogenesis after neuronogenesis, as it occurs in vivo (Figure R10B). Next, we found that *Foxg1* activation in the neuronal lineage promotes a profound reshaping of neuritic trees, reminiscent of the cytoarchitectonic phenotype occurring in *Foxg1*-GOF *natural* neuronal cells (Brancaccio et al., 2010). Specifically, the arborization index, i.e. the ratio between the number of neuritic end points and soma attachment points, was increased almost three fold ($p<0.001$, $n=3,3$) (Figure R10C-E). Last but not least, *Foxg1* overactivation in neural stem cells, while not impairing neuronogenesis, exerted a powerful inhibitory effect on generation of S100β^+ astrocytes (Figure R10F,G), again as previously described in *natural* neuronal cells (Brancaccio et al., 2010).

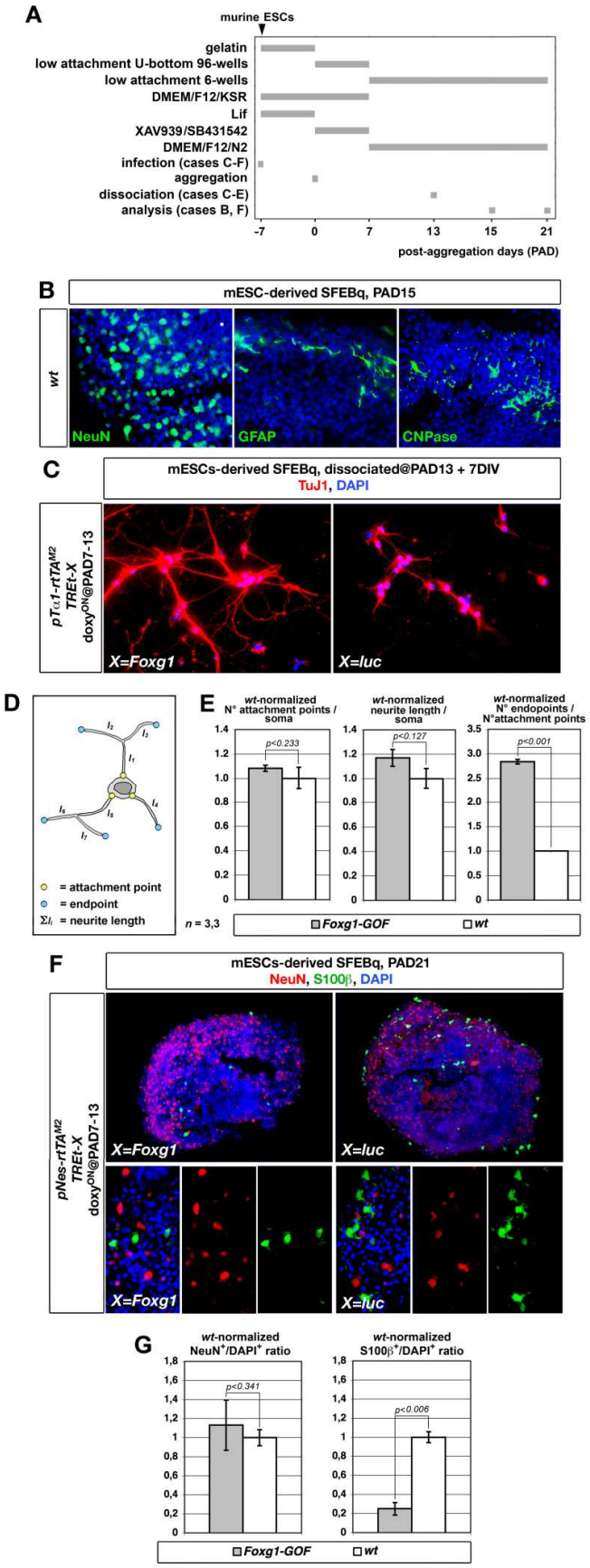
A
murine ESCs
gelatin
low attachment U-bottom 96-wells
low attachment 6-wells
DMEM/F12/KSR
Lif
XAV939/SB431542
DMEM/F12/N2
infection (cases C-F)
aggregation
dissociation (cases C-E)
analysis (cases B, F)
-7
0
7
13
15
21
post-aggregation days (PAD)
B
mESC-derived SFEBq, PAD15
wt
NeuN
GFAP
CNPase
C
mESCs-derived SFEBq, dissociated@PAD13 + 7DIV
TuJ1, DAPI
pTα1-rtTA^M2
TREt-X
doxy^ON@PAD7-13
X=Foxg1
X=luc
D
= attachment point
= endpoint
Σl = neurite length
E
wt-normalized N° attachment points / soma
wt-normalized neurite length / soma
wt-normalized N° endopoints / N°attachment points
p<0.233
p<0.127
p<0.001
n = 3,3
Foxg1-GOF
wt
F
mESCs-derived SFEBq, PAD21
NeuN, S100β, DAPI
pNes-rtTA^M2
TREt-X
doxy^ON@PAD7-13
X=Foxg1
X=luc
G
wt-normalized NeuN+/DAPI+ ratio
wt-normalized S100β+/DAPI+ ratio
p<0.341
p<0.006
Foxg1-GOF
wt

Figure R10. In vitro differentiation of murine ESCs to pallium-like, "serum-free embryoid bodies, quick" (SFEBq). (A) Graphical abstract and temporal articulation of the differentiation procedure. **(B)**. Immunoprofiling of PAD15 SFEBq's for neuronal (NeuN), astrocytic (GFAP) and oligodendrocytic (CNPase) markers. **(C)** Tubβ3 immunoprofiling of neuronal cultures originating from dissociated PAD13 SFEBq cells. Here SFEBq's were generated from ESCs made conditional gain-of-function for *Foxg1* 7 days prior to aggregation, via lentiviral transduction and TetON technology. The $rtTA^{M2}$ transactivator was driven by the neuron-specific *pTα1* promoter. Activation of the *Foxg1* transgene or its control was achieved by doxycycline medium addition, restricted to PAD7-13. **(D,E)** Morphometric analysis of neurons referred to in (C): idealized dendritic trees are schematized in (D), values of key morphometric parameters are shown in (E). Data normalized against "wt" controls. Statistical significance (*p*) evaluated by t-test. *n* is the number of biological replicates.**(F)** Immunoprofiling of PAD21 SFEBq's for neuronal (NeuN) and astrocytic (S100β) markers. Here, SFEBq's were generated as in (C). However, the $rtTA^{M2}$ transactivator was driven by the neural stem cell-specific *pNes* promoter. **(G)** Frequencies of $NeuN^+$ and $S100\beta^+$ cells shown in (F). Data normalization and their statistical analysis as in (E).

Encouraged by these results, we decided to move to generation of *human* SFEBq organoids. For this purpose, we reprogrammed fibroblasts from one WS patient harboring a *FOXG1* duplication to iPSCs, by the classical Yamanaka gene cocktail (Takahashi and Yamanaka, 2006) delivered by engineered Sendai viruses (Fusaki et al., 2009)(Seki et al., 2012). Human wild type fibroblasts from a commercial provider, were used as a positive control. Briefly, for each fibroblast preparation, 100,000 cells were transduced by Sendai viruses and, 7 days later, they were transferred to a feeder carpet under DMEM-F12/KSR/Fgf2 human-iPSC medium. 19-24 days after infection, about 20 colonies were picked. They were individually expanded on feeder cells. One week later, they were stringently screened for morphology and three of them were selected and further expanded. 50 days after picking, presumptive iPSCs were transferred onto matrigel. 15 more days later, they were profiled for pluripotency markers (Figure R11A). mRNAs of *TERT*, *NANOG*, *OCT3/4* and *SOX2* resulted to be upregulated by more than 10 times as compared to naive fibroblasts, in both patient- and control iPSCs (Figure R11C). Moreover, all iPSC preparations were strongly and specifically immunoreactive for NANOG and Tra-1-60 (Figure R11D). Finally,

Sendai virus-specific RNAs, present in freshly picked iPSCs, were progressively lost. They were undetectable by the end of the reprogramming procedure (Figure R11B). In summary, both WS and control fibroblasts gave rise to bona fide iPSC clones, devoid of any remnants of the reprogramming process.

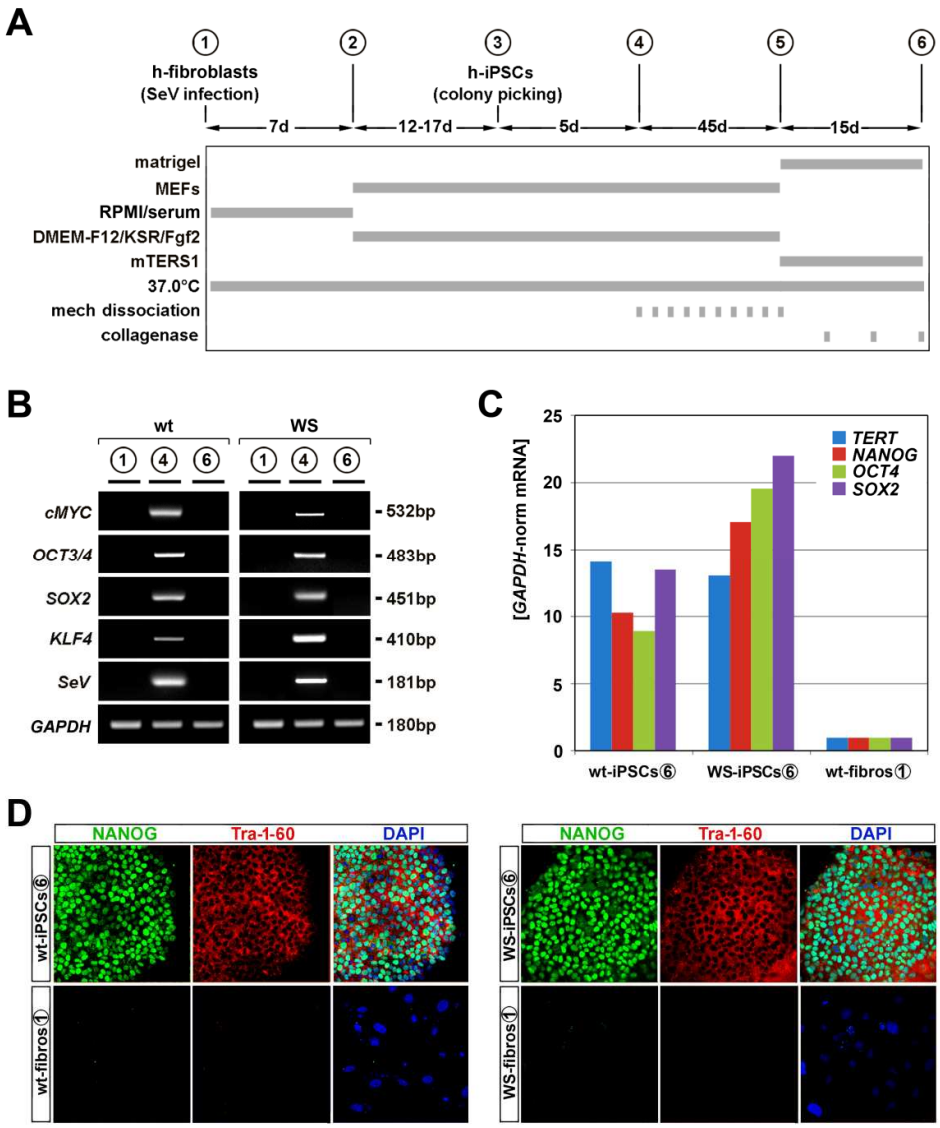

Figure R11. Reprogramming of human fibroblasts from a WS patient and a control individual to induced pluripotent stem cells (iPSCs), by recombinant Sendai viruses (SeV) expressing the Yamanaka gene cocktail. (A) Graphical abstract and temporal articulation of the reprogramming procedure. **(B)** RTPCR detection of SeV-encoded Yamanaka genes (*cMYC*, *OCT3/4*, *SOX2* and *KLF4*) and a SeV-specific tag, at different time

points of the procedure. Normalization against *GAPDH*. **(C)** Expression of endogenous, pluripotency genes *TERT*, *NANOG*, *OCT4* and *SOX2*, by WS-specific and control iPSCs (step 6 of the procedure), as evaluated by qRTPCR. Data double normalized, against *GAPDH* and wt not-reprogrammed fibroblasts. **(D)** Immunoprofiling of WS-specific and control iPSCs (step 6 of the procedure), for pluripotency markers NANOG and Tra-1-60. Not-reprogrammed fibroblasts provided as negative control reference.

Starting from one iPSC clone per type (WS and control), we generated SFEBq organoids, following the (Eiraku et al., 2008) protocol, as modified by (Mariani et al., 2012)(Figure R12A). Inspection of these organoids 30 days after iPSC aggregation (PAD30) revealed generalized activation of the pan-telencephalic marker FOXG1 and expression of the neural-dorsal marker PAX6, confined to presumptive apical precursors lining the "ventricular cavities" (Figure R12B). This suggests that these organoids acquired a genuine pallial identity. Moreover, starting from PAD30 and PAD70, these organoids also expressed the pan-neuronal marker Tubβ3 and the astroglial markers S100β and AldoC, respectively (Figure R12B,C), meaning that the natural neuronogenic-to-astrogenic sequence was implemented.

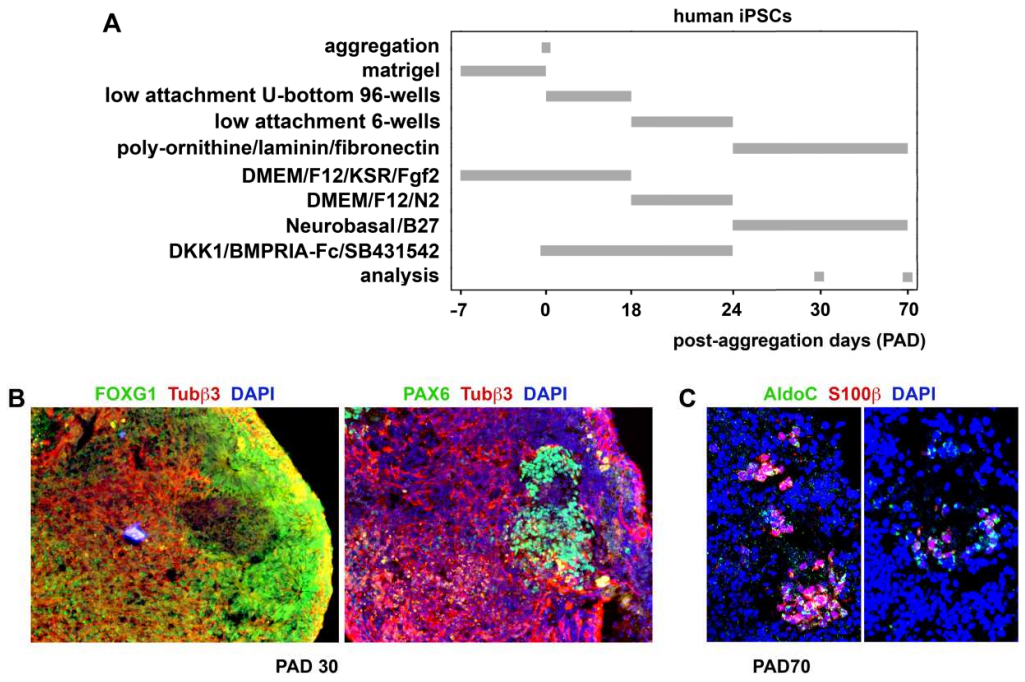

Figure R12. In vitro differentiation of human iPSCs to pallium-like, "serum-free embryoid bodies, quick" (SFEBq). (A) Graphical abstract and temporal articulation of the differentiation procedure. **(B,C)**. Immunoprofiling of SFEBq fixed at different post-aggregation times for selected markers: pan-telencephalic (FOXG1), neural-dorsal (PAX6), pan-neuronal (Tubβ3), astrocytic (AldoC and S100β).

However the frequency of S100β^+AldoC$^+$ cells displayed pronounced variability, even among organoids originating from the same iPSC clone. This variability prevented us from detecting any statistically significant changes of S100β^+AldoC$^+$ cell frequency between WS-type and control organoids (not shown). We suspected that such random variability could arise from geometrical and metabolic contingencies occurring to SFEBq organoids during the prolonged time elapsing from iPSC aggregation to activation of astrogenesis. To circumvent this issue, we dissociated early, PAD25 aggregates (already endowed with anterior-neural identity (Mariani et al., 2012) and cultured the resulting precursor cells on laminin, in a medium supporting proliferation and retention of the stem state (Figure R13A). 45 days later, at an in vitro stage corresponding to PAD70, we profiled these precursors for FOXG1, PAX6, SOX2, GFAP, ALDOC and ALDH1L1. They were immunopositive for all six markers (Figure R13B), regardless of the genotype, suggesting they acquired an identity of late pallial precursors, prone to astrogenesis. Next, we stimulated these precursors to differentiate as astrocytes, by transferring them into a prodifferentiative medium supplemented with Lif (Figure R13A). The vast majority of them activated the S100β astrocytic marker. However, the frequency of S100β^+ cells did not display any statistically significant differences between control- and WS-patient-samples (Figure R13C).

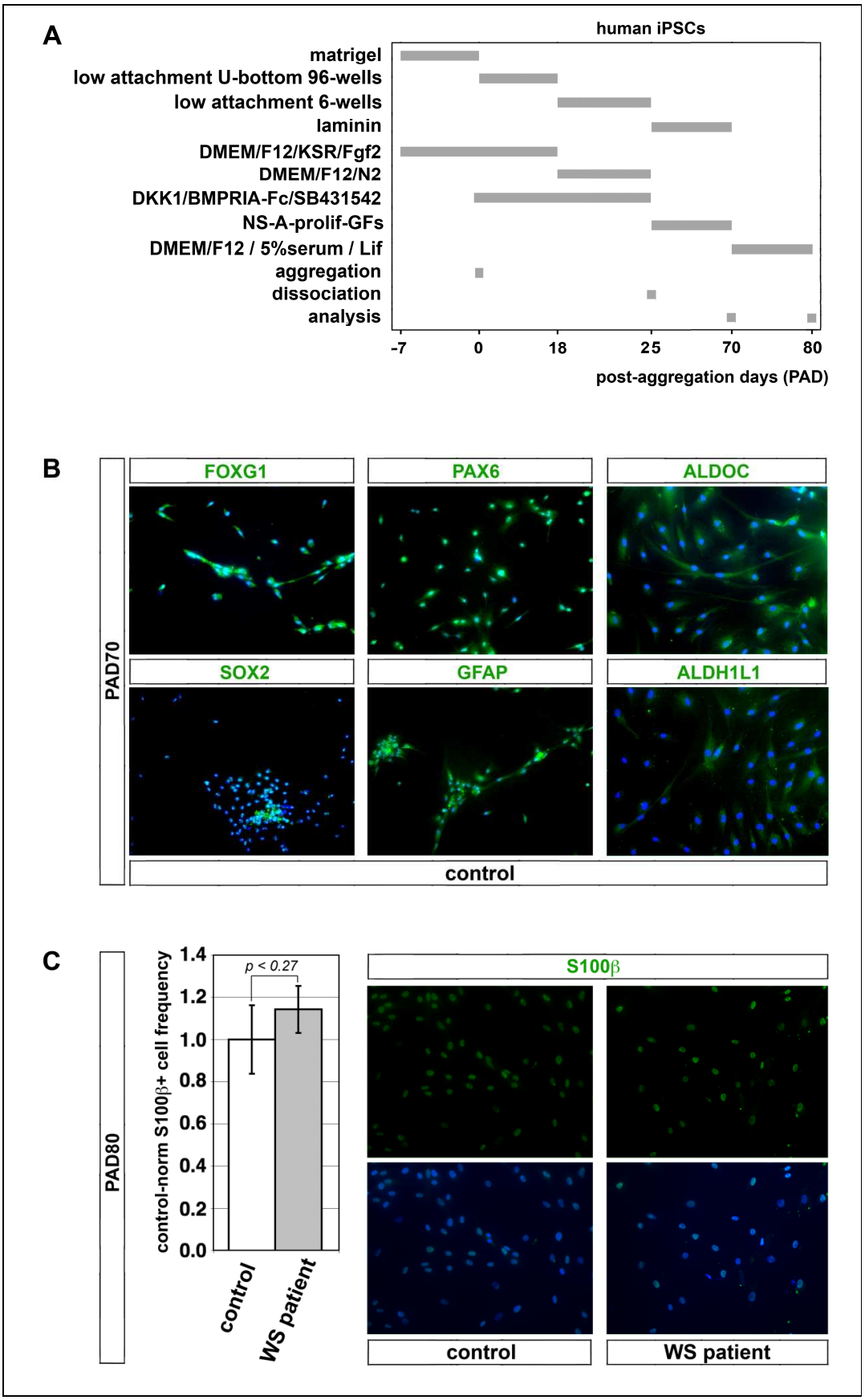
A
human iPSCs
matrigel
low attachment U-bottom 96-wells
low attachment 6-wells
laminin
DMEM/F12/KSR/Fgf2
DMEM/F12/N2
DKK1/BMPRIA-Fc/SB431542
NS-A-prolif-GFs
DMEM/F12 / 5%serum / Lif
aggregation
dissociation
analysis
-7
0
18
25
70
80
post-aggregation days (PAD)
B
PAD70
FOXG1
PAX6
ALDOC
SOX2
GFAP
ALDH1L1
control
C
PAD80
control-norm S100β+ cell frequency
1.4
1.2
1.0
0.8
0.6
0.4
0.2
0.0
p < 0.27
control
WS patient
S100β
control
WS patient

Figure R13. Generation of human, pallial-like radial glia and its differentiation to astrocytes. (A) Graphical abstract and temporal articulation of the procedure.**(B)** Coexpression of a panel of markers peculiar to pallial radial glia (FOXG1, PAX6, SOX2, GFAP, ALDOC, ALDH1L1) by neural precursors originating from human control iPSCs as in (A). **(C)** Control-normalized activation rates of the astrocytic marker S100β in derivatives of neural precursors originating from WS patient- and control-iPSCs. Absolute frequency of S100β^+ cells was 0.73±0.12 in controls.

4.5 *FOXG1* upregulation in human pallial astrocytes exposed to high extracellular K^+ [Figure R14]

We have found that astrocytes overexpressing *FOXG1* may undergo exaggerated release and/or diminished uptake of excitatory glio- and neuro-transmitters. If astrocyte stimulation would - in turn - upregulate *FOXG1*, this could result in a prominent positive loop, exacerbating aberrant consequences of increased *FOXG1* dosage. To preliminary address this issue, we challenged human *FOXG1* wild type astrocytes, generated as in Figure R1A, by 50mM K^+ and measured *FOXG1*-mRNA levels. Remarkably, this level was increased by 2.66±0.23 ($p<0.002$, n=4,4) 6 hours after ion addition and by 1.81±0.03 ($p<0.028$, n=4,3) 6 more hours later, suggesting that our suspicion was correct (Figure R14).

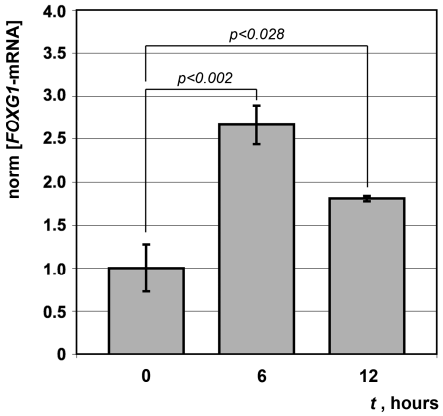

Figure R14. FOXG1 upregulation by extracellular K^+ in human astrocytes. Astrocytes, originating from human embryonic pallial precursors kept under "NS-A-differentiation medium" for 7 days, were challenged by extracellular 50mM [K^+], for 6 and 12 hours. *FOXG1*-mRNA was evaluated by qRTPCR. Data double normalized, against *GAPDH* and *t*=0 controls. Statistical significance (*p*) evaluated by t-test. *n* is the number of biological replicates.

5. DISCUSSION

Our study aimed at clarifying the impact of *FOXG1* overexpression on genesis and differentiation of cortico-cerebral astrocytes, as a first step towards the etiopathogenic dissection of the complex neurological dysfunctions peculiar to the *FOXG1*-duplication associated West syndrome.

We (1) monitored the impact of *FOXG1* overexpression in pallial precursors on general advancement of astrocytic differentiation. This was primarily done in cultures of human, wild type cortico-cerebral precursors, where *FOXG1* levels were manipulated by integrated lentiviral, TetON and RNAi technologies. Additionally, patient-specific fibroblasts and controls were dedifferentiated to iPSCs, which were used - in turn - as starting material for generation of organotypic cortico-cerebral cultures. It resulted from these studies that *FOXG1* overexpression antagonizes the advancement of astrocytic differentiation, in humans as previously described in mice.

We (2) investigated consequences of *FOXG1* overexpression on more specific aspects of astrocyte differentiation, linked to modulation of neuronal function. We approached this issue by an integrated design, including: (a) mRNA profiling of a small gene set implicated in astrocyte modulation of neuronal activity, (b) immunofluorescence analysis of a subset of their protein products, and (c) evaluation of select functional correlates of their activity. Briefly, we found: (a) an impairment of extracellular K^+ clearance machinery, (b) a defective capability to remove extracellular glutamate, (c) an upregulation of glutamate sensors and (d) anomalies in purinergic gliotransmitters, pointing to increased ATP/adenosine signaling ratio.

We (3) looked at consequences of neuronal activity on astrocytic *FOXG1* expression levels. We found that high $[K^+]_o$, mimicking sustained neuronal firing, in turn stimulates *FOXG1* expression.

Collectively, findings referred to at points (1) and (2) suggest that *FOXG1* overexpression may hamper the astrocytic control of neuronal

excitability, leading to neuronal hyperactivity. In turn, phenomena referred to in (3) further suggest that this may ignite a vicious loop, possibly exacerbating consequences of increased *FOXG1* gene dosage.

****

Our initial assessment of astrogenesis progression was largely based on immunoprofiling for S100β, preferentially expressed in grey matter protoplasmic astrocytes (Bignami et al., 1972), and was backed by inspection of AldoC, namely a pan-astrocytic lineage marker (Cahoy et al., 2008). We could not employ the alternative marker Gfap, active in rodent white matter fibrous astrocytes (Vaughn and Peters, 1967), as in primates this gene is also expressed by neural stem cells and astrocyte committed progenitors (Kriegstein and Alvarez-Buylla, 2009).

The *Foxg1*-evoked reduction of astrogenesis rates we found in this study is somehow reminiscent of a similar phenomenon previously reported in cultures of rodent pallial precursors overexpressing this gene (Brancaccio et al., 2010). However, in case of rodent cultures the reduction of the S100β^{+} astrocytic output has a dual origin. In fact, it reflects an inhibition of (1) the transition from Nesp-Egfp^{+}A2B5^{-} neural stem cells (NSCs) to A2B5^{+}PSANCAM^{-}Nesp-Egfp^{+}early glioblasts (eGPs), and the blockade of (2) further maturation of eGPs to more advanced A2B5^{+}PSANCAM^{-}Nesp-Egfp^{-} glial progenitors. Conversely, almost all pallial precursors subject of this study already expressed the pan-astrocytic markers AldoC and Aldh1L1, suggesting that step (1) was not accessible to the present investigation, while step (2) is modulated by *Foxg1* in primates similarly to rodents.

The kinetic anomalies we detected in human pallial precursors made *artificially* GOF for *Foxg1* were not replicated in derivatives of pallial organoids obtained via generation of WS-patient iPSCs and their differentiation. Reasons potentially undelying this discrepancy are variegated. Among them there is the random geometric variability of SFEBq aggregates (even if sharing the same genotype), as well as the stochastic epigenetic aberrancies which may affect single iPSC clones (associated to incomplete reprogramming and/or genomic instability). In fact, each radial glia preparation

we assayed originated from as little as two SFEBq aggregates. Moreover, our analysis was restricted to derivatives of *only one* iPSC clone per genotype. Scoring a much wider sample (e.g., 4 iPSC clones for genotype and 4 SFEBq aggregates per iPSC clone) and checking carefully the *FOXG1* copy number of SFEBq cells could help fix this issue. Beyond these technical issues, chronic *FOXG1* overexpression in patient-specific pre-astrogenic precursors might antagonize their early neuronal differentiation, so leading to a larger proliferating pool suitable to undergo astroglial differentiation (Hanashima et al., 2002). This might compensate for the intrinsic capability of *FOXG1* to counteract astrogenesis progression (Brancaccio et al., 2010), eventually resulting in an apparently normal S100β^+ complement. The articulation of the *human* preastrogenic pallial histogenesis over a high number of cell cycles (at least 3 times more than in mice; (Caviness et al., 2009) (Betizeau et al., 2013) makes this mechanism quite likely.

As for molecular mechanisms mediating *Foxg1*-dependent dampening of astroglial differentiation, we suspect that at least 2 distinct signalling pathways may be involved: the Bmp and the Tgfβ cascades. The former synergyzes with pStat3 in transactivating astroglial genes (Wen et al., 2009); the latter dictates conversion of late neuronogenic radial glia into astrocytes (Stipursky et al., 2014). *Foxg1* represses synthesis of Bmp4 (Dou et al., 1999), Bmp6 and Bmp7 (Hanashima et al., 2002). Moreover, it titrates Smad1, Smad2 and Smad4, preventing them from stimulating their targets (Rodriguez et al., 2001). Paradoxically, *Foxg1* also upregulates *Hes1* (Brancaccio et al., 2010), which, in turn, has been recognized for a long time as a key proastrogenic effector, which scaffolds Stat3 to Jak2 (Kamakura et al., 2004) and inhibits the antiastrogenic *Neurogenin*s (Nieto et al., 2001). We plan to address these issues in a future, dedicated study.

It was previously shown that, upon structured *Foxg1* overexpression in NSCs and neuronal progenitors followed by precursors exposure to differentiating cues, a pronounced increase of neuronal outputs takes place (see Figure 7A of (Brancaccio et al., 2010). Together with impaired astrogenesis, this may contribute to reduce the astrocyte-to-neuron ratio

(A/N), which may lead to complex emerging consequences. Among these, there is the defective clearance of ions and excitatory neurotransmitters released by discharging neurons, ultimately sustaining neuron hyperexcitability. It is possible that the A/N decline evoked by *Foxg1* overexpression is tempered in vivo. Astrogenesis rates - in fact - are tuned by two key signals coming from neurons: Ct1, which triggers the cardinal cytokine pathway promoting the astrogenic program (Barnabé-Heider et al., 2005), and Fgf9, sustaining proliferation of astrocyte progenitors (Tarabykin et al., 2001)(Falcone et al., 2015). Therefore, an increase of the neuronal population might lead to a compensating enlargement of the astrocyte pool. However, after birth, astrocytes also stimulate their own differentiation, thanks to the secretory product of the *Cntf* gene (Song and Ghosh, 2004). In this way, an even modest, initial defect of astrocyte generation might be exponentially amplified in vivo. A rodent *Foxg1* gain-of-function model is definitively needed to assay the final prevailing effect emerging in the living animal. On the other side, the clonal articulation of cortical histogenesis is much more complex in primates compared to rodents (Fietz et al., 2010)(Kriegstein et al., 2006)(Dehay et al., 2015). Therefore further validation in organotypic primate models will be needed, to secure the relevance of our findings to the etiopathogenesis of WS syndrome.

****

After bursts of neuronal discharge, astrocytes take care of K^+ removal from the extracellular space, which is crucial to proper tuning of neural tissue excitability. Three main molecular players are involved in this task, the sodium-potassium plasmamembrane pump Na^+K^+ATPase, the potassium inward rectifying channel Kir4.1 and the sodium-potassium-chloride cotransporter NKCC1. Their contributionsto K^+ influx into astrocytes depend on $[K^+]_o$. Na^+K^+ATPase predominates at lower $[K^+]_o$, (50% of K^+ flux at 1mM, only 20% at 30mM). NKCC1 activity prevails at higher $[K^+]_o$ (10% of K^+ flux at 1mM, 40% at 30mM). Kir4.1 might mediate up to 1/3 of this flux, regardless of $[K^+]_o$ (Larsen et al., 2014). Moreover, among the different Na^+K^+ATPase isoforms, the α2β2 displays an increase of K^+ affinity in depolarized cells (Larsen et al., 2014). We monitored expression levels of mRNAs encoding for

these players in engineered astrocytes. *Foxg1* resulted to inhibit *KIR4.1* expression, according to both GOF and LOF assays (Figures R5 and R6). It also antagonized *NKCC1* expression in a LOF assay (Figure R6), however the slight downregulation occurring upon *Foxg1* overexpression, -12%, did not reach statistical significance (Figure R5). *Foxg1* overexpression also upregulated mRNAs of Na^+K^+ATPase-α2 and -β2 (Figure R5). However, *FOXG1* knock-down, while not affecting β2 mRNA (Figure R6), elicited a paradoxical upregulation of α2 (Figure R5), suggesting that α2 upregulation observed in *Foxg1*-GOF astrocytes might originate from a dominant negative effect. In conclusion, we hypothesize that *FOXG1* overexpression, downregulating *KIR4.1* and - possibly - *NKCC1*, may severely jeopardize astrocytic K^+ uptake, leading to increased excitability of neural tissue.

After bursts of neuronal discharge, astrocytes also remove the excess of glutamate from the extracellular space, which - again -is needed to dampen neural tissue excitability. In this respect, we monitored expression levels of the two GLAST (EAAT1) and GLT-1 (EAAT2) glutamate transporters (Lehre et al., 1995), as well as of the Glutamine Synthetase (GS) enzyme (Shigeri et al., 2004). The first two take care of translocating glutamate and aspartate across the astrocyte plasmamembrane. The last one converts glutamate into glutamine within the astrocytic cytoplasm, so securing clearance of this neurotransmitter and paving the way to the synthesis of the GABA inhibitory neurotransmitter. None of these genes was apparently misregulated. However, glutamate transport through the astrocyte plasmamembrane is coupled to translocation of Na^+ towards cell interior and H^+ and K^+ towards cell exterior, according to the 1*glutamate/3*Na^+/1*K^+/1*H^+ stoichiometry ((Levy et al., 1998)(Owe et al., 2006). As such, glutamate transport tightly depends on ion gradients and an increase of $[K^+]_o$ may slow down or even reverse it (Levy et al., 1998). For this reason and following potential K^+ uptake anomalies inferred above, we monitored the actual capability of *FOXG1*-GOF astrocytes to remove glutamate from the extracellular space. As suspected, this capability resulted to be severely compromised, which may synergize with presumptive K^+ uptake disorders so exacerbating neural tissue excitability.

Extracellular glutamate acts not only on neurons (both synaptically and extrasynaptically), but also on astrocytes, mainly via stimulation of metabotropic glutamate receptors 5 and 1 (mGluR5 and mGluR1)(Devinsky et al., 2013)(Hamilton and Attwell, 2010). In this way, it promotes cytoplasmic Ca^{2+} waves, which in turn trigger further excitatory gliotransmitters release (Devinsky et al., 2013)(Hamilton and Attwell, 2010). *FOXG1* resulted to robustly upregulate mGluR5 expression, according to both GOF and LOF tests. This suggests that an increased *FOXG1* gene dosage not only leads to higher $[glutamate]_o$, but also makes astrocytes more sensitive to this transmitter, so priming a harmful vicious loop.

ATP is a key neuro- and glio-transmitter. It acts on purinergic 2 (P2) receptors, including ionotropic $P2X_{1-7}$ and metabotropic $P2Y_{1-14}$ receptors. Stimulation of the former ones allows the influx of a variety of cations, among which Na^+ and Ca^{2+}. Stimulation of the latter ones mainly leads to cytoplasmic cAMP and Ca^{2+} upregulation. In this respect, we found a more than doubled ATP concentration in the supernatant of *FOXG1*-GOF astrocytes. We presently ignore mechanisms leading to this phenotype. There was no evidence of increased ATP synthesis or degradation. The astrocyte ATP content did not arise upon Foxg1 overexpression (Figure D1).

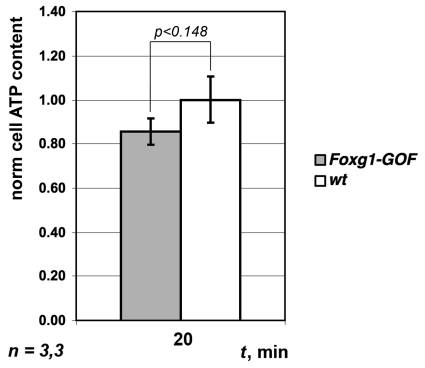

Figure D1. Unchanged ATP content of human *Foxg1*-GOF astrocytes. ATP content of lysates of astrocytes referred to in Figure R8, normalized values. Absolute average content of control samples was 66 nmol/200,000 cells.

The two enzymes ENTPDase2, converting extracellular ATP into the stable excitatory ADP metabolite, and ENTPDase1, initiating fast degradation of ATP to the inhibitory adenosine catabolite (Robson et al., 2006) were not misregulated. Hence we propose that an enhanced ATP release could have occurred. Regardless of the underlying mechanism, we suspect that an elevation of extracellular [ATP] triggered by *FOXG1* overexpression may significantly contribute to overexcitability of astrocytes (and associated neurons).

Adenosine is another key neuro- and glio-transmitter. It acts on purinergic 1A (P1A), metabotropic receptors. These include $P1A_1$ and $P1A_3$, downregulating cytoplasmic [cAMP] and $P1A_{2A}$ and $P1A_{2B}$, upregulating it. The prevailing adenosine impact on neural cells is inhibitory, as emerging from a large body of literature showing a tight association between depletion of the adenosine pool and increased excitability, in vitro as well as in vivo (Devinsky et al., 2013). Actually, we did not get any evidence of altered ATP-to-adenosine conversion upon *Foxg1* overexpression. Conversely, we found that the gene encoding for the key cytoplasmic enzyme phosphorylating adenosine, ADK, was upregulated by +25%. This might reduce adenosine availability, so contributing to neural cells hyperexcitability. Experimental measure of this gliotransmitter is definitively needed to corroborate this hypothesis.

CX43 and *CX30* encode for the building blocks of astrocyte hemichannels. These structures may stand alone as such or may juxtapose to hemichannels of adjacent astrocytes, so forming gap junctions. Hemichannels are permeable to small molecules and may mediate regulated release of excitatory gliotransmitters (Stout and Charles, 2003);(Ye et al., 2003)(Orellana and Stehberg, 2014). Gap junctions connect cytosols of adjacent astrocytes, giving rise to large syncitia, which exert a profound impact on physiology of neural tissue. Within these syncitia, cytoplasmic Ca^{2+} waves propagate over relatively long distances, allowing for large scale coordinated release of excitatory gliotransmitters. This may help synchronizing the electric activity of wide neuronal aggregates surrounded by these astrocytes (Kékesi et al., 2015). Within these syncitia, K^+ translocated from the extracellular space into

astrocyte cytosol after bursts of neuronal activity may diffuse, so allowing for so-called "spatial buffering" of K^+ transients (Wallraff et al., 2006)(Kozoriz et al., 2006)(Xu et al., 2009). We found that *Foxg1* overexpression led to a robust upregulation of *CX43*, as well as of *PANX1* (implicated in formation of hemichannels, but not included in gap junctions). *FOXG1* knock-down did not replicate this phenomenon, suggesting that it reflected a genuine gain-of-function effect. Moreover, at least in case of *CX43*, mRNA upregulation was accompanied by a consistent increase of its protein product, as easily detectable by immunofluorescence. We envisage that such *CX43* upregulation may affect neuronal activity in four main ways. First, it may facilitate hemichannel-mediated release of excitatory gliotransmitters. This might underlie the increased $[ATP]_o$ we detected in *FOXG1*-GOF cultures. Next, it may lead to neuronal hypersynchronization, thanks to stronger intrasyncitial propagation of Ca^{2+} waves and inclusion of a higher number of astrocytes in each syncitium. This could account for giant interictal EEG waves specifically characterizing WS patients. Third, *CX43* upregulation could ease spatial buffering of K^+, so limiting the neuronal hyperexcitability triggered by other concurrent mechanisms. Finally, astrocytic CX43 enhances glutamatergic transmission per se, by increasing pre-synaptic quantal neurotransmitter release (Chever et al., 2010).

In summary, we have got evidences that increased *FOXG1* expression affects astrocyte generation, in humans similarly to rodents, and specifically antagonizes key genes needed for astrocyte-dependent clearance of excitatory transmitters and potassium. Moreover, we discovered that high $[K^+]_o$ in turn upregulates *FOXG1* itself. Altogether, these findings help figuring out how an increased *FOXG1* dosage may jeopardize astrocyte control of neuronal activity, so leading to dramatic neurological aberrancies peculiar to the WS syndrome. Such astrocyte involvement in WS etiopathogenesis is of obvious operational interest. On one hand, it suggests a number of novel, potential therapeutic targets. On the other, confinement of astrogenesis to late gestational and early neonatal age makes this syndrome potentially amenable to preventive gene therapy.

6. SUPPLEMENTARY MATERIAL

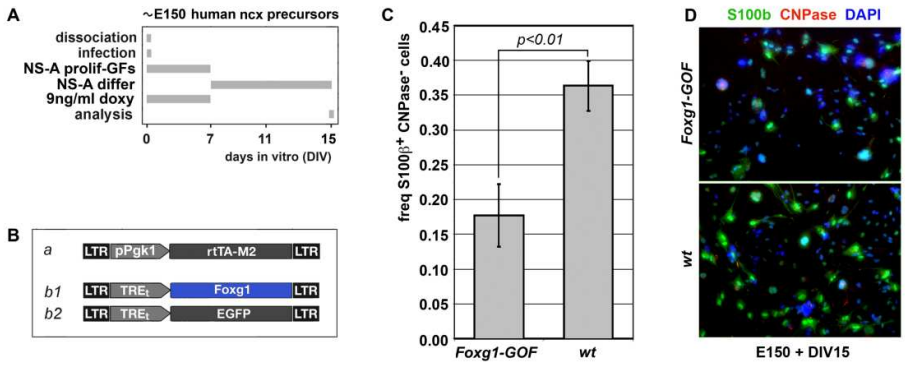

Supplementary Figure S1. Inhibition of astrogenesis upon *Foxg1* overexpression in human pallial precursors. (A,B) Temporal articulation of the assay and lentiviral vectors employed for it. Please notice that, differently from Figure R2A, here doxycycline was restricted to days in vitro 0 through 7. **(C)** Absolute frequencies of S100β^{+}CNPase^{-} astrocytes in *Foxg1*-GOF and control cultures at DIV15. Statistical significance (*p*) evaluated by t-test. *n* is the number of biological replicates.**(D)** Example of S100β^{+}CNPase^{-} astrocytes referred to in (C).

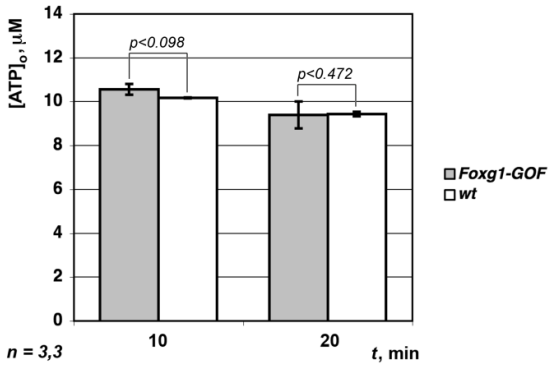

Supplementary Figure S2. Buffering of extracellular ATP by astrocytes gain-of-function for *Foxg1*. The assay was performed as described in Figure 8. However here cells were challenged by adding 10µM ATP to the medium at t=0.

ACKNOWLEDGEMENTS

It would not have been possible to write this doctoral thesis without the help and support of the kind people around me.

I would like to express my sincere gratitude to my supervisor, Antonello Mallamaci, for his meaningful assistance, enthusiasm, encouragement, tireless guidance, patience and for pushing me farther than I thought I could go.

I want to thank some people who partially contribute to this work: Stefano Pluchino (Cambridge, UK) for the human pallial precursor cells; Milka Pringsheim and collaborators in Schön Klinik Vogtareuth-Neuropaediatrics Clinic (Germany) for the possibility to have a skin biopsy and the family of the West' patient who accepted this surgery; GianMaria Severini (Burlo, Trieste) for teaching me how to generate a human fibroblast culture from a skin biopsy; Luca Braga for his technical support at the luminometer (ICGEB, Trieste); Manuela Santo, my master thesis' student, for helping me with the experiments of this last year especially the approach of Loss of function; all technical staff in Sissa for their support.

My deepest thanks go to all the people of the Mallamaci's lab that helped me and supported me during these years of PhD, creating a really very nice atmosphere in the lab. In particular, Marilena and Cristina for being two precious friends ("le mie ciccine").

Thanks also to Elena and Riccardo for all time spent together and for our Sissa's parties. I hope to meet you soon.

Finally, I want to say thank you to all my family and my love Alessio who suffered all my neurotic outbursts and depression in hard moment of this project.

REFERENCES

Alcamo, E.A., Chirivella, L., Dautzenberg, M., Dobreva, G., Fariñas, I., Grosschedl, R., and McConnell, S.K. (2008). Satb2 regulates callosal projection neuron identity in the developing cerebral cortex. Neuron *57*, 364–377.

Alcántara, S., Ruiz, M., D'Arcangelo, G., Ezan, F., de Lecea, L., Curran, T., Sotelo, C., and Soriano, E. (1998). Regional and cellular patterns of reelin mRNA expression in the forebrain of the developing and adult mouse. J. Neurosci. Off. J. Soc. Neurosci. *18*, 7779–7799.

Alvarez-Buylla, A., García-Verdugo, J.M., and Tramontin, A.D. (2001). A unified hypothesis on the lineage of neural stem cells. Nat. Rev. Neurosci. *2*, 287–293.

Amor, D.J., Burgess, T., Tan, T.Y., and Pertile, M.D. (2012). Questionable pathogenicity of FOXG1 duplication. Eur. J. Hum. Genet. *20*, 595–596.

Anderson, S.A. (2002). Determination of cell fate within the telencephalon. Chem. Senses *27*, 573–575.

Anderson, C.M., and Swanson, R.A. (2000). Astrocyte glutamate transport: review of properties, regulation, and physiological functions. Glia *32*, 1–14.

Angevine, J.B., and Sidman, R.L. (1961). Autoradiographic study of cell migration during histogenesis of cerebral cortex in the mouse. Nature *192*, 766–768.

Angulo, M.C., Kozlov, A.S., Charpak, S., and Audinat, E. (2004). Glutamate released from glial cells synchronizes neuronal activity in the hippocampus. J. Neurosci. Off. J. Soc. Neurosci. *24*, 6920–6927.

Aronica, E., Gorter, J.A., Jansen, G.H., van Veelen, C.W.M., van Rijen, P.C., Ramkema, M., and Troost, D. (2003). Expression and cell distribution of group I and group II metabotropic glutamate receptor subtypes in taylor-type focal cortical dysplasia. Epilepsia *44*, 785–795.

Aronica, E., Zurolo, E., Iyer, A., de Groot, M., Anink, J., Carbonell, C., van Vliet, E.A., Baayen, J.C., Boison, D., and Gorter, J.A. (2011). Upregulation of adenosine kinase in astrocytes in experimental and human temporal lobe epilepsy. Epilepsia *52*, 1645–1655.

Bao, B.A., Lai, C.P., Naus, C.C., and Morgan, J.R. (2012). Pannexin1 drives multicellular aggregate compaction via a signaling cascade that remodels the actin cytoskeleton. J. Biol. Chem. *287*, 8407–8416.

Barnabé-Heider, F., Wasylnka, J.A., Fernandes, K.J.L., Porsche, C., Sendtner, M., Kaplan, D.R., and Miller, F.D. (2005). Evidence that embryonic neurons regulate the onset of cortical gliogenesis via cardiotrophin-1. Neuron *48*, 253–265.

Barnes, A.P., Solecki, D., and Polleux, F. (2008). New insights into the molecular mechanisms specifying neuronal polarity in vivo. Curr. Opin. Neurobiol. *18*, 44–52.

Bertossi, C., Cassina, M., De Palma, L., Vecchi, M., Rossato, S., Toldo, I., Donà, M., Murgia, A., Boniver, C., and Sartori, S. (2014). 14q12 duplication including FOXG1: is there a common age-dependent epileptic phenotype? Brain Dev. *36*, 402–407.

Betizeau, M., Cortay, V., Patti, D., Pfister, S., Gautier, E., Bellemin-Ménard, A., Afanassieff, M., Huissoud, C., Douglas, R.J., Kennedy, H., et al. (2013). Precursor diversity and complexity of lineage relationships in the outer subventricular zone of the primate. Neuron *80*, 442–457.

Bezzi, P., Carmignoto, G., Pasti, L., Vesce, S., Rossi, D., Rizzini, B.L., Pozzan, T., and Volterra, A. (1998). Prostaglandins stimulate calcium-dependent glutamate release in astrocytes. Nature *391*, 281–285.

Bezzi, P., Gundersen, V., Galbete, J.L., Seifert, G., Steinhäuser, C., Pilati, E., and Volterra, A. (2004). Astrocytes contain a vesicular compartment that is competent for regulated exocytosis of glutamate. Nat. Neurosci. *7*, 613–620.

Bhat, K.M., van Beers, E.H., and Bhat, P. (2000). Sloppy paired acts as the downstream target of wingless in the Drosophila CNS and interaction between sloppy paired and gooseberry inhibits sloppy paired during neurogenesis. Dev. Camb. Engl. *127*, 655–665.

Bignami, A., Eng, L.F., Dahl, D., and Uyeda, C.T. (1972). Localization of the glial fibrillary acidic protein in astrocytes by immunofluorescence. Brain Res. *43*, 429–435.

Blume, W.T., and Dreyfus-Brisac, C. (1982). Positive rolandic sharp waves in neonatal EEG; types and significance. Electroencephalogr. Clin. Neurophysiol. *53*, 277–282.

Boison, D. (2012). A scaffold as a platform for new therapies? Epilepsy Curr. Am. Epilepsy Soc. *12*, 172–173.

Bourguignon, C., Li, J., and Papalopulu, N. (1998). XBF-1, a winged helix transcription factor with dual activity, has a role in positioning neurogenesis in Xenopus competent ectoderm. Dev. Camb. Engl. *125*, 4889–4900.

Brancaccio, M., Pivetta, C., Granzotto, M., Filippis, C., and Mallamaci, A. (2010). Emx2 and Foxg1 Inhibit Gliogenesis and Promote Neuronogenesis. STEM CELLS *28*, 1206–1218.

Braun, N., Sévigny, J., Robson, S.C., Enjyoji, K., Guckelberger, O., Hammer, K., Di Virgilio, F., and Zimmermann, H. (2000). Assignment of ecto-nucleoside triphosphate diphosphohydrolase-1/cd39 expression to microglia and vasculature of the brain. Eur. J. Neurosci. *12*, 4357–4366.

Britanova, O., Alifragis, P., Junek, S., Jones, K., Gruss, P., and Tarabykin, V. (2006). A novel mode of tangential migration of cortical projection neurons. Dev. Biol. *298*, 299–311.

Brunetti-Pierri, N., Paciorkowski, A.R., Ciccone, R., Della Mina, E., Bonaglia, M.C., Borgatti, R., Schaaf, C.P., Sutton, V.R., Xia, Z., Jelluma, N., et al. (2011). Duplications of FOXG1 in 14q12 are associated with developmental epilepsy, mental retardation, and severe speech impairment. Eur. J. Hum. Genet. EJHG *19*, 102–107.

Bulchand, S., Grove, E.A., Porter, F.D., and Tole, S. (2001). LIM-homeodomain gene Lhx2 regulates the formation of the cortical hem. Mech. Dev. *100*, 165–175.

Bulfone, A., Smiga, S.M., Shimamura, K., Peterson, A., Puelles, L., and Rubenstein, J.L. (1995). T-brain-1: a homolog of Brachyury whose expression defines molecularly distinct domains within the cerebral cortex. Neuron *15*, 63–78.

Burnstock, G. (2007). Purine and pyrimidine receptors. Cell. Mol. Life Sci. CMLS *64*, 1471–1483.

Bystron, I., Blakemore, C., and Rakic, P. (2008). Development of the human cerebral cortex: Boulder Committee revisited. Nat. Rev. Neurosci. *9*, 110–122.

Cahoy, J.D., Emery, B., Kaushal, A., Foo, L.C., Zamanian, J.L., Christopherson, K.S., Xing, Y., Lubischer, J.L., Krieg, P.A., Krupenko, S.A., et al. (2008). A transcriptome database for astrocytes, neurons, and oligodendrocytes: a new resource for understanding brain development and function. J. Neurosci. Off. J. Soc. Neurosci. *28*, 264–278.

Calegari, F., and Huttner, W.B. (2003). An inhibition of cyclin-dependent kinases that lengthens, but does not arrest, neuroepithelial cell cycle induces premature neurogenesis. J. Cell Sci. *116*, 4947–4955.

Caviness, V.S., Nowakowski, R.S., and Bhide, P.G. (2009). Neocortical neurogenesis: morphogenetic gradients and beyond. Trends Neurosci. *32*, 443–450.

Chen, Y., Warner, J.D., Yule, D.I., and Giovannucci, D.R. (2005). Spatiotemporal analysis of exocytosis in mouse parotid acinar cells. Am. J. Physiol. Cell Physiol. *289*, C1209–C1219.

Chever, O., Djukic, B., McCarthy, K.D., and Amzica, F. (2010). Implication of Kir4.1 channel in excess potassium clearance: an in vivo study on anesthetized glial-conditional Kir4.1 knock-out mice. J. Neurosci. Off. J. Soc. Neurosci. *30*, 15769–15777.

Cobos, I., Puelles, L., and Martínez, S. (2001). The avian telencephalic subpallium originates inhibitory neurons that invade tangentially the pallium (dorsal ventricular ridge and cortical areas). Dev. Biol. *239*, 30–45.

Collignon, F., Wetjen, N.M., Cohen-Gadol, A.A., Cascino, G.D., Parisi, J., Meyer, F.B., Marsh, W.R., Roche, P., and Weigand, S.D. (2006). Altered expression of connexin subtypes in mesial temporal lobe epilepsy in humans. J. Neurosurg. *105*, 77–87.

Coulter, D.A., and Eid, T. (2012). Astrocytic regulation of glutamate homeostasis in epilepsy. Glia *60*, 1215–1226.

D'Ambrosio, R., Gordon, D.S., and Winn, H.R. (2002). Differential role of KIR channel and Na(+)/K(+)-pump in the regulation of extracellular K(+) in rat hippocampus. J. Neurophysiol. *87*, 87–102.

Danesin, C., Peres, J.N., Johansson, M., Snowden, V., Cording, A., Papalopulu, N., and Houart, C. (2009). Integration of telencephalic Wnt and hedgehog signaling center activities by Foxg1. Dev. Cell *16*, 576–587.

D'Antoni, S., Berretta, A., Bonaccorso, C.M., Bruno, V., Aronica, E., Nicoletti, F., and Catania, M.V. (2008). Metabotropic glutamate receptors in glial cells. Neurochem. Res. *33*, 2436–2443.

Dehay, C., Kennedy, H., and Kosik, K.S. (2015). The outer subventricular zone and primate-specific cortical complexification. Neuron *85*, 683–694.

Desai, A.R., and McConnell, S.K. (2000). Progressive restriction in fate potential by neural progenitors during cerebral cortical development. Dev. Camb. Engl. *127*, 2863–2872.

Devinsky, O., Vezzani, A., Najjar, S., De Lanerolle, N.C., and Rogawski, M.A. (2013). Glia and epilepsy: excitability and inflammation. Trends Neurosci. *36*, 174–184.

Diodato, A., Pinzan, M., Granzotto, M., and Mallamaci, A. (2013). Promotion of cortico-cerebral precursors expansion by artificial pri-miRNAs targeted against the Emx2 locus. Curr. Gene Ther. *13*, 152–161.

Djukic, B., Casper, K.B., Philpot, B.D., Chin, L.-S., and McCarthy, K.D. (2007). Conditional knock-out of Kir4.1 leads to glial membrane depolarization, inhibition of potassium and glutamate uptake, and enhanced short-term synaptic potentiation. J. Neurosci. Off. J. Soc. Neurosci. *27*, 11354–11365.

Dou, C.L., Li, S., and Lai, E. (1999). Dual role of brain factor-1 in regulating growth and patterning of the cerebral hemispheres. Cereb. Cortex N. Y. N 1991 *9*, 543–550.

Dulac, O., Feingold, J., Plouin, P., Chiron, C., Pajot, N., and Ponsot, G. (1993). Genetic predisposition to West syndrome. Epilepsia *34*, 732–737.

Eagleson, G., Ferreiro, B., and Harris, W.A. (1995). Fate of the anterior neural ridge and the morphogenesis of the Xenopus forebrain. J. Neurobiol. *28*, 146–158.

Eiraku, M., Watanabe, K., Matsuo-Takasaki, M., Kawada, M., Yonemura, S., Matsumura, M., Wataya, T., Nishiyama, A., Muguruma, K., and Sasai, Y. (2008). Self-organized formation of polarized cortical tissues from ESCs and its active manipulation by extrinsic signals. Cell Stem Cell *3*, 519–532.

Evans, J.C., Archer, H.L., Colley, J.P., Ravn, K., Nielsen, J.B., Kerr, A., Williams, E., Christodoulou, J., Gécz, J., Jardine, P.E., et al. (2005). Early onset seizures and Rett-like features associated with mutations in CDKL5. Eur. J. Hum. Genet. EJHG *13*, 1113–1120.

Falace, A., Vanni, N., Mallamaci, A., Striano, P., and Zara, F. (2013). Do regulatory regions matter in FOXG1 duplications? Eur. J. Hum. Genet. EJHG *21*, 365–366.

Falcone, C., Filippis, C., Granzotto, M., and Mallamaci, A. (2015). Emx2 expression levels in NSCs modulate astrogenesis rates by regulating EgfR and Fgf9. Glia *63*, 412–422.

Fasano, C.A., Phoenix, T.N., Kokovay, E., Lowry, N., Elkabetz, Y., Dimos, J.T., Lemischka, I.R., Studer, L., and Temple, S. (2009). Bmi-1 cooperates with Foxg1 to maintain neural stem cell self-renewal in the forebrain. Genes Dev. *23*, 561–574.

Feinberg, A.P., and Leahy, W.R. (1977). Infantile spasms: case report of sex-linked inheritance. Dev. Med. Child Neurol. *19*, 524–526.

Fertuzinhos, S., Krsnik, Z., Kawasawa, Y.I., Rasin, M.-R., Kwan, K.Y., Chen, J.-G., Judas, M., Hayashi, M., and Sestan, N. (2009). Selective depletion of molecularly defined cortical interneurons in human holoprosencephaly with severe striatal hypoplasia. Cereb. Cortex N. Y. N 1991 *19*, 2196–2207.

Fields, R.D., and Burnstock, G. (2006). Purinergic signalling in neuron-glia interactions. Nat. Rev. Neurosci. *7*, 423–436.

Fietz, S.A., Kelava, I., Vogt, J., Wilsch-Bräuninger, M., Stenzel, D., Fish, J.L., Corbeil, D., Riehn, A., Distler, W., Nitsch, R., et al. (2010). OSVZ progenitors of human and ferret neocortex are epithelial-like and expand by integrin signaling. Nat. Neurosci. *13*, 690–699.

Fishell, G., and Kriegstein, A.R. (2003). Neurons from radial glia: the consequences of asymmetric inheritance. Curr. Opin. Neurobiol. *13*, 34–41.

Follenzi, A., and Naldini, L. (2002). HIV-based vectors. Preparation and use. Methods Mol. Med. *69*, 259–274.

Franco, S.J., Gil-Sanz, C., Martinez-Garay, I., Espinosa, A., Harkins-Perry, S.R., Ramos, C., and Müller, U. (2012). Fate-restricted neural progenitors in the mammalian cerebral cortex. Science *337*, 746–749.

Frantz, G.D., and McConnell, S.K. (1996). Restriction of late cerebral cortical progenitors to an upper-layer fate. Neuron *17*, 55–61.

Fujita, S. (2003). The discovery of the matrix cell, the identification of the multipotent neural stem cell and the development of the central nervous system. Cell Struct. Funct. *28*, 205–228.

Furness, D.N., Dehnes, Y., Akhtar, A.Q., Rossi, D.J., Hamann, M., Grutle, N.J., Gundersen, V., Holmseth, S., Lehre, K.P., Ullensvang, K., et al. (2008). A quantitative assessment of glutamate uptake into hippocampal synaptic terminals and astrocytes: new insights into a neuronal role for excitatory amino acid transporter 2 (EAAT2). Neuroscience *157*, 80–94.

Fusaki, N., Ban, H., Nishiyama, A., Saeki, K., and Hasegawa, M. (2009). Efficient induction of transgene-free human pluripotent stem cells using a vector based on Sendai virus, an RNA

virus that does not integrate into the host genome. Proc. Jpn. Acad. Ser. B Phys. Biol. Sci. *85*, 348–362.

Gaiano, N., Nye, J.S., and Fishell, G. (2000). Radial glial identity is promoted by Notch1 signaling in the murine forebrain. Neuron *26*, 395–404.

Gammill, L.S., and Bronner-Fraser, M. (2003). Neural crest specification: migrating into genomics. Nat. Rev. Neurosci. *4*, 795–805.

Giaume, C. (2010). Astroglial Wiring is Adding Complexity to Neuroglial Networking. Front. Neuroenergetics *2*.

Giaume, C., and McCarthy, K.D. (1996). Control of gap-junctional communication in astrocytic networks. Trends Neurosci. *19*, 319–325.

Goodenough, D.A., and Paul, D.L. (2003). Beyond the gap: functions of unpaired connexon channels. Nat. Rev. Mol. Cell Biol. *4*, 285–294.

Gorski, J.A., Talley, T., Qiu, M., Puelles, L., Rubenstein, J.L.R., and Jones, K.R. (2002). Cortical excitatory neurons and glia, but not GABAergic neurons, are produced in the Emx1-expressing lineage. J. Neurosci. Off. J. Soc. Neurosci. *22*, 6309–6314.

Götz, M., and Huttner, W.B. (2005). The cell biology of neurogenesis. Nat. Rev. Mol. Cell Biol. *6*, 777–788.

Grove, E.A., Tole, S., Limon, J., Yip, L., and Ragsdale, C.W. (1998). The hem of the embryonic cerebral cortex is defined by the expression of multiple Wnt genes and is compromised in Gli3-deficient mice. Dev. Camb. Engl. *125*, 2315–2325.

Guerrini, R. (2005). Genetic malformations of the cerebral cortex and epilepsy. Epilepsia *46 Suppl 1*, 32–37.

Gunhaga, L., Marklund, M., Sjödal, M., Hsieh, J.-C., Jessell, T.M., and Edlund, T. (2003). Specification of dorsal telencephalic character by sequential Wnt and FGF signaling. Nat. Neurosci. *6*, 701–707.

Guo, C., Eckler, M.J., McKenna, W.L., McKinsey, G.L., Rubenstein, J.L.R., and Chen, B. (2013). Fezf2 expression identifies a multipotent progenitor for neocortical projection neurons, astrocytes, and oligodendrocytes. Neuron *80*, 1167–1174.

Guthrie, P.B., Knappenberger, J., Segal, M., Bennett, M.V., Charles, A.C., and Kater, S.B. (1999). ATP released from astrocytes mediates glial calcium waves. J. Neurosci. Off. J. Soc. Neurosci. *19*, 520–528.

Gutin, G., Fernandes, M., Palazzolo, L., Paek, H., Yu, K., Ornitz, D.M., McConnell, S.K., and Hébert, J.M. (2006). FGF signalling generates ventral telencephalic cells independently of SHH. Dev. Camb. Engl. *133*, 2937–2946.

Hajós, F., Woodhams, P.L., Bascó, E., Csillag, A., and Balázs, R. (1981). Proliferation of astroglia in the embryonic mouse forebrain as revealed by simultaneous immunocytochemistry and autoradiography. Acta Morphol. Acad. Sci. Hung. *29*, 361–364.

Halassa, M.M., Florian, C., Fellin, T., Munoz, J.R., Lee, S.-Y., Abel, T., Haydon, P.G., and Frank, M.G. (2009). Astrocytic modulation of sleep homeostasis and cognitive consequences of sleep loss. Neuron *61*, 213–219.

Hamilton, N.B., and Attwell, D. (2010). Do astrocytes really exocytose neurotransmitters? Nat. Rev. Neurosci. *11*, 227–238.

Hanashima, C., Shen, L., Li, S.C., and Lai, E. (2002). Brain factor-1 controls the proliferation and differentiation of neocortical progenitor cells through independent mechanisms. J. Neurosci. Off. J. Soc. Neurosci. *22*, 6526–6536.

Hanashima, C., Li, S.C., Shen, L., Lai, E., and Fishell, G. (2004). Foxg1 suppresses early cortical cell fate. Science *303*, 56–59.

Hanashima, C., Fernandes, M., Hebert, J.M., and Fishell, G. (2007). The role of Foxg1 and dorsal midline signaling in the generation of Cajal-Retzius subtypes. J. Neurosci. Off. J. Soc. Neurosci. *27*, 11103–11111.

Hansen, D.V., Lui, J.H., Parker, P.R.L., and Kriegstein, A.R. (2010). Neurogenic radial glia in the outer subventricular zone of human neocortex. Nature *464*, 554–561.

Hardcastle, Z., and Papalopulu, N. (2000). Distinct effects of XBF-1 in regulating the cell cycle inhibitor p27(XIC1) and imparting a neural fate. Dev. Camb. Engl. *127*, 1303–1314.

Haydon, P.G., and Carmignoto, G. (2006). Astrocyte control of synaptic transmission and neurovascular coupling. Physiol. Rev. *86*, 1009–1031.

Herculano-Houzel, S. (2011). Not all brains are made the same: new views on brain scaling in evolution. Brain. Behav. Evol. *78*, 22–36.

Hevner, R.F., Shi, L., Justice, N., Hsueh, Y., Sheng, M., Smiga, S., Bulfone, A., Goffinet, A.M., Campagnoni, A.T., and Rubenstein, J.L. (2001). Tbr1 regulates differentiation of the preplate and layer 6. Neuron *29*, 353–366.

Hibino, H., Inanobe, A., Furutani, K., Murakami, S., Findlay, I., and Kurachi, Y. (2010). Inwardly rectifying potassium channels: their structure, function, and physiological roles. Physiol. Rev. *90*, 291–366.

Ho, S.-Y., Chao, C.-Y., Huang, H.-L., Chiu, T.-W., Charoenkwan, P., and Hwang, E. (2011). NeurphologyJ: an automatic neuronal morphology quantification method and its application in pharmacological discovery. BMC Bioinformatics *12*, 230.

Hoogland, T.M., Kuhn, B., Göbel, W., Huang, W., Nakai, J., Helmchen, F., Flint, J., and Wang, S.S.-H. (2009). Radially expanding transglial calcium waves in the intact cerebellum. Proc. Natl. Acad. Sci. U. S. A. *106*, 3496–3501.

Hrachovy, R.A., and Frost, J.D. (1989). Infantile spasms. Pediatr. Clin. North Am. *36*, 311–329.

Ichikawa, M., Shiga, T., and Hirata, Y. (1983). Spatial and temporal pattern of postnatal proliferation of glial cells in the parietal cortex of the rat. Brain Res. *285*, 181–187.

Inoue, T., Nakamura, S., and Osumi, N. (2000). Fate mapping of the mouse prosencephalic neural plate. Dev. Biol. *219*, 373–383.

John Rubstenstein, and Pasko Rakic (2013). Patterning and Cell type specification in the developing Cns and Pns.

Kamakura, S., Oishi, K., Yoshimatsu, T., Nakafuku, M., Masuyama, N., and Gotoh, Y. (2004). Hes binding to STAT3 mediates crosstalk between Notch and JAK-STAT signalling. Nat. Cell Biol. *6*, 547–554.

Kang, J., Kang, N., Lovatt, D., Torres, A., Zhao, Z., Lin, J., and Nedergaard, M. (2008). Connexin 43 hemichannels are permeable to ATP. J. Neurosci. Off. J. Soc. Neurosci. *28*, 4702–4711.

Kanner, B.I., and Schuldiner, S. (1987). Mechanism of transport and storage of neurotransmitters. CRC Crit. Rev. Biochem. *22*, 1–38.

Kato, M., and Dobyns, W.B. (2003). Lissencephaly and the molecular basis of neuronal migration. Hum. Mol. Genet. *12 Spec No 1*, R89–R96.

Kékesi, O., Ioja, E., Szabó, Z., Kardos, J., and Héja, L. (2015). Recurrent seizure-like events are associated with coupled astroglial synchronization. Front. Cell. Neurosci. *9*, 215.

Kippin, T.E., Martens, D.J., and van der Kooy, D. (2005). p21 loss compromises the relative quiescence of forebrain stem cell proliferation leading to exhaustion of their proliferation capacity. Genes Dev. *19*, 756–767.

Kitamura, K., Yanazawa, M., Sugiyama, N., Miura, H., Iizuka-Kogo, A., Kusaka, M., Omichi, K., Suzuki, R., Kato-Fukui, Y., Kamiirisa, K., et al. (2002). Mutation of ARX causes abnormal development of forebrain and testes in mice and X-linked lissencephaly with abnormal genitalia in humans. Nat. Genet. *32*, 359–369.

Kofuji, P., and Newman, E.A. (2004). Potassium buffering in the central nervous system. Neuroscience *129*, 1045–1056.

Kofuji, P., Ceelen, P., Zahs, K.R., Surbeck, L.W., Lester, H.A., and Newman, E.A. (2000). Genetic inactivation of an inwardly rectifying potassium channel (Kir4.1 subunit) in mice: phenotypic impact in retina. J. Neurosci. Off. J. Soc. Neurosci. *20*, 5733–5740.

Köles, L., Leichsenring, A., Rubini, P., and Illes, P. (2011). P2 receptor signaling in neurons and glial cells of the central nervous system. Adv. Pharmacol. San Diego Calif *61*, 441–493.

Kopan, R., and Ilagan, M.X.G. (2009). The canonical Notch signaling pathway: unfolding the activation mechanism. Cell *137*, 216–233.

Kozoriz, M.G., Bates, D.C., Bond, S.R., Lai, C.P.K., and Moniz, D.M. (2006). Passing potassium with and without gap junctions. J. Neurosci. Off. J. Soc. Neurosci. *26*, 8023–8024.

Kriegstein, A., and Alvarez-Buylla, A. (2009). The glial nature of embryonic and adult neural stem cells. Annu. Rev. Neurosci. *32*, 149–184.

Kriegstein, A., Noctor, S., and Martínez-Cerdeño, V. (2006). Patterns of neural stem and progenitor cell division may underlie evolutionary cortical expansion. Nat. Rev. Neurosci. *7*, 883–890.

Kucheryavykh, Y.V., Pearson, W.L., Kurata, H.T., Eaton, M.J., Skatchkov, S.N., and Nichols, C.G. (2007). Polyamine permeation and rectification of Kir4.1 channels. Channels Austin Tex *1*, 172–178.

Kuffler, S.W., Nicholls, J.G., and Orkand, R.K. (1966). Physiological properties of glial cells in the central nervous system of amphibia. J. Neurophysiol. *29*, 768–787.

Kunzelmann, P., Schröder, W., Traub, O., Steinhäuser, C., Dermietzel, R., and Willecke, K. (1999). Late onset and increasing expression of the gap junction protein connexin30 in adult murine brain and long-term cultured astrocytes. Glia *25*, 111–119.

Larsen, B.R., Assentoft, M., Cotrina, M.L., Hua, S.Z., Nedergaard, M., Kaila, K., Voipio, J., and MacAulay, N. (2014). Contributions of the Na^+/K^+-ATPase, NKCC1, and Kir4.1 to hippocampal K^+ clearance and volume responses. Glia *62*, 608–622.

Lee, S.H., Magge, S., Spencer, D.D., Sontheimer, H., and Cornell-Bell, A.H. (1995). Human epileptic astrocytes exhibit increased gap junction coupling. Glia *15*, 195–202.

Lehre, K.P., Levy, L.M., Ottersen, O.P., Storm-Mathisen, J., and Danbolt, N.C. (1995). Differential expression of two glial glutamate transporters in the rat brain: quantitative and immunocytochemical observations. J. Neurosci. Off. J. Soc. Neurosci. *15*, 1835–1853.

Levy, L.M., Warr, O., and Attwell, D. (1998). Stoichiometry of the glial glutamate transporter GLT-1 expressed inducibly in a Chinese hamster ovary cell line selected for low endogenous Na+-dependent glutamate uptake. J. Neurosci. Off. J. Soc. Neurosci. *18*, 9620–9628.

Li, J., Chang, H.W., Lai, E., Parker, E.J., and Vogt, P.K. (1995). The oncogene qin codes for a transcriptional repressor. Cancer Res. *55*, 5540–5544.

Li, T., Ren, G., Lusardi, T., Wilz, A., Lan, J.Q., Iwasato, T., Itohara, S., Simon, R.P., and Boison, D. (2008). Adenosine kinase is a target for the prediction and prevention of epileptogenesis in mice. J. Clin. Invest. *118*, 571–582.

Lisman, J.E. (1999). Relating hippocampal circuitry to function: recall of memory sequences by reciprocal dentate-CA3 interactions. Neuron *22*, 233–242.

LoTurco, J.J., and Bai, J. (2006). The multipolar stage and disruptions in neuronal migration. Trends Neurosci. *29*, 407–413.

Louvi, A., and Artavanis-Tsakonas, S. (2006). Notch signalling in vertebrate neural development. Nat. Rev. Neurosci. *7*, 93–102.

Lux, A.L. (2001). West & son: the origins of West syndrome. Brain Dev. *23*, 443–446.

MacVicar, B.A., and Thompson, R.J. (2010). Non-junction functions of pannexin-1 channels. Trends Neurosci. *33*, 93–102.

Malatesta, P., Hartfuss, E., and Götz, M. (2000). Isolation of radial glial cells by fluorescent-activated cell sorting reveals a neuronal lineage. Dev. Camb. Engl. *127*, 5253–5263.

Mariani, J., Simonini, M.V., Palejev, D., Tomasini, L., Coppola, G., Szekely, A.M., Horvath, T.L., and Vaccarino, F.M. (2012). Modeling human cortical development in vitro using induced pluripotent stem cells. Proc. Natl. Acad. Sci. U. S. A. *109*, 12770–12775.

Marín-Padilla, M. (1998). Cajal-Retzius cells and the development of the neocortex. Trends Neurosci. *21*, 64–71.

Martynoga, B., Morrison, H., Price, D.J., and Mason, J.O. (2005). Foxg1 is required for specification of ventral telencephalon and region-specific regulation of dorsal telencephalic precursor proliferation and apoptosis. Dev. Biol. *283*, 113–127.

Matsumoto, A., Watanabe, K., Negoro, T., Sugiura, M., Iwase, K., Hara, K., and Miyazaki, S. (1981). Long-term prognosis after infantile spasms: a statistical study of prognostic factors in 200 cases. Dev. Med. Child Neurol. *23*, 51–65.

McKenna, W.L., Betancourt, J., Larkin, K.A., Abrams, B., Guo, C., Rubenstein, J.L.R., and Chen, B. (2011). Tbr1 and Fezf2 regulate alternate corticofugal neuronal identities during neocortical development. J. Neurosci. Off. J. Soc. Neurosci. *31*, 549–564.

Metea, M.R., and Newman, E.A. (2006). Calcium signaling in specialized glial cells. Glia *54*, 650–655.

Mikelonis, D., Jorcyk, C.L., Tawara, K., and Oxford, J.T. (2014). Stüve-Wiedemann syndrome: LIFR and associated cytokines in clinical course and etiology. Orphanet J. Rare Dis. *9*, 34.

Miller, F.D., and Gauthier, A.S. (2007). Timing is everything: making neurons versus glia in the developing cortex. Neuron *54*, 357–369.

Mission, J.P., Takahashi, T., and Caviness, V.S. (1991). Ontogeny of radial and other astroglial cells in murine cerebral cortex. Glia *4*, 138–148.

Mitsuhashi, T., and Takahashi, T. (2009). Genetic regulation of proliferation/differentiation characteristics of neural progenitor cells in the developing neocortex. Brain Dev. *31*, 553–557.

Miyata, T., Kawaguchi, A., Okano, H., and Ogawa, M. (2001). Asymmetric inheritance of radial glial fibers by cortical neurons. Neuron *31*, 727–741.

Miyoshi, G., and Fishell, G. (2011). GABAergic interneuron lineages selectively sort into specific cortical layers during early postnatal development. Cereb. Cortex N. Y. N 1991 *21*, 845–852.

Miyoshi, G., and Fishell, G. (2012). Dynamic FoxG1 expression coordinates the integration of multipolar pyramidal neuron precursors into the cortical plate. Neuron *74*, 1045–1058.

Mobbs, P., Brew, H., and Attwell, D. (1988). A quantitative analysis of glial cell coupling in the retina of the axolotl (Ambystoma mexicanum). Brain Res. *460*, 235–245.

Molliver, M.E., Kostović, I., and van der Loos, H. (1973). The development of synapses in cerebral cortex of the human fetus. Brain Res. *50*, 403–407.

Molyneaux, B.J., Arlotta, P., Menezes, J.R.L., and Macklis, J.D. (2007). Neuronal subtype specification in the cerebral cortex. Nat. Rev. Neurosci. *8*, 427–437.

Mondal, S., Ivanchuk, S.M., Rutka, J.T., and Boulianne, G.L. (2007). Sloppy paired 1/2 regulate glial cell fates by inhibiting Gcm function. Glia *55*, 282–293.

Mugnaini E. (1986). Cell junctions of astrocytes, ependyma, and related cells in the mammalian central nervous system, with emphasis on the hypothesis of a generalized functional syncytium of supporting cells. 339–371.

Muzio, L., and Mallamaci, A. (2005). Foxg1 confines Cajal-Retzius neuronogenesis and hippocampal morphogenesis to the dorsomedial pallium. J. Neurosci. Off. J. Soc. Neurosci. *25*, 4435–4441.

Nadarajah, B., and Parnavelas, J.G. (2002). Modes of neuronal migration in the developing cerebral cortex. Nat. Rev. Neurosci. *3*, 423–432.

Naka, H., Nakamura, S., Shimazaki, T., and Okano, H. (2008). Requirement for COUP-TFI and II in the temporal specification of neural stem cells in CNS development. Nat. Neurosci. *11*, 1014–1023.

Namihira, M., Kohyama, J., Semi, K., Sanosaka, T., Deneen, B., Taga, T., and Nakashima, K. (2009). Committed neuronal precursors confer astrocytic potential on residual neural precursor cells. Dev. Cell *16*, 245–255.

Nielsen, S., Nagelhus, E.A., Amiry-Moghaddam, M., Bourque, C., Agre, P., and Ottersen, O.P. (1997). Specialized membrane domains for water transport in glial cells: high-resolution immunogold cytochemistry of aquaporin-4 in rat brain. J. Neurosci. Off. J. Soc. Neurosci. *17*, 171–180.

Nieto, M., Schuurmans, C., Britz, O., and Guillemot, F. (2001). Neural bHLH genes control the neuronal versus glial fate decision in cortical progenitors. Neuron *29*, 401–413.

Noctor, S.C., Flint, A.C., Weissman, T.A., Dammerman, R.S., and Kriegstein, A.R. (2001). Neurons derived from radial glial cells establish radial units in neocortex. Nature *409*, 714–720.

Noctor, S.C., Martínez-Cerdeño, V., Ivic, L., and Kriegstein, A.R. (2004). Cortical neurons arise in symmetric and asymmetric division zones and migrate through specific phases. Nat. Neurosci. *7*, 136–144.

Ohkubo, Y., Chiang, C., and Rubenstein, J.L.R. (2002). Coordinate regulation and synergistic actions of BMP4, SHH and FGF8 in the rostral prosencephalon regulate morphogenesis of the telencephalic and optic vesicles. Neuroscience *111*, 1–17.

Ohtsuka, T., Sakamoto, M., Guillemot, F., and Kageyama, R. (2001). Roles of the basic helix-loop-helix genes Hes1 and Hes5 in expansion of neural stem cells of the developing brain. J. Biol. Chem. *276*, 30467–30474.

Ono, K., Takebayashi, H., Ikeda, K., Furusho, M., Nishizawa, T., Watanabe, K., and Ikenaka, K. (2008). Regional- and temporal-dependent changes in the differentiation of Olig2 progenitors in the forebrain, and the impact on astrocyte development in the dorsal pallium. Dev. Biol. *320*, 456–468.

Orellana, J.A., and Stehberg, J. (2014). Hemichannels: new roles in astroglial function. Front. Physiol. *5*, 193.

Orkand, R.K., Nicholls, J.G., and Kuffler, S.W. (1966). Effect of nerve impulses on the membrane potential of glial cells in the central nervous system of amphibia. J. Neurophysiol. *29*, 788–806.

O'Rourke, N.A., Dailey, M.E., Smith, S.J., and McConnell, S.K. (1992). Diverse migratory pathways in the developing cerebral cortex. Science *258*, 299–302.

Owe, S.G., Marcaggi, P., and Attwell, D. (2006). The ionic stoichiometry of the GLAST glutamate transporter in salamander retinal glia. J. Physiol. *577*, 591–599.

Paek, H., Gutin, G., and Hébert, J.M. (2009). FGF signaling is strictly required to maintain early telencephalic precursor cell survival. Dev. Camb. Engl. *136*, 2457–2465.

Parpura, and Haydon (2008). Astrocytes in (patho)physiology of the nervous system springer (Springer).

Petzold, G.C., Albeanu, D.F., Sato, T.F., and Murthy, V.N. (2008). Coupling of neural activity to blood flow in olfactory glomeruli is mediated by astrocytic pathways. Neuron *58*, 897–910.

Phelan, P., and Starich, T.A. (2001). Innexins get into the gap. BioEssays News Rev. Mol. Cell. Dev. Biol. *23*, 388–396.

Pontrelli, G., Cappelletti, S., Claps, D., Sirleto, P., Ciocca, L., Petrocchi, S., Terracciano, A., Serino, D., Fusco, L., Vigevano, F., et al. (2014). Epilepsy in patients with duplications of chromosome 14 harboring FOXG1. Pediatr. Neurol. *50*, 530–535.

Pow, D.V., and Robinson, S.R. (1994). Glutamate in some retinal neurons is derived solely from glia. Neuroscience *60*, 355–366.

Raciti, M., Granzotto, M., Duc, M.D., Fimiani, C., Cellot, G., Cherubini, E., and Mallamaci, A. (2013). Reprogramming fibroblasts to neural-precursor-like cells by structured overexpression of pallial patterning genes. Mol. Cell. Neurosci. *57*, 42–53.

Rakic, P. (1974). Neurons in rhesus monkey visual cortex: systematic relation between time of origin and eventual disposition. Science *183*, 425–427.

Rallu, M., Machold, R., Gaiano, N., Corbin, J.G., McMahon, A.P., and Fishell, G. (2002). Dorsoventral patterning is established in the telencephalon of mutants lacking both Gli3 and Hedgehog signaling. Dev. Camb. Engl. *129*, 4963–4974.

Ramon and Cajal, A. (1997). Histology of the Nervous System of Man and Vertebrates. Neurology *48*, 299–300.

Reichenbach, A., Derouiche, A., and Kirchhoff, F. (2010). Morphology and dynamics of perisynaptic glia. Brain Res. Rev. *63*, 11–25.

Riikonen, R. (2001). Long-term outcome of patients with West syndrome. Brain Dev. *23*, 683–687.

Del Río, J.A., Heimrich, B., Borrell, V., Förster, E., Drakew, A., Alcántara, S., Nakajima, K., Miyata, T., Ogawa, M., Mikoshiba, K., et al. (1997). A role for Cajal-Retzius cells and reelin in the development of hippocampal connections. Nature *385*, 70–74.

Robson, S.C., Sévigny, J., and Zimmermann, H. (2006). The E-NTPDase family of ectonucleotidases: Structure function relationships and pathophysiological significance. Purinergic Signal. *2*, 409–430.

Rodriguez, C., Huang, L.J., Son, J.K., McKee, A., Xiao, Z., and Lodish, H.F. (2001). Functional cloning of the proto-oncogene brain factor-1 (BF-1) as a Smad-binding antagonist of transforming growth factor-beta signaling. J. Biol. Chem. *276*, 30224–30230.

Roth, M., Bonev, B., Lindsay, J., Lea, R., Panagiotaki, N., Houart, C., and Papalopulu, N. (2010). FoxG1 and TLE2 act cooperatively to regulate ventral telencephalon formation. Dev. Camb. Engl. *137*, 1553–1562.

Rouach, N., Koulakoff, A., Abudara, V., Willecke, K., and Giaume, C. (2008). Astroglial metabolic networks sustain hippocampal synaptic transmission. Science *322*, 1551–1555.

Roux, L., Benchenane, K., Rothstein, J.D., Bonvento, G., and Giaume, C. (2011). Plasticity of astroglial networks in olfactory glomeruli. Proc. Natl. Acad. Sci. U. S. A. *108*, 18442–18446.

Saijo, K., Winner, B., Carson, C.T., Collier, J.G., Boyer, L., Rosenfeld, M.G., Gage, F.H., and Glass, C.K. (2009). A Nurr1/CoREST pathway in microglia and astrocytes protects dopaminergic neurons from inflammation-induced death. Cell *137*, 47–59.

Sardi, S.P., Murtie, J., Koirala, S., Patten, B.A., and Corfas, G. (2006). Presenilin-dependent ErbB4 nuclear signaling regulates the timing of astrogenesis in the developing brain. Cell *127*, 185–197.

Sastry, L., Johnson, T., Hobson, M.J., Smucker, B., and Cornetta, K. (2002). Titering lentiviral vectors: comparison of DNA, RNA and marker expression methods. Gene Ther. *9*, 1155–1162.

Sauer FC. (1935). Mitosis in the neural tube. :377–405.

Seifert, G., and Steinhäuser, C. (2013). Neuron-astrocyte signaling and epilepsy. Exp. Neurol. *244*, 4–10.

Seifert, G., Schilling, K., and Steinhäuser, C. (2006). Astrocyte dysfunction in neurological disorders: a molecular perspective. Nat. Rev. Neurosci. *7*, 194–206.

Seki, T., Yuasa, S., and Fukuda, K. (2012). Generation of induced pluripotent stem cells from a small amount of human peripheral blood using a combination of activated T cells and Sendai virus. Nat. Protoc. *7*, 718–728.

Seoane, J., Le, H.-V., Shen, L., Anderson, S.A., and Massagué, J. (2004). Integration of Smad and forkhead pathways in the control of neuroepithelial and glioblastoma cell proliferation. Cell *117*, 211–223.

Shaikh, T.H., Gai, X., Perin, J.C., Glessner, J.T., Xie, H., Murphy, K., O'Hara, R., Casalunovo, T., Conlin, L.K., D'Arcy, M., et al. (2009). High-resolution mapping and analysis of copy number variations in the human genome: a data resource for clinical and research applications. Genome Res. *19*, 1682–1690.

Shen, Q., Wang, Y., Dimos, J.T., Fasano, C.A., Phoenix, T.N., Lemischka, I.R., Ivanova, N.B., Stifani, S., Morrisey, E.E., and Temple, S. (2006). The timing of cortical neurogenesis is encoded within lineages of individual progenitor cells. Nat. Neurosci. *9*, 743–751.

Shigeri, Y., Seal, R.P., and Shimamoto, K. (2004). Molecular pharmacology of glutamate transporters, EAATs and VGLUTs. Brain Res. Brain Res. Rev. *45*, 250–265.

Shimamura, K., and Rubenstein, J.L. (1997). Inductive interactions direct early regionalization of the mouse forebrain. Dev. Camb. Engl. *124*, 2709–2718.

Shimojo, H., Ohtsuka, T., and Kageyama, R. (2011). Dynamic Expression of Notch Signaling Genes in Neural Stem/Progenitor Cells. Front. Neurosci. *5*.

Shitamukai, A., Konno, D., and Matsuzaki, F. (2011). Oblique radial glial divisions in the developing mouse neocortex induce self-renewing progenitors outside the germinal zone that resemble primate outer subventricular zone progenitors. J. Neurosci. Off. J. Soc. Neurosci. *31*, 3683–3695.

Siegenthaler, J.A., Tremper-Wells, B.A., and Miller, M.W. (2008). Foxg1 Haploinsufficiency Reduces the Population of Cortical Intermediate Progenitor Cells: Effect of Increased p21 Expression. Cereb. Cortex N. Y. NY *18*, 1865–1875.

Song, M.-R., and Ghosh, A. (2004). FGF2-induced chromatin remodeling regulates CNTF-mediated gene expression and astrocyte differentiation. Nat. Neurosci. *7*, 229–235.

Spigoni, G., Gedressi, C., and Mallamaci, A. (2010). Regulation of Emx2 expression by antisense transcripts in murine cortico-cerebral precursors. PloS One *5*, e8658.

Srinivasan, K., Leone, D.P., Bateson, R.K., Dobreva, G., Kohwi, Y., Kohwi-Shigematsu, T., Grosschedl, R., and McConnell, S.K. (2012). A network of genetic repression and derepression specifies projection fates in the developing neocortex. Proc. Natl. Acad. Sci. U. S. A. *109*, 19071–19078.

Stehberg, J., Moraga-Amaro, R., Salazar, C., Becerra, A., Echeverría, C., Orellana, J.A., Bultynck, G., Ponsaerts, R., Leybaert, L., Simon, F., et al. (2012). Release of gliotransmitters through astroglial connexin 43 hemichannels is necessary for fear memory consolidation in the basolateral amygdala. FASEB J. Off. Publ. Fed. Am. Soc. Exp. Biol. *26*, 3649–3657.

Stipursky, J., Francis, D., Dezonne, R.S., Bérgamo de Araújo, A.P., Souza, L., Moraes, C.A., and Alcantara Gomes, F.C. (2014). TGF-β1 promotes cerebral cortex radial glia-astrocyte differentiation in vivo. Front. Cell. Neurosci. *8*, 393.

Storm, E.E., Garel, S., Borello, U., Hebert, J.M., Martinez, S., McConnell, S.K., Martin, G.R., and Rubenstein, J.L.R. (2006). Dose-dependent functions of Fgf8 in regulating telencephalic patterning centers. Dev. Camb. Engl. *133*, 1831–1844.

Stout, C., and Charles, A. (2003). Modulation of intercellular calcium signaling in astrocytes by extracellular calcium and magnesium. Glia *43*, 265–273.

Strømme, P., Mangelsdorf, M.E., Scheffer, I.E., and Gécz, J. (2002). Infantile spasms, dystonia, and other X-linked phenotypes caused by mutations in Aristaless related homeobox gene, ARX. Brain Dev. *24*, 266–268.

Studer, F.E., Fedele, D.E., Marowsky, A., Schwerdel, C., Wernli, K., Vogt, K., Fritschy, J.M., and Boison, D. (2006). Shift of adenosine kinase expression from neurons to astrocytes during postnatal development suggests dual functionality of the enzyme. Neuroscience *142*, 125–137.

Sugai, K., Fukuyama, Y., Yasuda, K., Fujimoto, S., Ohtsu, M., Ohta, H., Ogawa, A., Hamano, S., Hirano, S., Yoshioka, H., et al. (2001). Clinical and pedigree study on familial cases of West syndrome in Japan. Brain Dev. *23*, 558–564.

Sun, T., and Hevner, R.F. (2014). Growth and folding of the mammalian cerebral cortex: from molecules to malformations. Nat. Rev. Neurosci. *15*, 217–232.

Supèr, H., Del Río, J.A., Martínez, A., Pérez-Sust, P., and Soriano, E. (2000). Disruption of neuronal migration and radial glia in the developing cerebral cortex following ablation of Cajal-Retzius cells. Cereb. Cortex N. Y. N 1991 *10*, 602–613.

Tabata, H., and Nakajima, K. (2003). Multipolar migration: the third mode of radial neuronal migration in the developing cerebral cortex. J. Neurosci. Off. J. Soc. Neurosci. *23*, 9996–10001.

Takahashi, K., and Yamanaka, S. (2006). Induction of pluripotent stem cells from mouse embryonic and adult fibroblast cultures by defined factors. Cell *126*, 663–676.

Takahashi, T., Nowakowski, R.S., and Caviness, V.S. (1995). The cell cycle of the pseudostratified ventricular epithelium of the embryonic murine cerebral wall. J. Neurosci. Off. J. Soc. Neurosci. *15*, 6046–6057.

Tarabykin, V., Stoykova, A., Usman, N., and Gruss, P. (2001). Cortical upper layer neurons derive from the subventricular zone as indicated by Svet1 gene expression. Dev. Camb. Engl. *128*, 1983–1993.

Theis, M., Söhl, G., Eiberger, J., and Willecke, K. (2005). Emerging complexities in identity and function of glial connexins. Trends Neurosci. *28*, 188–195.

Tian, G.-F., Azmi, H., Takano, T., Xu, Q., Peng, W., Lin, J., Oberheim, N., Lou, N., Wang, X., Zielke, H.R., et al. (2005). An astrocytic basis of epilepsy. Nat. Med. *11*, 973–981.

Tohyama, J., Yamamoto, T., Hosoki, K., Nagasaki, K., Akasaka, N., Ohashi, T., Kobayashi, Y., and Saitoh, S. (2011). West syndrome associated with mosaic duplication of FOXG1 in a patient with maternal uniparental disomy of chromosome 14. Am. J. Med. Genet. A. *155A*, 2584–2588.

Toma, K., Kumamoto, T., and Hanashima, C. (2014). The timing of upper-layer neurogenesis is conferred by sequential derepression and negative feedback from deep-layer neurons. J. Neurosci. Off. J. Soc. Neurosci. *34*, 13259–13276.

Vallejo, M. (2009). PACAP signaling to DREAM: a cAMP-dependent pathway that regulates cortical astrogliogenesis. Mol. Neurobiol. *39*, 90–100.

Vangeison, G., and Rempe, D.A. (2009). The Janus-faced effects of hypoxia on astrocyte function. Neurosci. Rev. J. Bringing Neurobiol. Neurol. Psychiatry *15*, 579–588.

Vaughn, J.E., and Pease, D.C. (1967). Electron microscopy of classically stained astrocytes. J. Comp. Neurol. *131*, 143–154.

Vaughn, J.E., and Peters, A. (1967). Electron microscopy of the early postnatal development of fibrous astrocytes. Am. J. Anat. *121*, 131–152.

Vigevano, F., Fusco, L., Cusmai, R., Claps, D., Ricci, S., and Milani, L. (1993). The idiopathic form of West syndrome. Epilepsia *34*, 743–746.

Wallraff, A., Köhling, R., Heinemann, U., Theis, M., Willecke, K., and Steinhäuser, C. (2006). The impact of astrocytic gap junctional coupling on potassium buffering in the hippocampus. J. Neurosci. Off. J. Soc. Neurosci. *26*, 5438–5447.

Watanabe, K., Negoro, T., Aso, K., and Matsumoto, A. (1993). Reappraisal of interictal electroencephalograms in infantile spasms. Epilepsia *34*, 679–685.

Weaving, L.S., Christodoulou, J., Williamson, S.L., Friend, K.L., McKenzie, O.L.D., Archer, H., Evans, J., Clarke, A., Pelka, G.J., Tam, P.P.L., et al. (2004). Mutations of CDKL5 cause a severe neurodevelopmental disorder with infantile spasms and mental retardation. Am. J. Hum. Genet. *75*, 1079–1093.

Wen, S., Li, H., and Liu, J. (2009). Dynamic signaling for neural stem cell fate determination. Cell Adhes. Migr. *3*, 107–117.

Wilson, S.W., and Houart, C. (2004). Early steps in the development of the forebrain. Dev. Cell *6*, 167–181.

Xiong, Z.Q., and Stringer, J.L. (2000). Sodium pump activity, not glial spatial buffering, clears potassium after epileptiform activity induced in the dentate gyrus. J. Neurophysiol. *83*, 1443–1451.

Xu, L., Zeng, L.-H., and Wong, M. (2009). Impaired astrocytic gap junction coupling and potassium buffering in a mouse model of tuberous sclerosis complex. Neurobiol. Dis. *34*, 291–299.

Xuan, S., Baptista, C.A., Balas, G., Tao, W., Soares, V.C., and Lai, E. (1995). Winged helix transcription factor BF-1 is essential for the development of the cerebral hemispheres. Neuron *14*, 1141–1152.

Yang, R., and Liang, B.T. (2012). Cardiac P2X(4) receptors: targets in ischemia and heart failure? Circ. Res. *111*, 397–401.

Yao, J., Lai, E., and Stifani, S. (2001). The winged-helix protein brain factor 1 interacts with groucho and hes proteins to repress transcription. Mol. Cell. Biol. *21*, 1962–1972.

Ye, Z.-C., Wyeth, M.S., Baltan-Tekkok, S., and Ransom, B.R. (2003). Functional hemichannels in astrocytes: a novel mechanism of glutamate release. J. Neurosci. Off. J. Soc. Neurosci. *23*, 3588–3596.

Yoshida, Y., Takahashi, K., Okita, K., Ichisaka, T., and Yamanaka, S. (2009). Hypoxia enhances the generation of induced pluripotent stem cells. Cell Stem Cell *5*, 237–241.

Yu, X., and Zecevic, N. (2011). Dorsal radial glial cells have the potential to generate cortical interneurons in human, but not in mouse brain. J. Neurosci. Off. J. Soc. Neurosci. *31*, 2413–2420.

Yu, Y.-C., Bultje, R.S., Wang, X., and Shi, S.-H. (2009). Specific synapses develop preferentially among sister excitatory neurons in the neocortex. Nature *458*, 501–504.

Yu, Y.-C., He, S., Chen, S., Fu, Y., Brown, K.N., Yao, X.-H., Ma, J., Gao, K.P., Sosinsky, G.E., Huang, K., et al. (2012). Preferential electrical coupling regulates neocortical lineage-dependent microcircuit assembly. Nature *486*, 113–117.

Zhang, J., Wang, H., Ye, C., Ge, W., Chen, Y., Jiang, Z., Wu, C., Poo, M., and Duan, S. (2003). ATP released by astrocytes mediates glutamatergic activity-dependent heterosynaptic suppression. Neuron *40*, 971–982.

Zupanc, M.L. (2003). Infantile spasms. Expert Opin. Pharmacother. *4*, 2039–2048.